Helsinki University of Technology Department of Signal Processing and Acoustics
Teknillinen korkeakoulu Signaalinkäsittelyn ja akustiikan laitos
Espoo 2009 Report 11

SPECTRUM SENSING FOR COGNITIVE RADIO AND RADAR SYSTEMS

Jarmo Lundén

Dissertation for the degree of Doctor of Science in Technology to be presented with due permission of the Faculty of Electronics, Communications and Automation for public examination and debate in Auditorium S1 at Helsinki University of Technology (Espoo, Finland) on the 13th of November, 2009, at 12 noon.

Helsinki University of Technology
Faculty of Electronics, Communications and Automation
Department of Signal Processing and Acoustics

Teknillinen korkeakoulu
Elektroniikan, tietoliikenteen ja automaation tiedekunta
Signaalinkäsittelyn ja akustiikan laitos

Distribution:
Helsinki University of Technology
Department of Signal Processing and Acoustics
P.O. Box 3000
FI-02015 TKK
Tel. +358-9-451 3211
Fax +358-9-452 3641
E-mail: Mirja.Lemetyinen@tkk.fi
Web page: http://signal.tkk.fi

ISBN 978-952-248-053-8 (Printed)
ISBN 978-952-248-054-5 (PDF)
ISSN 1797-4267

Multiprint Oy
Espoo, Finland 2009

ABSTRACT OF DOCTORAL DISSERTATION	HELSINKI UNIVERSITY OF TECHNOLOGY P. O. BOX 1000, FI-02015 TKK http://www.tkk.fi

Author Jarmo Lundén

Name of the dissertation

Spectrum sensing for cognitive radio and radar systems

Manuscript submitted July 9, 2009	Manuscript revised October 9, 2009
Date of the defence November 13, 2009	
☐ Monograph	☒ Article dissertation (summary + original articles)
Faculty	Faculty of Electronics, Communications and Automation
Department	Department of Signal Processing and Acoustics
Field of research	Signal Processing for Communications
Opponent(s)	Dr. Brian M. Sadler and Prof. Sergio Barbarossa
Supervisor	Prof. Visa Koivunen
Instructor	Prof. Visa Koivunen

Abstract

The use of the radio frequency spectrum is increasing at a rapid rate. Reliable and efficient operation in a crowded radio spectrum requires innovative solutions and techniques. Future wireless communication and radar systems should be aware of their surrounding radio environment in order to have the ability to adapt their operation to the effective situation. Spectrum sensing techniques such as detection, waveform recognition, and specific emitter identification are key sources of information for characterizing the surrounding radio environment and extracting valuable information, and consequently adjusting transceiver parameters for facilitating flexible, efficient, and reliable operation.

In this thesis, spectrum sensing algorithms for cognitive radios and radar intercept receivers are proposed. Single-user and collaborative cyclostationarity-based detection algorithms are proposed: Multicycle detectors and robust nonparametric spatial sign cyclic correlation based fixed sample size and sequential detectors are proposed. Asymptotic distributions of the test statistics under the null hypothesis are established. A censoring scheme in which only informative test statistics are transmitted to the fusion center is proposed for collaborative detection. The proposed detectors and methods have the following benefits: employing cyclostationarity enables distinction among different systems, collaboration mitigates the effects of shadowing and multipath fading, using multiple strong cyclic frequencies improves the performance, robust detection provides reliable performance in heavy-tailed non-Gaussian noise, sequential detection reduces the average detection time, and censoring improves energy efficiency.

In addition, a radar waveform recognition system for classifying common pulse compression waveforms is developed. The proposed supervised classification system classifies an intercepted radar pulse to one of eight different classes based on the pulse compression waveform: linear frequency modulation, Costas frequency codes, binary codes, as well as Frank, P1, P2, P3, and P4 polyphase codes.

A robust M-estimation based method for radar emitter identification is proposed as well. A common modulation profile from a group of intercepted pulses is estimated and used for identifying the radar emitter. The M-estimation based approach provides robustness against preprocessing errors and deviations from the assumed noise model.

Keywords Cognitive radio, detection, intercept receiver, pattern recognition, radar, spectrum sensing	
ISBN (printed) 978-952-248-053-8	ISSN (printed) 1797-4267
ISBN (pdf) 978-952-248-054-5	ISSN (pdf)
Language English	Number of pages 107 + 123
Publisher Helsinki University of Technology, Department of Signal Processing and Acoustics	
Print distribution Helsinki University of Technology, Department of Signal Processing and Acoustics	
☒ The dissertation can be read at http://lib.tkk.fi/Diss/2009/isbn9789522480545	

VÄITÖSKIRJAN TIIVISTELMÄ	TEKNILLINEN KORKEAKOULU PL 1000, 02015 TKK http://www.tkk.fi

Tekijä Jarmo Lundén

Väitöskirjan nimi

Spektrin aistinta kognitiivisissa radio- ja tutkajärjestelmissä

Käsikirjoituksen päivämäärä 9.7.2009	Korjatun käsikirjoituksen päivämäärä 9.10.2009
Väitöstilaisuuden ajankohta 13.11.2009	
☐ Monografia	☒ Yhdistelmäväitöskirja (yhteenveto + erillisartikkelit)

Tiedekunta	Elektroniikan, tietoliikenteen ja automaation tiedekunta
Laitos	Signaalinkäsittelyn ja akustiikan laitos
Tutkimusala	Tietoliikenteen signaalinkäsittely
Vastaväittäjä(t)	Dr. Brian M. Sadler and Prof. Sergio Barbarossa
Työn valvoja	Prof. Visa Koivunen
Työn ohjaaja	Prof. Visa Koivunen

Tiivistelmä

Radiotaajuuksien käyttö lisääntyy kasvavalla vauhdilla. Toimiakseen tehokkaalla ja luotettavalla tavalla ruuhkautuvassa radiospektrissä tulevaisuuden langattomilta tietoliikenne- ja tutkajärjestelmiltä vaaditaan parempaa kykyä sopeutua vallitsevaan radioympäristöön. Spektrin aistiminen ja siihen liittyvät tekniikat, kuten signaalien ilmaisu sekä aaltomuotojen ja yksittäisten lähettimien tunnistus, auttavat muodostamaan paremman tilannekuvan vallitsevista olosuhteista, täten mahdollistaen myös paremman radioiden toimintaparametrien sopeuttamisen ja tehokkaamman spektrin hyödyntämisen.

Tässä väitöskirjassa on kehitetty spektrin aistimiseen liittyviä algoritmeja kognitiivisiin radioihin sekä tiedusteluvastaanottimiin. Työssä on kehitetty syklostationäärisyyteen pohjautuvia ilmaisualgoritmeja sekä yksittäisille käyttäjille että useamman käyttäjän yhteistyöhön. Kehitetyt useampaa voimakasta syklistä taajuutta käyttävät algoritmit parantavat ilmaisutodennäköisyyttä. Lisäksi työssä on kehitetty tilastollisesti vankkoja parametrittomia syklisiä ilmaisualgoritmeja, jotka toimivat luotettavasti myös impulsiivisissa kohina- ja interferenssiympäristöissä. Parametrittomasta testistä on työssä johdettu myös sekventaalinen versio, joka pienentää ilmaisuun tarvittavaa näytemäärää. Testistatistiikkojen asymptoottiset jakaumat on johdettu nollahypoteesille. Usean käyttäjän yhteistyö mahdollistaa häipymisen vaikutuksen pienentämisen. Käyttäjien yhteistyön energiatehokkuuden parantamiseksi tässä työssä on johdettu menetelmä, jossa vain informatiiviset testistatistiikat lähetetään fuusiokeskukseen.

Tässä väitöskirjassa on myös kehitetty tutkasignaalien aaltomuodon tunnistusjärjestelmä tutkapulssien luokittelemiseen niiden pulssikompressioaaltomuodon perusteella. Kehitetty järjestelmä luokittelee vastaanotetut tutkapulssit kahdeksaan luokkaan: lineaarinen taajuusmodulaatio, Costas taajuuskoodit, binäärikoodit sekä Frank, P1, P2, P3 ja P4 monitaajuuskoodit.

Lisäksi työssä on kehitetty vankkaan M-estimointiin pohjautuva yksittäisten tutkalähettimien tunnistusmenetelmä. Ideana menetelmässä on estimoida ryhmästä vastaanotettuja pulsseja yhteinen modulaatio ja käyttää sitä lähettimen tunnistamiseen. M-estimaattorien käyttäminen parantaa menetelmän sietokykyä esikäsittelyvirheille ja virheoletuksille.

Asiasanat Kognitiivinen radio, signaalin ilmaisu, tiedusteluvastaanotin, hahmontunnistus, tutka, spektrin aistinta

ISBN (painettu) 978-952-248-053-8	ISSN (painettu) 1797-4267
ISBN (pdf) 978-952-248-054-5	ISSN (pdf)
Kieli Englanti	Sivumäärä 107 + 123

Julkaisija Teknillinen korkeakoulu, Signaalinkäsittelyn ja akustiikan laitos

Painetun väitöskirjan jakelu Teknillinen korkeakoulu, Signaalinkäsittelyn ja akustiikan laitos

☒ Luettavissa verkossa osoitteessa http://lib.tkk.fi/Diss/2009/isbn9789522480545

Preface

The research work leading to this thesis has been carried out in the Statistical Signal Processing research group of the Department of Signal Processing and Acoustics, Helsinki University of Technology (TKK), during the years 2005-2009. The period includes a research visit from September 2007 to March 2008 to the University of Pennsylvania, Philadelphia, USA. The Statistical Signal Processing research group, led by Prof. Visa Koivunen, is a part of SMARAD (Centre of Excellence in Smart Radios and Wireless Research), a Centre of Excellence appointed by the Academy of Finland.

I would like to thank all the people who have helped to make this thesis what it is. First and foremost, I wish to express my deep gratitude to my supervisor Prof. Koivunen for his continuous guidance and support during the course of this work. It has been invaluable in improving the quality of my work. Prof. Koivunen's dedication to helping his students is truly admirable. It has been a great pleasure to be working with him.

I wish to thank Prof. Saleem A. Kassam, my supervisor during my research visit to the University of Pennsylvania, for sharing his expertise on detection theory and for the inspiring discussions that gave me plenty to think about. It was a great privilege to have the opportunity to go abroad and broaden my perspective both professionally as well as personally. I am grateful to both Prof. Koivunen and Prof. Kassam for making it possible.

I would also like to thank Prof. H. Vincent Poor, Dr. Anu Huttunen, and Liisa Terho with whom I had the privilege of co-authoring some of the papers in this thesis for their contributions and comments that have been extremely important for improving the quality of my work.

I am also grateful to the thesis pre-examiners, Dr. Brian M. Sadler and Dr. Kimmo Kansanen, for the careful examination of the thesis and comments that helped me to improve the quality of the thesis.

Thanks to my current and former colleagues at the Department of Signal Processing and Acoustics for creating a very supportive and inspiring working environment. In particular, thanks to Keijo Pölönen, Tommi Koivisto, Dr. Jan Eriksson, Jan Oksanen, and Sachin Chaudhari for the many interesting discussions we have shared during the past few years. Special thanks to the department secretary Mirja Lemetyinen and to former secretaries Anne Jääskeläinen and Marika Ahlavuo for taking care of the many

practical matters and arrangements.

I would also like to acknowledge and thank the Graduate School in Electronics, Telecommunications and Automation (GETA), the Finnish Defence Forces Technical Research Center, the Nokia Research Center, and the Nokia Foundation for providing the funding for this research. Especially, I would like to acknowledge the GETA coordinator Marja Leppäharju as well as the director of GETA Prof. Ari Sihvola and the former director of GETA Prof. Iiro Hartimo for the great work they have been doing in the interest of all the GETA graduate school students.

Last but not least, I wish to express my warmest thanks to my parents Leila and Pekka and my brother Petteri for all their encouragement and support during this time.

Espoo, October 6, 2009

Jarmo Lundén

Contents

List of publications

(I) J. Lundén, V. Koivunen, A. Huttunen and H. V. Poor, "Spectrum sensing in cognitive radios based on multiple cyclic frequencies," in *Proceedings of the 2nd International Conference on Cognitive Radio Oriented Wireless Networks and Communications (CrownCom)*, Orlando, FL, USA, July 31–August 3, 2007, pp. 37–43.

(II) J. Lundén, V. Koivunen, A. Huttunen and H. V. Poor, "Censoring for collaborative spectrum sensing in cognitive radios," in *Proceedings of the 41st Asilomar Conference on Signals, Systems, and Computers*, Pacific Grove, CA, USA, November 4–7, 2007, pp. 772–776.

(III) J. Lundén, V. Koivunen, A. Huttunen and H. V. Poor, "Collaborative cyclostationary spectrum sensing for cognitive radio systems," *IEEE Transactions on Signal Processing*, vol. 57, no. 11, November 2009.

(IV) J. Lundén, S. A. Kassam and V. Koivunen, "Nonparametric cyclic correlation based detection for cognitive radio systems," in *Proceedings of the 3rd International Conference on Cognitive Radio Oriented Wireless Networks and Communications (CrownCom)*, Singapore, May 15–17, 2008.

(V) J. Lundén, S. A. Kassam and V. Koivunen, "Robust nonparametric cyclic correlation based spectrum sensing for cognitive radio," *IEEE Transactions on Signal Processing*, 2009, to appear.

(VI) J. Lundén, L. Terho and V. Koivunen, "Classifying pulse compression radar waveforms using time-frequency distributions," in *Proceedings of the 39th Annual Conference on Information Sciences and Systems (CISS)*, Baltimore, USA, March 16–18, 2005.

(VII) J. Lundén, L. Terho and V. Koivunen, "Waveform recognition in pulse compression radar systems," in *Proceedings of the IEEE International Workshop on Machine Learning for Signal Processing (MLSP)*, Mystic, CT, USA, September 28–30, 2005, pp. 271–276.

(VIII) J. Lundén and V. Koivunen, "Automatic radar waveform recognition," *IEEE Journal of Selected Topics in Signal Processing*, vol. 1, no. 1, pp. 124–136, June 2007.

(IX) J. Lundén and V. Koivunen, "Robust estimation of radar pulse modulation," in *Proceedings of the 6th IEEE International Symposium on*

Signal Processing and Information Technology (ISSPIT), Vancouver, Canada, August 27–30, 2006, pp. 271–276.

(X) J. Lundén and V. Koivunen, "Scaled conjugate gradient method for radar pulse modulation estimation," in *Proceedings of the IEEE International Conference on Acoustics, Speech, and Signal Processing (ICASSP)*, Honolulu, HI, USA, April 15–20, 2007, vol. 2, pp. 297–300.

List of abbreviations

AD	atomic decomposition
ADC	analog-to-digital converter
ATSC	advanced television systems committee
AWGN	additive white Gaussian noise
BPSK	binary phase shift keying
BSC	binary-symmetric channel
BW	bandwidth
cdf	cumulative density function
CDMA	code division multiple access
CFAR	constant false alarm rate
CUSUM	cumulative sum
CWD	Choi-Williams distribution
DTV	digital television
DVB-T	digital video broadcasting — terrestrial
DWT	discrete wavelet transform
EM	expectation maximization
ES	electronic support
ESC	early-stop committee
FAM	FFT accumulation method
FCC	Federal Communications Commission
FD	frequency diversity
FFT	fast Fourier transform
FM	frequency modulation
FSK	frequency shift keying
GLR	generalized likelihood ratio
GLRT	generalized likelihood ratio test
GPS	global positioning system
IEEE	Institute of Electrical and Electronics Engineers
i.i.d.	independent and identically distributed
IPFE	intrapulse frequency encoding
IRLS	iterative reweighted least-squares
I/Q	in-phase/quadrature
ISM	industrial, scientific, and medical
LAN	local area network
LDA	linear discriminant analysis
LFM	linear frequency modulation
LPI	low probability of intercept
LR	likelihood ratio
LRT	likelihood ratio test

MAC	medium access control
MDL	minimum description length
ML	maximum likelihood
MLP	multilayer perceptron
NIC	network interface card
NLFM	nonlinear frequency modulation
NP	Neyman-Pearson
OFDM	orthogonal frequency division multiplexing
PCA	principal component analysis
pdf	probability density function
PN	pseudo-random number
POMDP	partially observable Markov decision process
PSD	power spectral density
PSK	phase shift keying
PWVD	pseudo Wigner-Ville distribution
QMFB	quadrature mirror filter banks
QPSK	quadrature phase shift keying
RF	radio frequency
SCG	scaled conjugate gradient
SNR	signal-to-noise ratio
SOM	self-organizing map
SPRT	sequential probability ratio test
STFT	short time Fourier transform
SU	secondary user
SVM	support vector machine
TV	television
UMTS	universal mobile telecommunications system
UWB	ultra-wideband
VHF	very high frequency
WiMAX	worldwide interoperability for microwave access
WLAN	wireless local area network
WV	Wigner-Ville

List of symbols

$\mathcal{A}$	set
$\boldsymbol{A}$	matrix
$\boldsymbol{A}^{-1}$	inverse of matrix $\boldsymbol{A}$
$\boldsymbol{A}^{T}$	transpose of matrix $\boldsymbol{A}$
A_{mn}	(m,n) element of matrix $\boldsymbol{A}$
χ^2_N	central chi-square distribution with N degrees of freedom
$\chi^2_N(\gamma)$	non-central chi-square distribution with N degrees of freedom and non-centrality parameter γ
$e^{(\cdot)}, \exp(\cdot)$	exponential function
$E[\cdot]$	expectation operator
H_0	null hypothesis
H_1	alternative hypothesis
$\mathrm{Im}\{x\}$	imaginary part of x
j	imaginary unit
n	discrete time index
$o_p(1)$	quantity that converges in probability to zero
$p(\cdot)$	probability
$\mathbb{R}$	the set of real numbers
$R_s^{\alpha}(\cdot)$	cyclic autocorrelation function of signal s at cyclic frequency α
$\mathrm{Re}\{x\}$	real part of x
$S_s^{\alpha}(\cdot)$	spectral correlation function of signal s at cyclic frequency α
t	continuous time index
τ	time delay
$\mathrm{tr}(\boldsymbol{A})$	trace of a matrix $\boldsymbol{A}$
$\mathrm{Var}(\cdot)$	variance operator
$\hat{x}$	estimate of x, signified by the use of a caret (hat)
$\lvert x \rvert$	modulus of scalar x
$\lvert\lvert \boldsymbol{x} \rvert\rvert$	Euclidean norm of vector $\boldsymbol{x}$
$\boldsymbol{x}^T$	transpose of vector $\boldsymbol{x}$
$\boldsymbol{x}^H$	conjugate transpose of vector $\boldsymbol{x}$
$\boldsymbol{x}_n$	nth vector in a sample
$x_{n,r}$	real part of the nth element of vector $\boldsymbol{x}$
$x_{n,i}$	imaginary part of the nth element of $\boldsymbol{x}$
$\frac{\partial \boldsymbol{x}}{\partial \boldsymbol{\theta}}$	derivative of $\boldsymbol{x}$ with respect to $\boldsymbol{\theta}$
$\stackrel{D}{=}, \xrightarrow{D}$	convergence in distribution

$\xrightarrow{P}$	convergence in probability
$\sim$	distributed as
$\in$	symbol for "belongs to"
$\forall$	symbol for "for all"
$\cup$	symbol for "union of"

Chapter 1

Introduction

1.1 Motivation

Wireless communications and the utilization of the radio frequency spectrum have witnessed a tremendous boom during the past few decades. The multitude of different wireless devices and technologies, the dramatic increases in the number of wireless subscribers, the advent of new applications, and the continuous demand for higher data rates are all reasons for the radio frequency spectrum becoming more and more crowded. This development calls for systems and devices that are aware of their surrounding radio environment, hence, facilitating flexible, efficient, and reliable operation and utilization of the available spectral resources. Wireless communication and radar systems must collect information about the radio spectrum in order to adapt their operation and behavior to provide a better match to the prevailing conditions. Thus, spectrum sensing is becoming increasingly important to modern and future wireless communication and radar systems for identifying underutilized spectrum and characterizing interference, and consequently, achieving reliable and efficient operation.

Cognitive radio is a term coined by Mitola [1, 2] that refers to an intelligent radio that is aware of its surrounding environment. Moreover, a cognitive radio is capable of learning and adapting its behavior and operation to provide a better match to its surrounding environment as well as to the user's needs. Learning is based on the feedback received from the environment. The feedback is realized as the outcome of the cognitive radio's decisions and actions.

Currently, the most prominent application area of cognitive radios is dynamic spectrum access. The current spectrum regulation is based on a fixed frequency allocation policy. The frequency spectrum is divided to frequency bands with each frequency band allocated to a certain wireless system in a rigid manner. The result is a very uneven spectrum utilization that varies heavily depending on frequency, time, and spatial location. Hence, there

is a demand for more flexible and efficient utilization of the available spectral resources. This can be accomplished with dynamic spectrum access. In order to access the spectrum in dynamic fashion the cognitive radios need to sense the spectrum to identify spectrum opportunities and to avoid interfering with the licensed primary users.

In addition to dynamic spectrum access, spectrum sensing techniques are important in both civilian and military spectrum management operations. Typical civilian spectrum management applications may include, e.g., traffic analysis as well as detection, identification, and characterization of interference sources. With the increasing use of the radio frequency spectrum, the importance of automatic waveform or modulation recognition as well as signal and emitter identification systems is emphasized. In military applications spectrum sensing techniques are employed by systems such as cognitive radars and intercept receivers. Automatic waveform recognition and specific emitter identification are examples of electronic intelligence that has become an integral part of modern military operations. Applications such as signal reconnaissance as well as threat recognition and analysis are essential for building situational awareness.

Another potential major application of spectrum sensing and emitter identification techniques is wireless security. Specific emitter identification and radio frequency (RF) fingerprinting techniques enable the discrimination of rogue devices from the legitimate ones. For example, RF fingerprinting has been used for detecting phone cloning fraud in cellular networks [3]. Consequently, spectrum sensing and identification techniques may be used for spectrum monitoring by wireless operators and agencies in change of frequency allocation and for improving wireless security.

1.2 Scope of the thesis

The first goal of this thesis is to develop reliable detection algorithms and methods for spectrum sensing for cognitive radio and dynamic spectrum access. The objective is to develop algorithms that require minimal knowledge about the detected signals while still possessing the capability to distinguish among different signals, i.e., signals of interest and interference. The algorithms should be robust to noise uncertainties, non-idealities, and deviations from model assumptions, such as the assumed noise model. Collaborative energy efficient detection approaches and techniques are developed. Collaboration among spatially dispersed secondary users extracts spatial diversity, thus, improving the performance and reliability in the face of shadowing and fading effects. In addition, collaboration allows employing simpler local individual detectors and/or shorter detection time. The discussion in this thesis is limited to detection in the physical layer and to collaborative scenarios where a group of secondary users are trying to detect whether the

primary user is active or not in a single given frequency band. That is, sensing policies, how to distribute the sensing work among the secondary users in different locations to different frequency bands at different times, are not considered in this thesis.

The second goal of this thesis is to develop a radar waveform classification system for classifying common pulse compression waveforms based on spectrum sensing. The discussion is limited to pulsed radar systems and radar waveform recognition. The considered pulse compression waveforms are: linear frequency modulation, Costas frequency codes, binary codes, as well as Frank, P1, P2, P3, and P4 polyphase codes. A review of modulation recognition of communication signals may be found in [4]. The focus is aimed at developing classification methods, hence, detection is assumed to be successfully performed. The objective is to develop a classification method that performs reliable classification independently for each intercepted pulse. Waveform classification is used for characterizing the emitters. Such information is important in both civilian and military spectrum management applications.

The third goal of this thesis is to develop spectrum sensing methods for specific emitter identification. The discussion in this thesis is limited to identifying a specific radar emitter operating in a single mode. That is, tracking the modes of multifunction radars is not considered. RF fingerprinting literature related to identifying communication devices is reviewed in the thesis; however, the proposed identification algorithms are aimed at radar signals. Moreover, only pulsed radar signals are considered. The goal is to develop general, yet reliable identification methods that do not require any prior information about the intercepted emitters but may apply multiple pulses to identify the emitter or estimate its modulation profile for future identification.

1.3 Contributions of the thesis

The contributions of this thesis are in three fields related to spectrum sensing: signal detection, waveform classification, and signal identification.

The contributions of the thesis to signal detection and spectrum sensing for cognitive radios are listed as follows.

- A multicycle detector requiring minimal prior knowledge of the primary system is proposed. The asymptotic distributions of the detector are established. Two simplified detectors based on the sum and maximum over the cyclic frequencies of interest are proposed as well. The asymptotic distributions of these two detectors under the null hypothesis are established. The use of multiple cyclic frequencies improves the performance compared to single-cycle detector when the signal has multiple strong cyclic frequencies.

- Robust spatial sign cyclic correlation based fixed sample size and sequential detectors are proposed. The asymptotic distribution of the fixed sample size detector under the null hypothesis is established and an upper bound for the false alarm rate of the sequential detector is derived. The asymptotic relative efficiency of the spatial sign cyclic correlation based detector compared to the single-cycle detector of [5] is derived. The proposed spatial sign cyclic correlation based detector has highly reliable performance in heavy-tailed non-Gaussian noise experienced commonly in wireless communication systems.

- Collaborative detection tests for the cooperation of multiple secondary users are proposed. The asymptotic distributions under the null hypothesis are established. Collaboration among spatially dispersed secondary users extracts diversity gain, thus, mitigating the effects of shadowing and multipath fading. Hence, collaboration allows using simpler local detectors and/or shorter detection times.

- A censoring scheme for improving the energy efficiency of collaborative detection is introduced. Censoring denotes a scheme where only informative local test statistics are transmitted to the fusion center. A technique for approximating the asymptotic distribution of the censoring test statistic under the null hypothesis by numerically inverting the characteristic function of the test statistic is derived. The proposed scheme results in only a minimal loss in performance compared to uncensored collaborative detection even under very strict communication rate constraints. That is, the proposed censoring scheme improves the energy efficiency significantly with only a minimal loss in performance.

The contributions of this thesis to radar waveform recognition are as follows.

- A radar waveform recognition system for classifying intercepted radar pulses to eight classes based on the pulse compression waveform is developed. The considered classes are: linear frequency modulation, Costas frequency codes, binary codes, as well as Frank, P1, P2, P3, and P4 polyphase codes.

- A supervised waveform classifier structure consisting of two parallel multilayer perceptron (MLP) networks is proposed. Two different MLP classifiers, the ensemble averaging early-stop committee and the Bayesian MLP, are compared.

- Novel features based on the Wigner and Choi-Williams time-frequency distributions are proposed. In addition, a large set of features gathered from communication signal modulation recognition literature are considered. The final feature vectors are selected using a mutual information based feature selection algorithm.

- The proposed classification system has highly reliable performance: the overall correct classification rate exceeds 98 % at SNR of 6 dB on data similar to the training data.

The contributions of this thesis to radar emitter identification are listed below.

- A robust M-estimation method for estimating a common modulation from a group of intercepted radar pulses is proposed. An iterative reweighted least-squares procedure is derived with two different weighting strategies. A gradient based algorithm is proposed for improving the frequency alignment of the intercepted pulses.
- A robust likelihood ratio-type test is proposed for radar emitter identification. The asymptotic distribution of the proposed test statistic under the null hypothesis is established. The proposed robust likelihood ratio-type test has very good resolution for distinguishing among emitters with similar modulation profiles.

1.4 Summary of the publications and the structure of the thesis

This thesis consists of an introductory part and ten original publications. The introductory part is organized as follows. Chapter 2 reviews spectrum sensing methods for dynamic spectrum access and cognitive radio. In addition, the cyclostationarity-based spectrum sensing algorithms proposed in Publications I-V are briefly described. Chapter 3 provides a literature review of radar waveform classification. Moreover, the radar waveform classification system proposed in Publications VI-VIII is summarized in Chapter 3. Chapter 4 reviews specific emitter identification and RF fingerprinting methods. The robust M-estimation method for estimating a common modulation from a group of intercepted radar pulses proposed in Publications IX and X is introduced in Chapter 4 as well. The system model is presented and a robust likelihood-ratio type test is proposed for radar emitter identification. Finally, Chapter 5 provides the concluding remarks.

In Publication I, multicycle detectors for single-user and collaborative spectrum sensing for cognitive radio systems have been proposed. The asymptotic distributions of the proposed test statistics under the null hypothesis have been established. Simulation results illustrating the very good performance of the proposed methods have been provided.

A censoring scheme for improving the energy efficiency of collaborative spectrum sensing has been proposed in Publication II. Simulation results demonstrating the reliable and close to ideal performance even under very strict communication rate constraints have been provided.

In Publication III, the methods proposed in Publications I and II have been further extended to more general situations. The asymptotic distribution of the proposed multicycle detector under the alternative hypothesis has been established. Extensive simulations have been provided to illustrate the highly reliable performance of the proposed methods even in very low signal-to-noise ratio (SNR) regimes and in the face of shadowing and fading.

A robust spatial sign cyclic correlation based detector has been proposed in Publication IV. The asymptotic distribution of the proposed detector under the null hypothesis has been derived and simulation examples demonstrating the robust performance of the proposed detector in heavy-tailed non-Gaussian noise have been provided.

In Publication V, the asymptotic relative efficiency of the spatial sign cyclic correlation detector proposed in Publication IV compared to the single-cycle detector of [5] has been derived. A sequential detection test based on the spatial sign cyclic correlation has been proposed. The proposed sequential detection test reduces detection times significantly compared to the fixed sample size test with roughly the same performance. Extensive simulation experiments illustrating the robust performance of the proposed spatial sign cyclic correlation detector in heavy-tailed non-Gaussian noise have been presented.

In Publication VI, a time-frequency distribution based supervised classification system for classifying the Frank, P1, P2, P3, and P4 polyphase pulse compression radar waveforms has been introduced. Choi-Williams distribution based features as well as a symmetry based cross-correlation feature have been proposed. The reliable classification performance has been demonstrated through simulation experiments.

The classification system proposed in Publication VI has been extended to other waveforms in addition to polyphase codes in Publication VII. The additional waveform classes that have been considered are the linear frequency modulation, Costas discrete frequency codes, and binary phase codes. A parallel classifier structure consisting of two parallel MLP networks has been proposed. In addition to the features proposed in Publication VI, a large set of features from modulation recognition literature have been collected and adapted to radar waveform recognition. Simulation results showing the highly reliable classification performance of the proposed system even at relatively low SNRs have been presented.

In Publication VIII, the classification system proposed in Publications VI and VII has been further improved. Wigner distribution based features have been proposed for improving the reliability of the classification. Extensive simulation experiments have been provided to demonstrate the highly reliable performance of the proposed classification system.

A robust M-estimation method for estimating a common modulation from a group intercepted radar pulses has been proposed in Publication IX. Two M-estimators using an iterative reweighted least-squares procedure

with different weighting schemes have been introduced. Simulation results highlighting the robustness of the proposed M-estimation technique against preprocessing errors and non-Gaussian noise have been provided.

In Publication X, the robust M-estimators proposed in Publication IX have been further improved by using the scaled conjugate gradient algorithm to improve the frequency alignment of the intercepted pulses. Simulation examples demonstrating the improved performance have been presented.

In Publication I, the author of this thesis proposed the final version of the algorithms, derived the asymptotic distributions of all detectors, as well as performed the simulation experiments. The co-authors contributed the idea for the multicycle sum detector as well as contributed in steering the research and helped writing the publication.

In Publication II, the author of this thesis proposed the final versions of the test statistics, derived the numerical approximation method for the asymptotic distributions of the censoring test statistics, as well as performed all the simulations. The initial idea and development of the censoring tests was done by the co-authors. In addition, the co-authors helped writing the publication.

The novel results in Publication III were derived by the author of this thesis. The co-authors helped in steering the research and writing the publication.

In Publications IV and V, the results and methods were derived by the author of this thesis. The co-authors provided guidance during the work and helped writing the publications.

The results in Publications VI and VII were derived by the author of this thesis. The co-authors contributed in steering the research and writing the publications.

In Publication VII, the author of this thesis derived most of the algorithms, features, as well as the other results. The co-author provided the idea for the statistical runs test feature, helped writing the publication, as well as provided guidance during the research work.

The results in Publications IX and X as well as the novel identification test in Chapter 4 have been derived by the author of this thesis. The co-author provided guidance during the development of the algorithms and contributed to the writing of the publications.

Chapter 2

Spectrum sensing techniques for cognitive radio systems

Current spectrum regulation is based on a fixed frequency allocation policy. The radio frequency spectrum is divided to frequency bands that are then allocated to different systems. The allocations are decided by the regulatory authorities in each country such as the Federal Communications Commission (FCC) in the United States. Most of the spectrum has already been allocated to different systems. Moreover, the allocations vary from country to country. Whenever a new wireless system is introduced a frequency band needs to be made available for it, which may require worldwide collaboration. Hence, although the current frequency allocation policy guarantees low interference because each system operates in a different band, it is also very rigid and inflexible. This has resulted in apparent spectrum scarcity that realizes as heavy congestion in certain frequency bands. However, many of the frequency bands have been allocated to legacy systems that are rarely used or to systems whose degree of frequency band utilization varies sharply from time to time and location to location. Hence, there is still plenty of spectrum available. Merely because of the fixed frequency allocation policy it cannot be exploited. Consequently, the radio frequency spectrum is very inefficiently utilized depending on time, frequency band, and location. Hence, there is an increasing need for more dynamic way of utilizing the radio frequency spectrum. Dynamic spectrum access provides a flexible way of utilizing the available resources more evenly.

Dynamic spectrum access may be broadly categorized under three different models [6]: dynamic exclusive use model, spectrum commons model, and hierarchical access model. Similar categorization with slightly different terminology and more subcategories for the three main models has been given in [7] as well. The dynamic exclusive use model maintains the current spectrum allocation structure where frequency bands are licensed to different systems for exclusive use. The difference is that the spectrum is al-

located in more dynamic manner either by using spatial and temporal traffic analysis or by allowing the licensees to lease out and trade spectrum. For more information, see the discussion and references in [6, 7].

The spectrum commons model refers to a concept found successful in the unlicensed industrial, scientific, and medical (ISM) bands where different users share the spectrum, for example, by competing equally for the available resources in a fair manner. The spectrum commons model entails both the fully open sharing model, where the spectrum is unowned and access is available to anyone, as well as managed commons where the spectrum is owned and controlled, for example, by a group of entities [7]. In managed commons there are stronger restrictions and rules on how to use the spectrum than under the open sharing model. For a more detailed discussion of the spectrum commons model, see [6–8] and the references therein.

The hierarchical access model adopts the current structure, where frequency bands are licensed to different primary systems, and opens the licensed spectrum to secondary users. The access by secondary users is allowed under the condition that the interference caused to the primary systems is maintained below an allowed level. The allowed level of interference is defined by the regulating bodies. The hierarchical access model may be subdivided to spectrum overlay and spectrum underlay approaches [6]. Spectrum underlay is based on ultra-wideband (UWB) devices that operate at short ranges with low transmit powers. By imposing severe constraints on the allowed transmit powers, the interference caused to the primary systems is maintained at low level. Hence, there is no need for spectrum sensing in spectrum underlay. As opposed to spectrum underlay, spectrum overlay is based on the cognitive radios sensing the spectrum in order to find spectrum opportunities. Hence, rather than imposing severe constraints on transmit powers, the interference caused to the primary users is kept below the allowed level by the secondary users' ability to identify through sensing when the spectrum is unoccupied and thus may be utilized. In this thesis, we focus on the spectrum overlay approach, referred to as opportunistic spectrum access in the literature as well. Moreover, we focus on spectrum sensing and more precisely on spectrum sensing in the physical layer. However, first we briefly discuss the other main challenges faced by the cognitive radios in obtaining awareness of the state of the radio spectrum and achieving dynamic spectrum access.

Fig. 2.1 presents a network of cognitive radios operating in the midst of licensed primary systems. The operation of a cognitive radio for dynamic spectrum access consists of two main components: spectrum sensing and spectrum opportunity exploitation.

Due to hardware limitations and energy constraints, a cognitive radio may not be able to sense the whole spectrum simultaneously. Hence, a sensing policy that defines when and which frequency band to sense must be implemented. Sensing policy may be implemented either individually

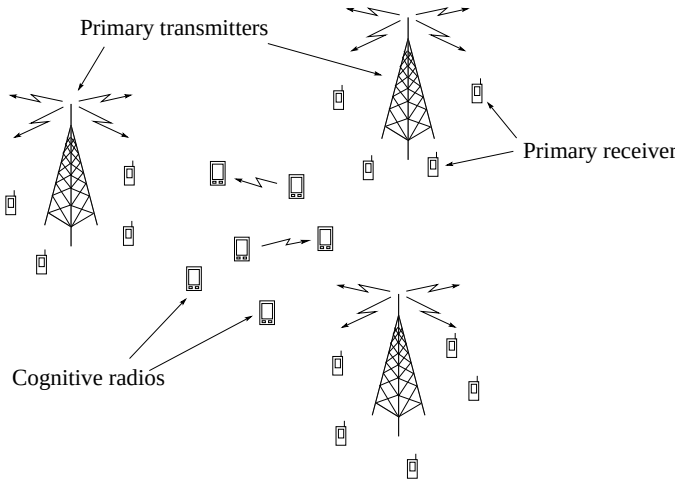

Figure 2.1: A network of cognitive radios. The cognitive radios sense the radio frequency spectrum for spectrum opportunities and exploit them in an agile manner.

or collaboratively. Note that here we assume that the sensing periods are already synchronized among different cognitive radios. This is necessary because simultaneous transmission and sensing on the same frequency band is not in general possible. The sensing policy defines whether a cognitive radio performs sensing in a given sensing period and, if so, which channel or channels it senses. It is expected that collaborative sensing policies offer benefits over individually selected policies in scenarios where the users perform collaborative sensing in the physical layer as well. This is due to a guaranteed "diversity order" by the collaborative policies, i.e., it can be guaranteed that there are multiple spatially dispersed cognitive radios sensing the same band simultaneously. Individual sensing policies using a decision-theoretic approach by formulating the design of optimal sensing policy as a partially observable Markov decision process (POMDP) have been proposed in [9–11]. Myopic sensing policies that seek at maximizing the immediate reward have been analyzed in [12, 13].

After sensing the spectrum and finding spectral opportunities, the cognitive radios need to decide their access policy in order to exploit the available opportunities. Access policy answers question such as when and on which channels to transmit or whether to transmit at all in order to conserve the energy of battery-operated terminals if the channel quality is bad. Similarly as sensing policy, access policy can be individually or collectively decided as well. An integral part of spectrum exploitation is also interference management. The cognitive radio system must ensure that its combined interference caused to the primary systems stays within the bounds set by the regulatory bodies.

Sensing and access policies are closely connected to each other. For example, if it is noticed that the throughput on a certain frequency band is constantly very low, there may not be any reason to sense that frequency band either. That is, it is desirable to sense bands where persistent spectral resources are available. Or if the cognitive user does not expect to transmit anything in the near future, it may be wise to refrain from sensing as well in order to conserve energy. Moreover, both sensing policy and access policy are areas where cognition most naturally comes into play. In dynamic signal environments techniques such as reinforcement learning [14, 15] have great potential for achieving the most efficient utilization of the available resources [16, 17]. The feedback from the past decisions and actions may be used to learn the state of the environment and thus enable making better decisions in the future.

In addition to the above issues, there are several other issues that cognitive radios need to resolve such as employed modulation formats, transmit powers, routing issues, etc. Moreover, in addition to the technological challenges, there are regulatory challenges that have to be met. Regulatory policies that define the rules for opportunistic spectrum access have to be established and it must be ensured that the cognitive radios conform to the established rules.

In the following, an overview of spectrum sensing methods and algorithms for cognitive radios is presented. However, first a short discussion of the main challenges, requirements, and techniques of physical layer spectrum sensing is given.

2.1 Spectrum sensing challenges, requirements, and techniques

Opportunistic spectrum access by the secondary users is inherently dictated by the characteristics and operation of the primary users. The primary users have the privileged access to the frequency band for which they possess a license. Hence, the secondary users must guarantee their ability to share the spectrum while maintaining the interference caused to the primary users at an acceptable level. General treatments discussing the requirements and implementation issues of spectrum sensing may be found in [18–20]. In the following few of the most important concepts regarding spectrum sensing and opportunistic spectrum use are briefly discussed.

Interference temperature concept has been introduced by the FCC as a model for measuring and limiting interference in wireless communications [19, 21–23]. Fig. 2.2 illustrates two possible realizations of the interference temperature concept. The idea is that each primary receiver has an interference temperature limit that defines how much noise and interference it can tolerate. This opens up opportunities for secondary users that

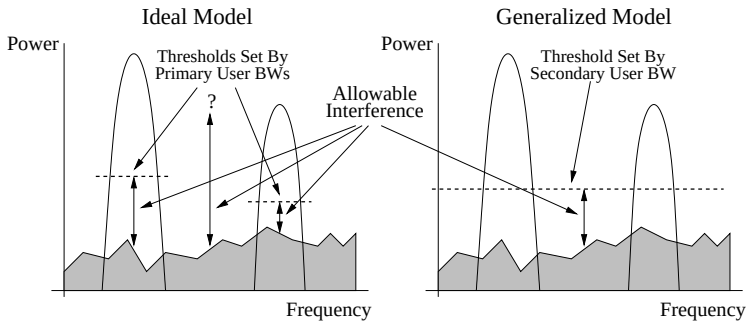

Figure 2.2: Interference temperature model: (a) ideal and (b) generalized interpretations [23]. The generalized model applies to a situation where there is no prior knowledge of the possible primary systems.

are consequently allowed to transmit provided that the interference their transmissions cause to the primary receivers do not increase the interference temperature above the limit. However, the problem arises from measuring the interference temperature at the primary receivers which may be infeasible in practice [19]. The interference temperature concept has been recently abandoned by the FCC as unworkable [24].

A more practical opportunistic access concept relies on secondary users identifying frequency bands unused by the primary users and transmitting at those frequency bands until a primary user becomes active. Such a frequency band or channel is called a spectrum opportunity [6, 25, 26]. Spectrum opportunity is a local concept that may be defined as follows [25]: *A channel is an opportunity to a secondary transmitter A and secondary receiver B if they can communicate successfully over this channel while limiting the interference to primary users below a prescribed level determined by the regulatory policy.*

Fig. 2.3 illustrates the spectrum opportunity concept. A spectrum opportunity means that there are no primary receivers that would be interfered by the secondary transmitter A transmitting and no primary transmitters that would interfere the secondary receiver B from receiving in the same band at the same time.

The inherent requirement is that the secondary users must vacate the spectrum as quickly as possible when the primary user appears. Moreover, in order to guarantee low-interference operation of the primary users, the detection sensitivity of the cognitive radio users has to be very high. Note that some interference must be tolerated otherwise opportunistic access based on spectrum sensing is not possible.

The interference takes place at the primary receivers. However, the sensing problem is typically formulated as detecting primary transmitters instead of primary receivers. In practice, this is the only feasible option if

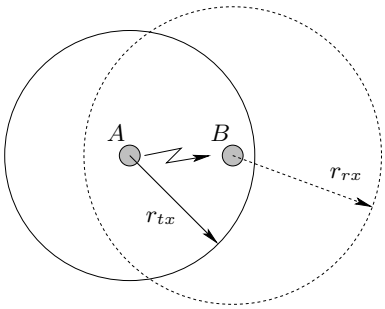

Figure 2.3: A spectrum opportunity exists if there are no primary receivers within a distance of r_{tx} from the secondary transmitter A and no primary transmitters within a distance of r_{rx} from the secondary receiver B where r_{tx} is the interference range of A and r_{rx} is the interference range of the primary transmitters [6, 25, 26].

the primary receivers are passive. This is the case, for example, in broadcast systems such as the DVB-T (digital video broadcasting — terrestrial). Detecting the primary transmitters from a far enough distance that considerably exceeds the primary system's operation range allows protection of primary receivers. Moreover, the detection has to be performed reliably in highly varying propagation environments in the face of shadowing and multipath fading effects, as well as challenging, possibly heavy-tailed, noise and interference environments. This requires very high sensitivity from the cognitive radios. Fig. 2.4 illustrates spectrum opportunity detection through detecting primary transmitters.

There are multiple ways to improve the detection sensitivity of a cognitive radio network. The sensitivity of the cognitive radios may be improved by enhancing the cognitive radio's RF front-end sensitivity, designing and employing powerful signal processing algorithms well-suited for the task, as well as by exploiting spatial diversity through collaborative sensing among multiple cognitive radios.

Another important consideration for the cognitive radios is the sensing policy that includes decisions such as when and how long to sense, and which frequency band to sense. In order to maximize performance, the sensing policies should be coordinated among the secondary users. Simultaneous transmission and sensing on a given frequency is not possible in general. Hence, sensing and transmission have to be done in an alternating manner. Moreover, the sensing periods must be synchronized among the cognitive radios. Ideally a cognitive radio user wants to minimize the time required for identifying spectral opportunities in order to maximize the time available for transmission. Different primary systems impose different constraints for sensing. For example, broadcast TV systems that typically operate continuously for hours may tolerate a longer interference period at

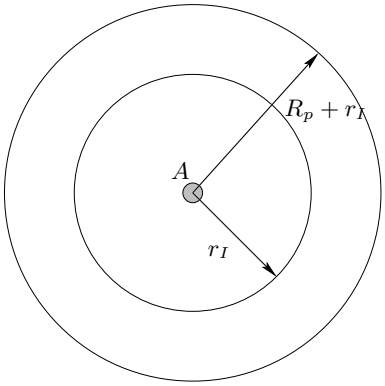

Figure 2.4: A conservative approach to spectrum opportunity detection that transforms the spectrum sensing problem to detecting the primary transmitters: The secondary transmitter A can determine that a channel is available if there are no primary transmitters within a distance of $R_p + r_I$ where R_p is the transmission range of the primary transmitter and r_I is the interference range of the secondary transmitter.

the beginning of their transmission than burstier cellular phone or wireless LAN traffic, for example. Hence, one of the questions that regulators must address is how quickly must the secondary users vacate the channel after the primary user's activity starts.

In addition to sensing, cognitive radios may benefit from using geolocation information for avoiding primary systems and managing interference [27]. Geolocation database consisting of primary transmitter geolocations and employed channels would enable the cognitive radio that is aware of its own geolocation to avoid using those bands whenever the primary user could potentially be interfered by the secondary user's transmissions. The cognitive radio may determine its geolocation using global positioning system (GPS) or through other means, such as cell tower or Wi-Fi access point based positioning or through mutual ranging of radios. Note that only relative locations may be obtained through mutual ranging, thus, one of the radios has to be aware of its geolocation and pass that information to the other radios as well. Such a node is called an anchor node. For static applications, such as the digital television broadcasts, the geolocation information of the transmitters is already available or may be easily obtained. In more dynamic applications, where radios may be mobile, additional benefits would be obtained by using a geolocation database that would be constantly updated by the licensed systems. The cognitive users would need to query the database frequently for updated information. Moreover, a geolocation based system as well as any other cognitive radio system would greatly benefit from knowledge about the local propagation environment and propagation statistics when estimating the interference caused to the primary

systems.

Another possible protection mechanism for the primary systems would be to use beacons [27]. Beacons might be either transmitter beacons or area beacons. Area beacons could provide a service announcing the frequency band, location, and coverage area of each primary system in the area [27]. A more elaborate discussion of issues and benefits of using geolocation databases and beacons for enabling opportunistic spectrum use may be found in [27].

However, both the application of beacons as well as the form of geolocation databases that require primary system updates has the obvious drawback that under the current spectrum regulation the primary systems have no requirement to change their infrastructure to enable coexistence with secondary opportunistic users. Hence, no help from the primary systems can be expected unless it is forced by the regulating bodies or if the flexible spectrum use is coordinated by the primary systems.

In the following sections, an overview of spectrum sensing algorithms and collaborative detection techniques proposed in the literature is presented. Moreover, cyclostationarity-based spectrum sensing algorithms proposed in Publications I-V are briefly presented. Detailed descriptions may be found in Publications I-V.

The spectrum sensing algorithms proposed in the literature may be broadly divided to three classes: matched filters, energy based detectors, and feature detectors. This categorization is used in the following. Moreover, the detection problem may be formulated as a binary hypothesis test

$$\begin{aligned} H_0 : &\quad x(t) = n(t) \\ H_1 : &\quad x(t) = s(t) + n(t) \end{aligned} \tag{2.1}$$

where $x(t)$ and $n(t)$ denote the received signal and the noise, respectively, and $s(t)$ denotes the signal to be detected.

In a binary hypothesis test there are two types of errors that can be made. These errors are called type I and type II errors, respectively. A type I error is made if H_1 is accepted when H_0 is true. The probability of making a type I error is often called the probability of false alarm. In spectrum sensing the probability of false alarm of a detector is an important design parameter since false alarms lead to overlooking spectral opportunities. A type II error is made if H_0 is accepted when H_1 is true. Type II errors are a result of a missed detection and hence lead to collisions with primary transmissions and reduced rate for both the primary system and the secondary system.

In general, a cognitive radio system should satisfy constraints on both the probability of false alarm and the probability of miss detection. Designing a detection rule presents a trade-off between these two probabilities. However, provided that the detector behaves reasonably, i.e. the probability of error (the probability of false alarm + the probability of miss detection) decreases

as the number of samples increases, both constraints may be satisfied by selecting the number of samples to be large enough. From the implementation point of view it is desirable to have algorithms whose threshold may be set analytically and whose performance may be analyzed analytically. However, in practice especially the probability of detection and the number of samples required to achieve a given probability of detection will most likely have to be determined experimentally due to the large number of variables, such as the fading channel, synchronization errors, noise power uncertainty, etc., affecting their values.

2.2 Matched filter

Matched filter is the optimum detector of a known signal in the presence of additive Gaussian noise. It is the linear filter that maximizes the SNR of the output. The output of the matched filter is given by

$$y = \boldsymbol{s}^H \boldsymbol{\Sigma}_n^{-1} \boldsymbol{x} \tag{2.2}$$

where $\boldsymbol{x}$ is the observation vector, $\boldsymbol{s}$ is the known deterministic signal to be detected, and $\boldsymbol{\Sigma}_n$ is the noise covariance matrix.

Assuming that the noise is Gaussian it follows that the output y is Gaussian as well since it is a linear transformation of a Gaussian random vector. The mean of y is zero under H_0 and $\boldsymbol{s}^H \boldsymbol{\Sigma}_n^{-1} \boldsymbol{s}$ under H_1. The variance is $\boldsymbol{s}^H \boldsymbol{\Sigma}_n^{-1} \boldsymbol{s}$ under both hypotheses. Consequently, the hypothesis test may be defined as $y \underset{H_0}{\overset{H_1}{\gtrless}} \lambda$ where λ is the test threshold selected to obtain a specified false alarm rate.

From (2.2) it can be seen that the matched filter requires explicit knowledge of the transmitted signal $\boldsymbol{s}$ and the noise covariance matrix $\boldsymbol{\Sigma}_n$. Hence, the usability of the matched filter is limited to cases where explicit information about the waveform such as pilot signals or preambles is known. In addition, the performance may severely deteriorate with synchronization errors. Experimental measurements of matched filter pilot detection performance with synchronization errors (frequency offset) have been provided in [28,29]. In [30], an entropy-based matched filter method is proposed. The proposed detector compares the estimated entropy of the matched filter output to a threshold. The method can be applied when the variance of the assumed Gaussian noise is unknown.

2.2.1 ATSC field sync detectors

Coherent detectors for ATSC DTV (Advanced Television Systems Committee, digital television standard in North America) signals employing the field sync segment have been proposed in [31, 32]. The field sync segment

includes a known 511 symbol pseudo-random number (PN) sequence that can be employed for detection. Detection times required for the field sync detectors are typically relatively long since the field sync is inserted to the data stream only every 24.2 ms. Asymptotic distribution of the field sync correlation detector under the null hypothesis has been established in [33]. The probability of detection at SNR of -13 dB exceeds 99 % for a false alarm rate of 10 % in good channel conditions [33].

2.3 Energy based detection

2.3.1 Energy detector

Energy detector (or radiometer) measures the received energy and compares it to a threshold. The basic energy detector is given by [34]

$$y_M = \frac{2}{N_0} \sum_{n=1}^{M} |x(n)|^2, \tag{2.3}$$

where $x(n)$ is the received complex valued discrete time signal, N_0 is the noise power, and M is the number of observations. Factor 2 comes from the fact that under circularity assumption the complex noise power is equally divided between the real and imaginary parts. Fig. 2.5 depicts the block diagram of the energy detector.

Considering the detection of a deterministic signal in the presence of zero mean independent and identically distributed (i.i.d.) complex Gaussian noise, the energy detector test statistic obeys the following distribution [34]

$$\begin{aligned} H_0: &\quad y_M \sim \chi^2_{2M} \\ H_1: &\quad y_M \sim \chi^2_{2M}(2\gamma) \end{aligned} \tag{2.4}$$

where γ is the signal-energy-to-noise-spectral-density defined as $\gamma = E_S/N_0$ where $E_S = \sum_{n=1}^{M} |s(n)|^2$ is the signal energy. That is, the test statistic follows central chi-square distribution with $2M$ degrees of freedom under H_0 and non-central chi-square distribution with $2M$ degrees of freedom and non-centrality parameter 2γ under H_1.

Energy detection may be applied for the detection of unknown random signals. In fact, in case of i.i.d. Gaussian noise with known noise power the energy detector is the optimum detector for detecting a random uncorrelated Gaussian signal and at least a generalized likelihood ratio test (GLRT) for completely unknown random signals [35, 36]. Equation (2.4) holds for random signals as well assuming that the distribution under H_1 is considered to be a conditional distribution given the amount of signal energy [34]. Consequently, energy detection does not require any prior knowledge of the primary user signals. However, it has drawbacks as well. First, the energy

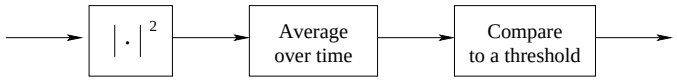

(a) Energy detector (radiometer)

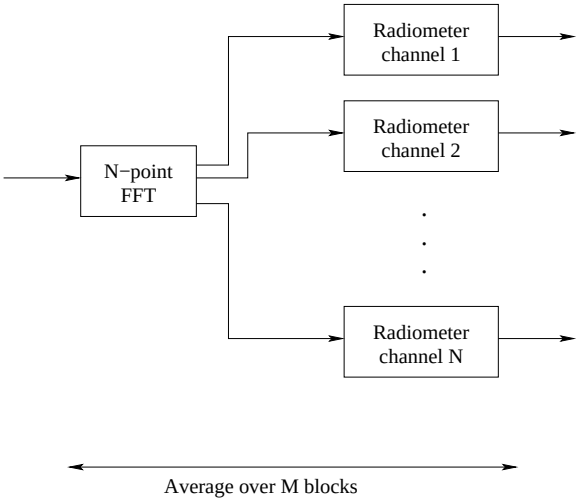

(b) Energy detector in frequency domain

Figure 2.5: Block diagram of (a) the basic energy detector and (b) an energy detector in frequency domain. Frequency domain energy detector may provide either a global decision or local decisions for each channel.

detector cannot distinguish among the primary user signals, secondary user signals, and interference. Second, energy detection is susceptible to uncertainty in noise power. Prior knowledge of noise power or a reliable estimate of it is needed to obtain reliable performance.

Noise level uncertainty renders robust detection below certain SNR impossible [37, 38]. To constrain the resulting false alarm rate, the detection threshold has to be set based on the worst case noise level uncertainty. Consequently, if the signal power is below a certain level, the energy detector cannot distinguish the signal from a slightly larger noise power regardless of the detection time. This threshold is called *the SNR wall* in [38]. For example, for a real-valued signal a 1 dB noise uncertainty renders robust detection below SNR of -3.3 dB impossible [38]. Consequently, the energy detector performance depends heavily on the accuracy and reliability of the noise level estimate. The noise level may be estimated from guard bands or the detection may be performed in the frequency domain using a channelized radiometer [39, 40] which divides the total frequency band to smaller channels and then integrates energy from each channel separately using a radiometer (see Fig. 2.5 (b) for a simple example). In the end a final global decision can be made for the whole frequency band by combining the radiometer outputs or decisions from the different channels (e.g., maximum or sum over outputs; sum or OR of decisions). If the noise bandwidth is significantly larger than the signal bandwidth, a reasonably accurate noise level estimate may be obtained. In addition, collaboration among secondary users that employ energy detection mitigates the effects of noise uncertainty when the users are experiencing i.i.d. fading or shadowing [41–43].

A review of energy based detection literature has been provided in [40]. In addition, constant false alarm rate (CFAR) strategies for the channelized radiometer, such as cell-averaging (see also [44]), have been considered in [40]. Recent performance analyses of energy detection in fading channels have been carried out in [41, 45–48] as well. Experimental measurements of energy detection performance with noise uncertainty have been provided in [28,29]. Energy detection of WiMAX systems for ultra-wideband/WiMAX coexistence has been considered in [49]. The detection of wireless microphone signals using the maximum of the frequency domain energy measurements has been proposed in [10]. Energy detectors have been proposed for colored Gaussian [50], independent non-Gaussian [36, 51], and colored non-Gaussian noise [36] as well.

2.3.2 Pilot energy detection for ATSC

Pilot energy detection algorithm for ATSC signals has been proposed in [52]. The received signal is first band-pass filtered around the pilot frequency. After the filtering, frequency domain energy detection is performed. The test statistic is the maximum squared fast Fourier transform (FFT) output

that is compared to a threshold.

2.3.3 Multi-resolution multiantenna energy detector

In [53], a multi-resolution multiple antenna energy detector for spectrum sensing has been proposed. The proposed multi-resolution detector performs the sensing first at a coarse frequency resolution. The fine resolution sensing that follows the coarse sensing is performed only for a small range of frequencies that have the smallest power in the coarse sensing stage. Using multiple antennas allows for faster sensing since in the coarse sensing stage each antenna block senses only a part of the spectrum. In the fine sensing stage all the antenna blocks sense the same frequency band thus achieving spatial diversity gain. In [54] multiantenna energy detection schemes based on maximum ratio and selection combining have been considered. Maximum ratio combining is difficult to implement in practice since it requires explicit channel information. In conclusion, using multiple antennas offers benefits through diversity but on the other hand it also requires an expensive structure because of multiple antennas.

2.3.4 Spectrum estimation and detection

Frequency domain energy detector illustrated in Fig. 2.5 essentially estimates the power spectral density (PSD) using the periodogram or the Bartlett's method if block averaging in time is employed. Naturally other spectrum estimation methods may be applied as well. Introduction to spectral analysis and various spectrum estimation methods may be found in [55–57]. Note, however, that the analysis and distributions derived for the energy detector apply in general only for the periodogram or the Bartlett's method. In practice, one may need to resort to less rigorous ad-hoc techniques for setting the thresholds and detecting the spectrum holes.

Spectrum estimation methods may be divided to parametric and nonparametric methods. Nonparametric methods are better suited for detecting an unknown signal than parametric methods. Hence, the focus for spectrum sensing has been on nonparametric methods. In [58], single-user and collaborative energy detection using Welch's periodogram has been considered. The test statistic averages multiple frequency bins around zero frequency. Welch's periodogram is an extension of the Bartlett's method that employs window functions and possibly overlapping segments. In [21, 22] the multitaper method has been proposed for PSD estimation and spectrum hole detection. In [59] a filter bank approach for wideband spectral estimation for spectrum sensing has been proposed. In [60] a multi-resolution frequency subband detection algorithm based on frequency smoothed periodograms has been proposed.

2.3.5 Wavelet based spectrum estimation and spectrum hole detection

Wavelets are a good tool for modeling and detecting singularities in the spectrum such as band edges. A wavelet based approach for spectrum hole detection has been proposed in [61]. In [62] the wavelet approach has been further developed: The PSD is first estimated for a wide bandwidth using compressive sampling and then the wavelet approach is applied for edge detection to locate the different spectrum areas (black, gray, white spaces) in the estimated PSD. Moreover, in order to reduce computational complexity, the edge spectrum whose peaks correspond to changes between different spectrum areas may be directly estimated from the compressed measurements without reconstructing the PSD.

In [63], another compressive sampling approach for wide-band spectrum estimation and spectrum hole detection has been proposed. The idea in the proposed scheme is to directly sample the signal at the information rate of the signal. Conceptually this can be viewed as an analog-to-digital converter (ADC) operating at the Nyquist rate, followed by compressive sampling. After the compressive sampling based PSD reconstruction performed using a wavelet edge detector along the approach of [62], the spectrum holes are detected using an energy detector in frequency domain. In [64], a collaborative detection approach based on the compressive sampling based spectrum sensing method of [63] has been proposed. The local autocorrelations of the compressed signal are transmitted to the fusion center that then performs spectrum reconstruction followed by energy detection in frequency domain.

Another wavelet based multi-resolution approach has been proposed in [65, 66]. The wavelet transform is performed in analog domain using an adjustable wavelet pulse to obtain the desired resolution. Detection is performed first at a coarse resolution after which the spectrum segments that appear to be unoccupied are sensed again using a finer resolution. Similar detector has been proposed in [67] where a discrete wavelet packet transform based energy detector has been proposed for performing initial coarse sensing for wide bandwidths.

2.3.6 Forward methods

Spectrum sensing using forward methods has been proposed in [68,69]. Forward methods are aimed at detecting outliers (i.e., highly-deviating samples) from a data set. In the cognitive radio context the outliers are the occupied frequency channels in the frequency domain. The algorithm in [68, 69] is based on energy measurements in the frequency domain (i.e., channelized radiometer). Frequency channels are sorted in an increasing order of energy, and using an iterative algorithm the number of occupied channels is determined. Contrary to typical energy detection based methods the algorithm

does not require the knowledge of the noise level; the noise level is adaptively estimated. However, the method requires a few vacant channels, although their location does not have to be known in advance.

2.3.7 Localization algorithm based spectrum hole detection

Spectrum hole detection using localization algorithm based on double-thresholding has been proposed in [70]. The proposed method iteratively updates two thresholds for clustering energy measurements in frequency domain. In the basic algorithm every cluster consisting of adjacent samples above the final lower threshold is considered to be a primary signal if at least one of the frequency domain samples is above the final upper threshold. This method is suitable only for narrowband signals with sufficiently high SNR. Furthermore, it is not able to distinguish among different signals.

2.4 Feature detection

Feature detection refers to extracting features from the received signal and performing the detection based on the extracted features. Generally speaking, a feature can be any measurement that can be extracted from the data. Typical features used for detection are, for example, correlation based features. Moreover, cyclostationarity-based detection has received considerable attention [71–76]. The benefit of feature detection compared to energy detection is that it typically allows distinction among different signals or waveforms. In the following different feature detection methods are reviewed. The main emphasis is on cyclostationarity-based detectors.

2.4.1 Cyclostationarity-based detection

A process $x(t)$ is said to be second-order cyclostationary in the wide sense if its mean and autocorrelation function are periodic with some period $T > 0$ [77]:

$$E[x(t)] = E[x(t+T)], \tag{2.5}$$

$$E[x(t)x(t+\tau)] = E[x(t+T)x(t+T+\tau)] \tag{2.6}$$

for all t and τ.

Man-made signals such as wireless communication and radar signals typically exhibit cyclostationarity at multiple cyclic frequencies that may be related to the carrier frequency, symbol, chip, code, or hop rates, as well as their harmonics, sums, and differences. Exploiting these periodicities allows designing powerful feature detectors that possess very appealing properties.

Cyclostationarity-based detectors have the potential to distinguish among the primary users, secondary users, and interference exhibiting cyclostationarity at different cyclic frequencies. Moreover, random noise commonly does

Table 2.1: Cyclostationarity-based detectors. $\mathcal{A}$ denotes the set of cyclic frequencies of the primary signal. (opt. = optimum, det. = detector, SC = single-cycle, MC = multicycle, τ = time delay)

Detector	**Minimum required information**
Opt. MC det. in Gaussian noise $y_{mc}(t)$ [71]	Signal phase, $S_s^\alpha(f), \forall f, \forall \alpha \in \mathcal{A}$
Opt. MC det. in non-Gaussian noise Z^{MC} [74]	Signal phase, $S_s^\alpha(f), \forall f, \forall \alpha \in \mathcal{A}$, noise pdf
SC detectors in Gaussian noise $\lvert y_{sc}^\alpha(t)\rvert$ [71]	$S_s^\alpha(f), \forall f$, for one $\alpha \in \mathcal{A}$
SC detectors in non-Gaussian noise Z^{SC} [74]	$S_s^\alpha(f), \forall f$, for one $\alpha \in \mathcal{A}$, noise pdf
Suboptimum MC detector $y_{mcm}(t)$ [73]	At least one $\alpha \in \mathcal{A}$
GLRT for cyclostationarity $\mathcal{T}_{xx}$ [5]	One $\alpha \in \mathcal{A}$, at least one suitable τ
GLRT MC detector [Publications I and III]	At least two $\alpha \in \mathcal{A}$, at least one suitable τ
Spatial sign detector [Publications IV and V]	At least one $\alpha \in \mathcal{A}$, at least one suitable τ
DVB-T detector $J_x(N_b)$ [85]	Symbol freq. $\alpha \in \mathcal{A}$, symbol data length N_d
Spread-spectrum signal detector $J_e(V)$ [86]	Length of the spreading sequence P
Synchronized averaging-based test $\mathcal{L}$ [87]	Cyclic frequencies to select proper N

not possess cyclostationarity property. In practice, however, the noise experienced in wireless communication and radar systems contains interference from various sources, such as ultra-wideband devices, device-to-device communication, leakage from adjacent channels, etc., that may exhibit cyclostationarity. This is the case especially for interference limited wireless communication systems.

In cognitive radio applications, it is reasonable to assume explicit knowledge of the cyclic frequencies of the primary users since primary user signals and their key parameters are specified in wireless standards and disclosure of such information is required by the regulatory bodies that allocate frequencies. Cyclostationary properties of many common modulated waveforms and air interfaces have been established in [77–82].

The caveat of requiring and employing prior information is that it can make cyclostationarity-based detection very sensitive to synchronization errors, such as carrier frequency and sampling clock frequency offsets. Moreover, sampling clock frequency offset may result in smearing of the spectral correlation features if block averaging is used in the estimation [29,83]. However, this problem can be alleviated with noncoherent block averaging.

Cyclostationarity-based detection has received considerable amount of attention in the past [71–76]. Two recent bibliographies on cyclostationarity, including a large number of references on cyclostationarity-based detection, are provided in [77, 84].

In the following an overview of cyclic detectors is provided. The detectors may be divided to single-cycle and multicycle detectors depending on the number of cyclic frequencies employed. Moreover, the amount of prior knowledge required by the detectors may be used to categorize them further. Table 2.1 lists the most important methods that will be introduced in the following and the prior knowledge they require.

2.4.2 Multicycle and single-cycle spectral correlation detectors in Gaussian noise

Optimum spectral correlation detector in additive stationary white Gaussian noise is given by [71]

$$y_{mc}(t) = \frac{1}{N_0^2} \sum_{\alpha} \int_{-\infty}^{\infty} S_s^{\alpha}(f)^* \hat{S}_x^{\alpha}(t,f) df \tag{2.7}$$

where the sum is over all cyclic frequencies α for which the spectral correlation function $S_s^{\alpha}(f)$ of the transmitted signal $s(t)$ is not identically zero. N_0 is the spectral density of the white noise and f denotes the frequency. The function

$$\hat{S}_x^{\alpha}(t,f) = \frac{1}{T} X_T(t,f) X_T^*(t, f-\alpha) \tag{2.8}$$

is called the cyclic periodogram, and

$$X_T(t,f) = \int_{t-T/2}^{t+T/2} x(u) e^{-j2\pi f u} du. \tag{2.9}$$

The above multicycle detector is optimum in the sense that it maximizes the SNR of the regenerated spectral lines. However, it cannot be implemented without knowledge of the signal phase since the values of $S_s^{\alpha}(f)$ depend on it. For example, for a delayed signal $u(t) = s(t-\tau)$ the spectral correlation function is given by

$$S_u^{\alpha}(f) = S_s^{\alpha}(f) e^{-j2\pi\alpha\tau}. \tag{2.10}$$

Hence, if the employed value for τ is wrong, the individual terms in (2.7) may add destructively. Consequently in practice, one typically needs to resort to a suboptimum single-cycle detector [71]

$$|y_{sc}^{\alpha}(t)| = \left| \frac{1}{N_0^2} \int_{-\infty}^{\infty} S_s^{\alpha}(f)^* \hat{S}_x^{\alpha}(t,f) df \right|. \tag{2.11}$$

Although the signal phase is no longer required, utilizing (2.11) still requires knowledge of the modulation type and its parameters, such as carrier frequency, pulse shape and symbol rate, in order to calculate the spectral correlation function $S_s^{\alpha}(f)$. In addition, if unknown, the noise spectral density N_0 may be replaced by its maximum likelihood (ML) estimate, $\hat{N}_0 = \frac{1}{M} \sum_{n=1}^{M} |x(n)|^2$ where M is the number of received samples [72]. Under weak-signal assumption $\hat{N}_0$ is approximately the same under both hypotheses.

The multicycle detector test statistic in (2.7) is asymptotically complex normal distributed under both hypotheses [76] while the single-cycle test statistic in (2.11) is asymptotically Rayleigh distributed under H_0 and Rician distributed under H_1 [75].

In case $S_s^\alpha(f)$ is not known, a suboptimum multicycle detector requiring only the knowledge of the cyclic frequency/frequencies is obtained by replacing $S_s^\alpha(f)$ in (2.7) by its estimate $\hat{S}_x^\alpha(t,f)$ in (2.8) [71, 73]

$$y_{mcm}(t) = \frac{1}{N_0^2} \sum_\alpha \int_{-\infty}^{\infty} |\hat{S}_x^\alpha(t,f)|^2 df \tag{2.12}$$

where the sum over α can be taken over any number of cyclic frequencies of $s(t)$.

A performance comparison of the detectors presented in this section may be found in [73]. In addition, variants of the above detectors have been proposed recently for spectrum sensing in cognitive radios, e.g., in [88, 89]. Single-cycle detector based on (2.12) has been proposed for detecting CDMA (code division multiple access) signals used in UMTS (universal mobile telecommunications system) in [88]. The estimate for the noise power is obtained from the cyclic spectrum areas where signal features do not exist. Furthermore, DVB-T signal detection using simplified versions of the single-cycle detector of (2.11) has been considered in [89].

2.4.3 Generalized likelihood ratio tests for the presence of cyclostationarity

In [5], GLRTs for the presence of cyclostationarity have been proposed. A GLRT is obtained from the likelihood ratio test by replacing the unknown parameters with their estimates. In the following we will consider a time-domain test for the presence of second-order cyclostationarity for a given cyclic frequency. The tests are based on testing whether the expected value of the estimated cyclic autocorrelation is zero or not. Let α denote the cyclic frequency of interest and

$$\begin{aligned} \hat{\boldsymbol{r}}_{xx} = \Big[& \mathrm{Re}\{\hat{R}_x^\alpha(\tau_1)\}, \ldots, \mathrm{Re}\{\hat{R}_x^\alpha(\tau_N)\}, \\ & \mathrm{Im}\{\hat{R}_x^\alpha(\tau_1)\}, \ldots, \mathrm{Im}\{\hat{R}_x^\alpha(\tau_N)\} \Big]. \end{aligned} \tag{2.13}$$

denote a $1 \times 2N$ vector containing the real and imaginary parts of the estimated cyclic autocorrelations for N time delays at the cyclic frequency α stacked in a single vector.

A sample estimate of the cyclic autocorrelation $\hat{R}_x^\alpha(\tau)$ may be obtained using M observations as

$$\hat{R}_x^\alpha(\tau) = \frac{1}{M} \sum_{n=1}^{M} x(n) x(n+\tau) e^{-j2\pi\alpha n} \tag{2.14}$$

where $x(n)$ denotes the received discrete-time complex valued signal. Moreover, a sample estimate of the nonconjugate cyclic autocorrelation may be obtained by complex conjugating $x(n+\tau)$ in (2.14).

In order to test for the presence of second-order cyclostationarity at the cyclic frequency of interest α, the hypotheses may be formulated as follows [5]

$$\begin{aligned} H_0 &: \hat{\boldsymbol{r}}_{xx} = \boldsymbol{\epsilon}_{xx}, \\ H_1 &: \hat{\boldsymbol{r}}_{xx} = \boldsymbol{r}_{xx} + \boldsymbol{\epsilon}_{xx}, \end{aligned} \tag{2.15}$$

where $\boldsymbol{r}_{xx}$ is assumed to be non-random and $\boldsymbol{\epsilon}_{xx}$ denotes the estimation error. Furthermore, under commonly assumed circumstances, i.e., when samples well separated in time are approximately independent, $\boldsymbol{\epsilon}_{xx}$ is asymptotically normally distributed, i.e., $\lim_{M\to\infty} \sqrt{M}\boldsymbol{\epsilon}_{xx} \overset{D}{=} N(\mathbf{0}, \boldsymbol{\Sigma}_{xx})$ where $\boldsymbol{\Sigma}_{xx}$ is the $2N \times 2N$ asymptotic covariance matrix of $\hat{\boldsymbol{r}}_{xx}$ [5].

The generalized log-likelihood ratio test statistic is given by [5]

$$\mathcal{T}_{xx} = M\hat{\boldsymbol{r}}_{xx}\hat{\boldsymbol{\Sigma}}_{xx}^{-1}\hat{\boldsymbol{r}}_{xx}^{T}. \tag{2.16}$$

The asymptotic covariance matrix $\boldsymbol{\Sigma}_{xx}$ is constructed of sums and differences of conjugated and nonconjugated cyclic spectrum terms [5]. The cyclic spectrum terms may be estimated using, e.g., frequency-smoothed cyclic periodograms.

Under the null hypothesis $\mathcal{T}_{xx}$ is asymptotically chi-square distributed with $2N$ degrees of freedom, i.e. χ^2_{2N}, and under the alternative asymptotically non-central chi-square distributed with $2N$ degrees of freedom and non-centrality parameter $M\boldsymbol{r}_{xx}\hat{\boldsymbol{\Sigma}}_{xx}^{-1}\boldsymbol{r}_{xx}^{T}$, i.e. $\chi^2_{2N}(M\boldsymbol{r}_{xx}\hat{\boldsymbol{\Sigma}}_{xx}^{-1}\boldsymbol{r}_{xx}^{T})$, where $\boldsymbol{r}_{xx}$ is the true cyclic correlation.

In [90], the GLRT has been formulated for the presence of nonconjugated 2nd-order cyclostationarity as well. Moreover, in [5] generalization of the above test for the presence of kth-order cyclostationarity as well as frequency domain tests have been provided as well.

The above test was initially proposed as a method for finding out the cyclic frequencies of the received signal. This may be accomplished by performing the test for various values of α (in the interval [0,1)). However, this is computationally very expensive. If a particular primary user signal whose cyclic frequencies are known is to be detected, the test may be performed only for one of the cyclic frequencies of the primary user signal at a time. Such an approach has been employed in [90] for spectrum sensing for cognitive radio systems.

The GLRT makes only minimal assumptions on the primary systems. That is, only the knowledge of the cyclic frequencies of the primary signals and a few suitable time delays are required. This also means that sensitivity to non-idealities and synchronization errors such as carrier frequency offsets is reduced. In fact the GLRT does not require the knowledge of the carrier frequency, unless of course cyclic frequencies related to the carrier frequency are used as features. However, the fact that the algorithm requires and employs only minimal prior knowledge of the primary systems means also that some performance loss may be sustained compared to detectors using

full, explicit information, such as the ideal spectral correlation function, if such information is in fact available. On the other hand, parameters such as pulse shapes and carrier frequencies may be known in practice only approximately.

2.4.4 Generalized likelihood ratio (GLR) based multicycle detectors

In Publications I and III, multicycle detectors that extend (2.16) to multiple cyclic frequencies have been proposed. The proposed multicycle generalized log-likelihood ratio statistic has the similar quadratic form as the single-cycle test statistic in (2.16) and is thus given by

$$\mathcal{T}_{\mathcal{A},xx} = M\hat{\boldsymbol{r}}_{\mathcal{A},xx}\hat{\boldsymbol{\Sigma}}_{\mathcal{A},xx}^{-1}\hat{\boldsymbol{r}}_{\mathcal{A},xx}^{T} \tag{2.17}$$

where M is the number of observations.

However, the differences are in contents of the cyclic autocorrelation vector $\hat{\boldsymbol{r}}_{\mathcal{A},xx}$ and its covariance matrix $\hat{\boldsymbol{\Sigma}}_{\mathcal{A},xx}$. Here

$$\begin{aligned}\hat{\boldsymbol{r}}_{\mathcal{A},xx} = \Big[&\mathrm{Re}\{\hat{R}_{xx}^{\alpha_1}(\tau_{1,1})\},\ldots,\mathrm{Re}\{\hat{R}_{xx}^{\alpha_1}(\tau_{1,N_1})\},\\ &\mathrm{Im}\{\hat{R}_{xx}^{\alpha_1}(\tau_{1,1})\},\ldots,\mathrm{Im}\{\hat{R}_{xx}^{\alpha_1}(\tau_{1,N_1})\},\\ &\qquad\qquad\ldots\\ &\mathrm{Re}\{\hat{R}_{xx}^{\alpha_P}(\tau_{P,1})\},\ldots,\mathrm{Re}\{\hat{R}_{xx}^{\alpha_P}(\tau_{P,N_P})\},\\ &\mathrm{Im}\{\hat{R}_{xx}^{\alpha_P}(\tau_{P,1})\},\ldots,\mathrm{Im}\{\hat{R}_{xx}^{\alpha_P}(\tau_{P,N_P})\}\Big]\end{aligned} \tag{2.18}$$

denotes a $1 \times 2N$ vector containing the real and imaginary parts of the estimated cyclic autocorrelations at the cyclic frequencies of interest stacked in a single vector. P is the number of cyclic frequencies in the set of cyclic frequencies of interest $\mathcal{A} = \{\alpha_k | k = 1,\ldots,P\}$ and $N = \sum_{k=1}^{P} N_k$ where $N_k, k = 1,\ldots,P$, are the number of time delays for each different cyclic frequency in (2.18). That is, the cyclic autocorrelations for each cyclic frequency may be calculated for different time delays as well. Consequently, (2.18) is an extension of $\hat{\boldsymbol{r}}_{xx}$ in (2.13) to multiple cyclic frequencies, each with a set of possibly distinct time delays.

The asymptotic covariance matrix $\hat{\boldsymbol{\Sigma}}_{\mathcal{A},xx}$ is again constructed of sums and differences of conjugated and nonconjugated cyclic spectrum terms. The detailed construction may be found in Publication III.

Under the null hypothesis $\mathcal{T}_{\mathcal{A},xx}$ is asymptotically chi-square distributed with $2N$ degrees of freedom, i.e. χ^2_{2N}, and under the alternative asymptotically non-central chi-square distributed with $2N$ degrees of freedom and non-centrality parameter $M\boldsymbol{r}_{\mathcal{A},xx}\hat{\boldsymbol{\Sigma}}_{\mathcal{A},xx}^{-1}\boldsymbol{r}_{\mathcal{A},xx}^{T}$, i.e. $\chi^2_{2N}(M\boldsymbol{r}_{\mathcal{A},xx}\hat{\boldsymbol{\Sigma}}_{\mathcal{A},xx}^{-1}\boldsymbol{r}_{\mathcal{A},xx}^{T})$, where $\boldsymbol{r}_{\mathcal{A},xx}$ is the true cyclic correlation.

In Publications I and III, two simplified multicycle test statistics have been proposed as well. These test statistics are defined as the sum and maximum over the set of test statistics $\mathcal{T}_{xx}(\alpha)$ calculated for different cyclic frequencies of interest $\alpha \in \mathcal{A}$, i.e.

$$\mathcal{D}_s = \sum_{\alpha \in \mathcal{A}} \mathcal{T}_{xx}(\alpha), \tag{2.19}$$

$$\mathcal{D}_m = \max_{\alpha \in \mathcal{A}} \mathcal{T}_{xx}(\alpha). \tag{2.20}$$

The multicycle detector of (2.17) and the multicycle sum detector of (2.19) are best suited for signals that have multiple strong cyclic frequencies, i.e., cyclic frequencies at which the signal exhibits significant spectral correlation. An example of such a signal is the orthogonal frequency division multiplexing (OFDM) signal that exhibits strong spectral correlation at the symbol frequency and its multiples. If weak cyclic frequencies are included in the test, the performance may deteriorate since each test statistic for different cyclic frequency increases the number of degrees of freedom of the asymptotic distribution. Consequently, including cyclic frequencies that do not provide substantial contribution is not beneficial.

The maximum detector of (2.20) may prove to be useful if the cyclic frequencies are due to different signal properties or if the primary user system has multiple alternating operation modes that result in different cyclic frequencies. For example, adaptive modulation and coding may lead to such signals. In such scenarios the maximum detector may improve the detection reliability. For example, a maximum detector using cyclic frequencies induced both by the carrier frequency and the symbol frequency, could improve the reliability of the detector in the presence of carrier frequency or symbol frequency offsets. Moreover, the location of the maximum could serve as a feature for cyclostationarity-based waveform classification systems.

Detailed description of the multicycle tests, derivation of the asymptotic distributions of the test statistics, as well as simulation results demonstrating the gain of using multiple cyclic frequencies may be found in Publications I and III.

2.4.5 DVB-T and spread-spectrum signal detectors

In [85] and [86] similar detectors to the ones in (2.17) and (2.19) have been proposed for the OFDM-based DVB-T [85] and spread spectrum signals [86].

The proposed DVB-T signal detector is given by [85]

$$J_x(N_b) = \frac{1}{2N_b + 1} \sum_{k=-N_b}^{N_b} \left| \hat{R}_x^{k/T_s}(N_d) \right|^2 \tag{2.21}$$

where N_d is the length of the data part of the OFDM symbol, T_s is the OFDM symbol length, and $2N_b + 1$ is the number of cyclic frequencies employed. $\hat{R}_x^\alpha(\tau)$ denotes the estimate of the cyclic autocorrelation for cyclic frequency α and time delay τ.

The spread spectrum signal detector is given by [86]

$$J_e(V) = \sum_{v=1}^{V} \sum_{k=0}^{P-1} \left| \hat{R}_x^{k/P}(v) \right|^2 \tag{2.22}$$

where P is the length of the spreading sequence of the primary user system.

Both detectors are asymptotically chi-square distributed under the null hypothesis assuming only i.i.d. white Gaussian noise is present. The noise power required for the CFAR tests may be estimated as [86]

$$\hat{N}_0 = \frac{1}{M} \sum_{n=1}^{M} |x(n)|^2, \tag{2.23}$$

where $x(n)$ is the received signal and M is the number of observations.

The proposed detectors use multiple cyclic frequencies and are thus very closely related to the multicycle detectors proposed in Publications I and III. The work in [85,86] has been done by Jallon independently of our work. The differences between our work and Jallon's work are the assumption of OFDM and spread-spectrum signals in [85,86] and the assumption in [85,86] that under the null hypothesis only i.i.d. white Gaussian noise is present. The detectors of Publications I and III may be applied for any almost cyclostationary signal and under other noise distributions, in addition to the i.i.d. white Gaussian noise. The i.i.d white Gaussian noise assumption in [85, 86] means that the whitening of the cyclic correlation coefficients using the asymptotic covariance matrix as in (2.17) is not required since the asymptotic covariance matrix is diagonal under H_0.

2.4.6 Synchronized averaging based test for cyclostationarity

In [87] a multicycle detector based on the Fourier series representation of the autocorrelation function has been proposed. That is, the autocorrelation function $r_x(t, \tau)$ of a cyclostationary signal $x(t)$ may be expressed as

$$r_x(t, \tau) = R_x^0(\tau) + \sum_{\alpha} R_x^\alpha(\tau) e^{j2\pi\alpha t} \tag{2.24}$$

where the $R_x^\alpha(\tau)$ are called the cyclic autocorrelation functions. The sum over α goes over all non-zero cyclic frequencies of $x(t)$. For a stationary signal the second term is zero. The detection is based on this property.

The autocorrelation function $r_x(n,\tau)$ of a discrete-time signal $x(n)$ is estimated using a technique called synchronized averaging [87, 91]

$$\hat{r}_x^{(S)}(n,\tau) = \frac{1}{S}\sum_{s=0}^{S-1} x(n+sN)x(n+sN+\tau), \quad n \in [0,1,\ldots,N-1] \quad (2.25)$$

where N is any period. The total number of observations is $M = SN + \tau$. Employing this method limits the possible cyclic periods into the set $\{N, \frac{N}{2}, \ldots, \frac{N}{N-1}\}$. That is, the presence of cyclostationarity is detected at the cyclic frequencies given by (defined in the interval $[0,1)$)

$$\mathcal{A} = \left\{ \alpha = \frac{k}{N} \middle| k = 1,2,\ldots,N-1 \right\}. \quad (2.26)$$

The test statistic is given by [87]

$$\mathcal{L} = S\hat{\hat{\boldsymbol{r}}}_x^{(S)}\hat{\boldsymbol{\Sigma}}^{-1}\hat{\hat{\boldsymbol{r}}}_x^{(S)^T}, \quad (2.27)$$

where $\hat{\hat{\boldsymbol{r}}}_x^{(S)}$ is $1 \times q$ vector of estimated autocorrelation function values. It is assumed in (2.27) that the mean of the autocorrelation values has been first calculated and subtracted from $\hat{\hat{\boldsymbol{r}}}_x^{(S)}$. $\hat{\boldsymbol{\Sigma}}^{-1}$ is the inverse of the estimated covariance matrix and superscript T denotes the transpose.

Under the null hypothesis when no cyclostationarity is present $\mathcal{L}$ is asymptotically chi-square distributed with q degrees of freedom. That is, $\lim_{S\to\infty} \mathcal{L} \overset{D}{=} \chi_q^2$ where D denotes convergence in distribution [87].

The above multicycle detector may be used when no prior knowledge of the primary system is available. However, the performance depends highly on the choice of N since N defines the set of cyclic frequencies. Prior knowledge of the cyclic frequencies of the primary signal may be used to select the value of N appropriately. Moreover, prior knowledge is required in order to be able to distinguish among different systems.

The problem with this approach is that it is computationally very intensive especially if the cyclic period is long. Furthermore, according to the simulation experiments in [87], the CFAR property may be achieved only for extremely large number of samples (tens of thousands of samples) which may not be feasible in cognitive radio applications.

2.4.7 Multicycle and single-cycle spectral correlation detectors in non-Gaussian noise

In [74] a locally optimum multicycle detector in non-Gaussian noise has been derived. The detection statistic is given by [74]

$$\begin{aligned} Z^{MC} &= \sum_{\alpha} Z^{\alpha} \\ &= M\sum_{\alpha}\left(\sum_{\tau=1-M}^{M-1} R_s^{\alpha}(\tau)^* \hat{R}_g^{\alpha}(\tau) + R_s^{\alpha}(0)^* \hat{A}_{g'}^{\alpha}\right) \end{aligned} \quad (2.28)$$

where the summation of index α ranges over all cyclic frequencies of $s(n)$ and M denotes the number of received observations. $R_s^\alpha(\cdot)$ denotes the cyclic autocorrelation function of $s(n)$ defined by

$$R_s^\alpha(\tau) = \lim_{L\to\infty} \frac{1}{2L+1} \sum_{n=-L}^{L} E[s(n)s(n+\tau)]e^{-j2\pi\alpha(n+\tau/2)}. \tag{2.29}$$

$\hat{R}_g^\alpha(\tau)$ is the estimate of the cyclic autocorrelation function after a nonlinearity $g(\cdot)$, i.e.,

$$\hat{R}_g^\alpha(\tau) = \frac{1}{M} \sum_{n=1}^{M-|\tau|} g(x(n))g(x(n+|\tau|))e^{-j2\pi\alpha(n+|\tau/2|)} \tag{2.30}$$

and

$$\hat{A}_{g'}^\alpha = \frac{1}{M} \sum_{n=1}^{M} g'(x(n))e^{-j2\pi\alpha n} \tag{2.31}$$

where $g'(\cdot)$ denotes the derivative of $g(\cdot)$. The nonlinear function $g(\cdot)$ is defined by

$$g(x) = \frac{f'(x)}{f(x)} \tag{2.32}$$

where $f(\cdot)$ and $f'(\cdot)$ denote the probability density function (pdf) of the noise and its derivative, respectively. The function $g(x)$ is the partial derivative of the log-likelihood function, i.e. $g(x) = \frac{\partial}{\partial x}\log f(x) = f'(x)/f(x)$. It is called the score function.

Similarly as the optimum multicycle detector in Gaussian noise in (2.7), the locally optimum multicycle detector in non-Gaussian noise cannot be implemented without the knowledge of the signal phase. Moreover, its implementation requires also the knowledge of the noise pdf and the noise power as well as the knowledge of the modulation type and its parameters. However, a robust method could also be obtained by using a heavy-tailed nominal pdf, such as t-distribution, for $f(x)$.

When a suboptimal single-cycle detector structure is employed, knowledge of the signal phase is not required. The single-cycle detector in non-Gaussian noise is given by [74]

$$Z^{SC} = |Z^\alpha|, \alpha \neq 0, \tag{2.33}$$

where Z^α is defined as in (2.28).

2.4.8 Spatial sign cyclic correlation based detector

In Publications IV and V, a robust nonparametric cyclic detector based on the spatial sign function has been proposed. Unlike the optimum cyclic

detectors in non-Gaussian noise, the proposed spatial sign cyclic correlation based detector does not require the noise pdf to be known.

The spatial sign function for complex-valued data $x(n)$ is defined as [92, 93]

$$S(x(n)) = \begin{cases} \frac{x(n)}{|x(n)|}, & x(n) \neq 0 \\ 0, & x(n) = 0, \end{cases} \tag{2.34}$$

where $|\cdot|$ denotes the modulus of the complex-valued argument. That is, the data is projected on a unit circle, thus, eliminating the effect of the amplitude. However, the spatial sign function preserves the phase information exploited by cyclostationarity-based methods.

We define the test statistic for the spatial sign cyclic correlation based test for a single secondary user as

$$\lambda_S = M||\hat{\boldsymbol{r}}_S(\alpha)||^2, \tag{2.35}$$

where $||\cdot||$ denotes the Euclidean vector norm and $\hat{\boldsymbol{r}}_S(\alpha)$ denotes a $1 \times N$-vector that contains the estimated spatial sign cyclic correlations at cyclic frequency α for a set of time delays $\tau_1, \ldots, \tau_N$,

$$\hat{\boldsymbol{r}}_S(\alpha) = [\hat{R}_S(\alpha, \tau_1), \ldots, \hat{R}_S(\alpha, \tau_N)]^T. \tag{2.36}$$

The spatial sign cyclic correlations may be estimated using the spatial sign cyclic correlation estimator as

$$\hat{R}_S(\alpha, \tau) = \frac{1}{M} \sum_{n=0}^{M-1} S(x(n)) S(x^*(n+\tau)) e^{-j2\pi\alpha n}, \ \forall \tau \neq 0 \tag{2.37}$$

where $x(n)$ is a discrete time signal, τ is a discrete time delay, M is the number of observations, and α is the cyclic frequency.

Under the null hypothesis when only i.i.d. circularly symmetric noise with zero mean is present λ_S is asymptotically chi-square distributed with N complex degrees of freedom.

The spatial sign cyclic correlation based detector of (2.35) can be easily extended to accommodate multiple cyclic frequencies in the same way as the multicycle detectors in Section 2.4.4.

Detailed description of the spatial sign cyclic correlation based detector, derivation of the asymptotic distribution, as well as simulation results demonstrating the robust performance of the spatial sign cyclic correlation based detector in non-Gaussian heavy-tailed noise may be found in Publications IV and V.

2.4.9 Other cyclic detectors

In [94] CFAR spectral correlation detectors based on the estimated cyclic spectrum that make no assumptions on the intercepted signal have been

proposed. Thus, they are suited for unknown signal detection. However, the caveat is that without prior knowledge they cannot distinguish among different systems. The proposed method employs the computationally efficient FFT accumulation method (FAM) [95] for estimating the cyclic spectrum and uses the normalized peak values of the cyclic spectrum as the test statistic. A similar type of cyclic spectrum based CFAR detector has been proposed and applied for ATSC pilot tone detection in [96] as well.

In [60] a multi-resolution frequency subband spectral correlation detection algorithm based on frequency smoothed periodograms has been proposed. The presence of spectral correlation is detected at a given cyclic frequency.

In addition to signal detection, cyclostationarity may be used for modulation classification as well. This is especially helpful for characterizing unknown signals. In addition, many of the techniques could be used for detection as well. Many of the cyclostationarity-based modulation classification methods are based on the cyclic frequency domain profile [97]

$$I(\alpha) = \max_f |C_x^\alpha(f)|, \tag{2.38}$$

where f denotes the frequency axis and $C_x^\alpha(f)$ is the spectral coherence defined by

$$C_x^\alpha(f) = \frac{\hat{S}_x^\alpha(f)}{[\hat{S}_x^0(f+\alpha/2)\hat{S}_x^0(f-\alpha/2)]^{1/2}}. \tag{2.39}$$

Methods based on the cyclic frequency domain profile have been used for modulation classification, e.g., in [97–99] and in [100] where the cyclic frequency domain profile of the cyclic spectrum $\hat{S}_x^\alpha(f)$ is used instead of the cyclic frequency domain profile of $C_x^\alpha(f)$. Other cyclostationarity-based modulation classification approaches include, for example, the second- and higher-order cyclic cumulant based approach [101–103] and the binary classification tree based on the GLRT of Section 2.4.3 [104]. A more detailed discussion of cyclostationarity-based modulation classification may be found in [4].

In certain cases, cyclostationarity may also be intentionally induced to the primary user signals for simplifying the detection and improving the performance. Such an approach has been successfully applied for blind channel equalization [105]. In [106] the authors propose to intentionally embed distinctive *cyclostationary signatures* to OFDM signals for detection purposes. The proposed cyclostationary signatures are formed by creating an intentional correlation pattern by transmitting the same data symbols on more than one subcarrier. Similar type of approach has been proposed in [107,108]. That is, in [107,108] two strategies, one using specific preamble on a distinct subset of subcarriers in the beginning of each OFDM frame and the other using a subset of subcarriers in each OFDM symbol transmitting specific signals, have been proposed. The main problem with these

kinds of approaches is that in order to be applied they require changes to be made to existing primary user systems. This is neither generally desirable nor possible because it would typically lead to changes in a wireless standard, which may be difficult to accomplish in practice. However, the cyclic prefixes or pilot subcarriers already used in many wireless standards induce cyclostationarity as well. These can be considered as intentionally embedded cyclostationary signatures although their main purpose is typically not to help detection.

2.5 Other feature detectors

2.5.1 Energy based feature detection

In [109] the authors propose a detector based on energy detection in frequency domain followed by a feature extraction of the bandwidths and center frequencies. The extracted features are used to classify the primary user system using a Bayesian classifier.

2.5.2 Pilot location detector for ATSC

Pilot location detection algorithm for ATSC signals has been proposed in [52]. The received signal is first band-pass filtered around the pilot frequency. After the filtering, frequency domain energy detection is performed. The location of the FFT peak is compared over successive intervals. If the distance of the peak locations is below a prescribed threshold, H_1 is selected.

2.5.3 ATSC data segment sync detector

At the beginning of each ATSC DTV signal data segment there is a fixed data segment sync sequence that consists of 4 symbols. In [33], a correlation based detector of ATSC DTV signals has been proposed. The proposed detector is based on finding the correlation peak due to the correlation between two consecutive data segment sync sequences.

2.5.4 Correlation feature detectors for OFDM signals

In [110, 111] a correlation detector for cyclic prefix OFDM signals has been proposed. The proposed detector is based on the fact that the cyclic prefix that precedes every OFDM symbol is the exact copy of the end part of that same OFDM symbol. This creates intrinsic correlation within the OFDM signal that can be exploited for detection. Moreover, in [111, 112] a sequential collaborative detection approach based on the autocorrelation method of [110] for the fusion of local secondary user test statistics has been proposed. Another correlation detector using the same cyclic prefix property of OFDM signals has been proposed in [113].

2.6 Other detectors

2.6.1 Blind correlation detectors

In [114] a detection method based on the estimated covariance matrix has been proposed. The proposed detector calculates the ratio of the sum of the absolute values of the correlation matrix and the sum of the diagonal elements. Hence in essence, the detection is based on whether the absolute values of the non-diagonal elements are approximately zero or not. This allows detection of correlated signals since i.i.d. noise has diagonal covariance matrix. However, detection of signals with i.i.d. samples is not possible. Two other detection algorithms using the same formulation have been proposed in [115]. These two detectors are based on the eigenvalues of the sample covariance matrix: One calculates the ratio of the maximum and minimum eigenvalues, i.e. the condition number, and the other calculates the ratio of the received energy and minimum eigenvalue. The detection algorithms proposed in [114] and [115] are robust against receiver noise uncertainty and can be implemented without the knowledge of the signal and channel. However, the algorithms cannot distinguish among different signals or interference.

2.6.2 Detecting RF receivers by exploiting local oscillator leakage power

Vast majority of the published spectrum sensing research focuses on detecting primary transmitters. However from the interference point of view and for truly finding a spectral opportunity, more important is detecting the primary receivers since that is where the interference to the primary systems takes place. Moreover, detecting the presence of primary transmitters allows setting only approximate bounds on the possible location of the primary receivers.

Detecting the presence of primary receivers by exploiting the local oscillator leakage power emitted by the RF front-end of the primary receivers during the receiving process has been considered in [27, 116]. The problem with the approach is that the local oscillator leakage has very low power thus restricting the reliable detection range below 20 m [27, 116]. Hence, in practice the detection would require a deployment of a sensor network with sensors positioned in close proximity of the primary receivers.

2.7 Collaborative detection

The interest in distributed signal processing in wireless communication and radar systems stems from the desire for reliable, low cost solutions with increased coverage and capacity. Distributed systems such as wireless sen-

sor networks and multistatic radars exploit the benefits of spatial diversity that geographically dispersed sensors provide. Distributed systems can be either centralized or decentralized. In centralized systems the local sensors transmit all the local data to a central processor that performs the optimal processing. Contrary to centralized systems, decentralized systems employ intelligent sensors that perform preliminary processing of the local data before transmitting it to a central processor called the fusion center. Decentralized detection approach is better suited for the cognitive radio context where the local sensors already have intelligent processing capabilities. Moreover, in cognitive radio applications the local sensors are typically installed on battery-operated devices. Hence, in order to conserve energy, the amount of data transmitted should be constrained. In addition, the capacity requirements a central scheme necessarily inflicts on the control channel used for transmitting data to the central processor may be prohibitive in practice. Hence, we concentrate on decentralized distributed (collaborative) spectrum sensing for cognitive radios. Introduction to distributed detection theory and various decentralized detection topologies as well as a discussion of advanced topics may be found in [117–119].

Collaboration among secondary users offers many benefits. Most notably, it allows mitigation of shadowing and multipath fading effects, thus enabling the use of less sensitive individual detectors or shorter detection time. Spatially dispersed secondary users extract diversity gain that improves the overall detection performance. The foundation for this originates from the properties of wireless propagation environments. Depending on the scattering environment multipath fading may exhibit significant spatial correlation on distances up to several tens of wavelengths [120]. However, in rich scattering environments coherence distance may be less than half a wavelength [120]. Hence, the multipath fading experienced by the secondary users may typically be considered to be uncorrelated among spatially dispersed secondary users. Shadowing, on the other hand, may exhibit correlation even for relatively large distances from few tens of meters in urban environments to hundreds of meters in suburban environments [121]. Hence, if the secondary users are closely spaced, shadowing correlation reduces potential collaboration gains. Nevertheless, the probability that each user suffers from severe shadowing and multipath fading decreases as the number of spatially dispersed collaborating secondary users increases. Moreover, the maximum diversity is obtained when the secondary users experience independent shadowing and multipath fading.

Collaboration among secondary users increases coverage as well. It allows more efficient utilization of system resources, such as extended battery life in mobile terminals, and more efficient utilization of available spectral resources.

In this work we are concerned with the secondary user collaboration in the physical layer for sensing a certain frequency band. That is, we assume

there is a group of dispersed secondary users that collaborate for sensing a given frequency band for the presence of primary users. We assume that the higher layers determine which secondary users collaborate with each other in the physical layer detection. Our formulation allows the presence of primary users to be either local or global concept within the coverage area of the cognitive network. If the presence of primary users is a local concept, each secondary user (or the fusion center) will make a local decision for the presence of primary users in the given frequency band for the location of that particular secondary user. In order to mitigate fading effects, these "local" decisions may be formed through collaborative detection among nearby secondary users. In practice, such a scheme would require that each secondary user knows its position relative to the other secondary users in order to determine which users should be included in the "local" collaborative detection. However, in order to keep the presentation concise we focus on the global concept approach without any loss of generality. Moreover, in order to avoid confusion in the following terms local test statistic and local decision refer to a test statistic or decision formed only from local measurements.

In cognitive radio applications, we are most interested in parallel topologies, illustrated in Fig. 2.6, where each secondary user performs some preliminary processing of data (e.g., calculates a test statistic or makes a local decision) and then sends the quantized information directly to a fusion center which makes the final decision. A parallel network can operate either with a dedicated fusion center or in an ad-hoc manner without a dedicated fusion center. Fig. 2.7 illustrates the two approaches. The dedicated fusion center approach is well suited for applications with a base station, such as unlicensed wireless wide-area networks that are mostly intended for providing wireless broadband access. In such networks the natural choice is for the base station that is already part of the infrastructure of the wireless network to assume the role of the fusion center. The IEEE 802.22 draft standard advocates this type of approach [122, 123]. In addition, the dedicated fusion center approach can be organized with one of the terminals assuming the job of the fusion center as well.

The other option is to organize the distributed spectrum sensing without a dedicated fusion center. In such a network each user distributes its quantized information to the other users. After receiving the local information from the other users, each user performs the fusion of the information locally. This type of an approach without a dedicated fusion center would be most suited for small-area networks with limited life-span and/or rapidly changing topology, i.e., networks not fixed to a certain place or time.

The other major topology used in distributed processing is the serial topology [117]. In serial configurations the intermediate information is passed from user to user until the last user receives the information and makes the final decision. Each user updates the intermediate information with its local information. Serial networks with wireless links suffer from

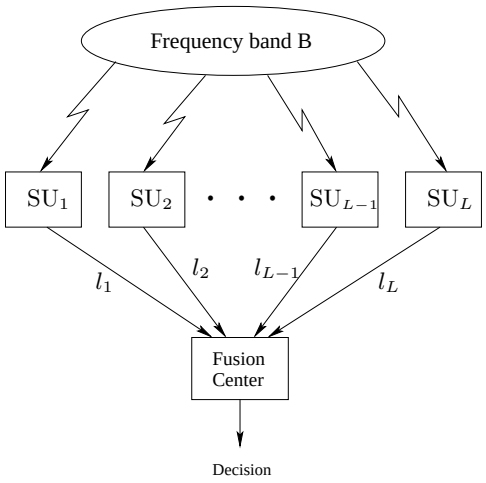

Figure 2.6: Parallel topology for collaborative spectrum sensing. The l_i, $i = 1, \ldots, L$, denote the local test statistics or binary decisions of the secondary users.

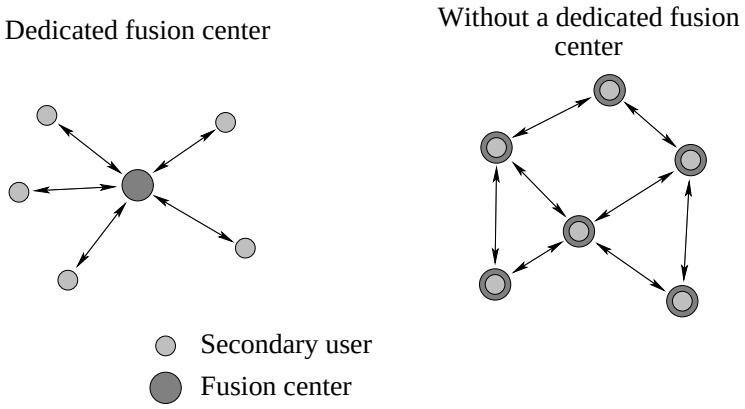

Figure 2.7: A parallel network can operate either with a dedicated fusion center or in an ad-hoc manner without a dedicated fusion center. The fusion center may or may not have sensing capability. Moreover, in the dedicated fusion center approach one of the secondary users may act as a fusion center.

severe reliability issues; a single broken link or a missing node will degrade the performance considerably.

Let L denote the number of secondary users collaborating in a parallel network topology. Common assumption is to assume conditional independence (conditioned on the hypothesis) of the secondary user observations. If this assumption is not valid, the optimal solution is in general intractable. Assuming conditional independence of the secondary user observations given H_0 or H_1, the optimal fusion center test in both the Neyman-Pearson (NP) and the Bayesian formulation is a likelihood ratio test (LRT) [117]. Moreover, the optimal local decision rules are LRTs as well [117]. However, finding the actual optimal LRT thresholds is rather difficult and computationally very complex for other than very small values of L.

When the local detection rules are fixed, the optimal fusion rule under conditional independence, the LRT, at the fusion center is a weighted sum of local decisions [117]. The weights are functions of the probabilities of detection and false alarm of the local detectors. However, these probabilities may not be known in practice, hence, various (in general) suboptimal decision rules involving fusion of binary decisions can be devised as well. These include the K-out-of-L fusion rule and its special cases the AND and OR rules. Depending on the form of processing performed at the local sensors, the detection approaches are commonly termed as soft or hard combining strategies. In hard combining only binary decisions are sent to the fusion center while soft combining involves sending less-processed or less-quantized information, such as likelihood ratios (LRs), to the fusion center.

Distributed detection using optimal Bayesian formulation and cyclostationarity-based local detectors at secondary users has been considered in [99]. The secondary users perform local tests and send their binary decisions to the fusion center. The thresholds are found using person-by-person optimization where the idea is to keep all other thresholds fixed while optimizing any one of the thresholds. An iterative Gauss-Seidel algorithm that requires multiple transmissions between the fusion center and the secondary users is employed for finding the thresholds.

Asymptotic performance analysis in the limit of large number of users of collaborative SNR based (e.g., energy detection) optimal soft combining, the LRT, and hard K-out-of-L spectrum sensing strategies under i.i.d. and exponentially correlated log-normal shadowing has been performed in [124, 125]. Collaboration among secondary users was observed to provide performance gain that depends heavily on the degree of correlation in the shadowing experienced by the secondary users. High correlation among secondary users reduces collaboration gains. In addition, soft combining of the SNR values at the fusion center produces better performance than hard combining [124]. However, if the ideal covariances among the secondary users are not known the performance difference between soft and hard combining can be relatively small [126]. Other studies considering collaborative energy detection

in Rayleigh, Nakagami, and Rician fading channels [46], Rayleigh and Nakagami fading [42], Rayleigh fading and log-normal shadowing [41,47,48,127, 128], Suzuki fading with correlated and uncorrelated shadowing [129], and Rayleigh fading with a block obstacle shadowing model [126]. The performance of collaborative energy detection with equal gain combining, selection combining, as well as switch-and-stay combining has been considered in [46]. Maximal ratio and equal gain combining for collaborative energy detection have been considered and compared to OR decision rule in [42]. In addition, a two-bit hard combining scheme is proposed. Equal gain combining has been considered and compared to OR rule also in [127]. Effects of quantization on the performance have been considered as well. In [128], the authors propose and compare several soft combining techniques, i.e. SNR weighted and equal gain combining and LRT, to OR decision rule as well. The optimum number of cooperating users for energy detection based cooperation has been investigated in [130] for AND and OR fusion rules and for K-out-of-L fusion rules in [131]. In [130], it was observed that including secondary users in bad channels in the cooperation may degrade the performance. In [131], the optimal K that minimizes the total error probability for i.i.d. sensors with identical local decision rules for the general K-out-of-L fusion rule was found to be $L/2$ for typical error probabilities.

In [132–135], linear combination of local frequency domain radiometer outputs in the fusion center has been proposed for collaborative wideband spectrum sensing. The collaborative spectrum sensing is formulated and solved as an optimization problem for maximizing the throughput of the secondary users given interference, detection probability, and false alarm constraints. The collaborative spectrum sensing improves the aggregate throughput of the secondary users. However, since the method is based on energy detection, it is susceptible to noise uncertainty.

As already noted above, given predetermined local decision strategies the optimal fusion of the local decisions at the fusion center requires the knowledge of the probabilities of detection and false alarm. In addition, when implementing the optimal Bayesian decision rule the prior probabilities of the hypotheses should be known as well. Unfortunately, these probabilities are not known in general. However, using the NP formulation at the local detectors fixes the probabilities of false alarm under nominal conditions. Moreover, the required probabilities may be estimated. Adaptive algorithms for estimating these probabilities have been proposed in [136–138]. Since the global decisions at the fusion center are more reliable than the local decisions, the algorithms are typically based on updating the local probabilities of detection and false alarm based on the decisions made at the fusion center.

Other cooperative sensing strategies have been proposed as well. Cooperative energy detection techniques for cognitive radios using amplify-and-forward relay strategy have been proposed in [139] for two user networks and in [140] for multiuser networks. The idea in the two user cooperation

is that the user with the better channel to the primary user operates as a relay for the other user. Hence, while relaying the message transmitted by the first user, the relay will also amplify and forward the primary user signal which the first user can receive. Consequently, the received SNR at the first user is improved and thus in the process the collaborative detection performance of the two users is improved as well. The problem with the proposed strategy is that it requires transmissions by the secondary users on the same channel as employed by the primary user in order to detect its presence. These transmissions will cause interference to the primary user. Hence, the proposed method is more suitable for detecting the appearance of the primary user during the secondary user transmissions and for reducing the detection time.

In [141] a cooperative spectrum sensing technique where a group of secondary users detect the primary in a round robin fashion has been proposed for reducing the average detection time. That is, for a group of L secondary users each user will sense only in every Lth time slot. The average detection time is reduced through spatial diversity.

In [142], collaborative distributed spectrum sensing with correlated observations has been considered. Since shadowing can be correlated even for relatively large distances, correlated observation situation might arise, for example, when the secondary users do not experience multipath fading. A linear quadratic deflection-optimizing detector for the fusion of the binary decisions of the local energy detectors at the fusion center has been proposed. Improved performance has been observed compared to K-out-of-L rules in correlated log-normal shadowing. Detection thresholds depend on correlation statistics of the secondary user decisions that have to be estimated in practice.

Most of the above assumes ideal reporting channels, i.e. no errors, between the secondary users and the fusion center. The optimality of the LRT for local sensor decisions and the fusion center test under conditional independence assumption has been established for a binary-symmetric channel (BSC) model between each sensor and the fusion center under the NP criterion in [143]. Optimal LR-based and suboptimum decision fusion rules under Rayleigh fading channels between the sensors and the fusion center have been proposed in [144, 145]. Under the Bayesian criterion, the optimality of the LRT for local sensor decisions under conditional independence assumption has been established in [146] for more general channels. Energy detection and optimal linear cooperation (i.e., weighted sum of received local energies) for spectrum sensing under additive white Gaussian noise (AWGN) channels between the secondary users and the fusion center has been considered in [147]. In [148], clustering of close by secondary users and collective transmission of their fused decision to the fusion center by the cluster head has been proposed. The reporting channels are assumed to experience Rayleigh fading. Selecting the secondary user with the best

channel to the fusion center as the cluster head extracts spatial diversity and improves performance. Selecting the proper cluster size and the number of secondary users that perform sensing within the cluster in correlated shadowing environments has been considered in [43]. The goal is to extract sufficient amount of diversity gain. However, the effect of non-ideal reporting channels is not taken into account.

2.7.1 Collaborative detection using local cyclostationarity-based detectors

We have proposed collaborative tests for the multicycle detectors of Section 2.4.4 in Publications I and III, and for the spatial sign detector of Section 2.4.8 in Publications IV and V. These tests will be described in the following.

In order to maximize performance we have proposed collaborative detection tests that employ soft combining at the fusion center. Under the conditional independence assumption, the optimal fusion rule at the fusion center in the NP formulation is the LRT. Here, since we do not assume the knowledge of the likelihood parameters, we employ generalized log-likelihood ratios. Hence, assuming that the test statistics of the secondary users are independent given H_0 or H_1, the single-user test statistics can be combined as follows

$$\mathcal{T}_{\mathcal{A},L} = \sum_{i=1}^{L} \mathcal{T}_{\mathcal{A},xx}^{(i)} \tag{2.40}$$

$$\lambda_{L,S} = \sum_{i=1}^{L} \lambda_{S}^{(i)} \tag{2.41}$$

for the multicycle and spatial sign cyclic correlation based detectors, respectively. Here, L is the number of collaborating secondary users and the superscript (i) denotes the local test statistic of the ith user.

Under the null hypothesis $\mathcal{T}_{\mathcal{A},L}$ and λ_L are chi-square distributed with $2LN$ real degrees of freedom and LN complex degrees of freedom, respectively. Under the alternative $\mathcal{T}_{\mathcal{A},L}$ is asymptotically non-central chi-square distributed with $2LN$ real degrees of freedom and non-centrality parameter $\sum_{i=1}^{L} M_i \boldsymbol{r}_{\mathcal{A},xx,i} \hat{\boldsymbol{\Sigma}}_{\mathcal{A},xx,i}^{-1} \boldsymbol{r}_{\mathcal{A},xx,i}$.

2.8 Energy efficiency

Energy efficiency is particularly important in mobile applications where the secondary user terminals are typically battery-operated with limited battery life. Hence, it is important to design algorithms and detection strategies that are energy efficient. Energy efficiency of collaborative spectrum sensing depends on several factors, such as network topology, number of collaborating

users, with or without a dedicated fusion center, computational complexity, the amount of local processing vs. processing at the fusion center, transmitter and receiver structure, amount of data to be transmitted, etc.

In this thesis we focus on improving energy efficiency by reducing the amount of data transmitted during the cooperative detection. Most of the cooperation strategies require information exchange between the local sensors and the fusion center, i.e., transmission of test statistics or decisions, and depending on the implementation possibly also the sensed channels. This creates overhead transmissions that consume energy. Moreover, the control channel employed for exchanging the information may have a very limited capacity. Hence, there is a need to constrain the amount of data transmitted during the collaboration. One very appealing approach is to use censoring [149]. Censoring refers to a technique where only informative test statistics or decisions, i.e., information relevant to making the global decision, are transmitted to the fusion center. Censoring techniques for wireless sensor networks have been proposed in [149–153]. Fusion of censored decisions transmitted over fading reporting channels has been investigated in [154]. Energy efficiency of distributed detection can be further improved by ordering the transmissions [155]. That is, the idea is to transmit the most informative observations first. This technique may be applied without censoring as well. Other approaches for distributed detection with constrained resources can be found in [156–158].

Cooperative energy detection with censoring of binary decisions has been proposed in [159, 160]. The fusion center employs the OR rule. The authors consider also the effect of imperfect reporting channels. Considerable savings in the number of bits transmitted are obtained at the expense of a small performance loss.

In Publications II and III, a censoring approach based on cyclostationary local detectors and transmission of local log-likelihood ratios under communication rate constraints has been proposed. The proposed approach has been formulated for cyclostationarity-based detectors but it can be applied to other local detectors such as energy detectors as well. The proposed approach will be described briefly in the following. Detailed description and derivation of the proposed algorithm as well as simulation results may be found in Publications II and III. Similar framework has later been employed in [110] for the correlation detector of OFDM signals.

2.8.1 A cyclostationarity-based censoring scheme for improving energy efficiency

Let L denote the total number of collaborating secondary users and K denote the number of users transmitting their test statistics to the fusion center. Each secondary user is assigned an individual communication rate constraint

as follows

$$p\left(\mathcal{T}^{(i)} > t_i \middle| H_0\right) \leq \kappa_i,\ i = 1, \ldots, L, \tag{2.42}$$

where $\mathcal{T}^{(i)}$ is the local test statistic of the user i, e.g., (2.17) or (2.19), $\kappa_i \in [0, 1]$ is the communication rate constraint of user i, and t_i is the upper limit of the censoring (no-send) region of the user i. That is, each user will transmit its test statistic to the fusion center only if its value is above t_i. The t_i is chosen such that the probability of the user i transmitting its test statistic to the fusion center under H_0 is κ_i. This type of strategy in which each user is assigned a separate communication rate constraint has been suggested in [150] for censoring in sensor networks. The choice is natural in a scenario where the secondary user terminals may have very different capabilities for data transmission. Moreover, the threshold values t_i needed to meet the communication rate constraints can easily be selected independently by the secondary users. However, the threshold values or the communication rate constraints must be communicated to the fusion center.

Assuming that the test statistics of the secondary users are independent given H_0 or H_1, the test statistic of the proposed censoring test at the fusion center may be formulated as

$$\mathcal{D}_L = \sum_{i=1}^{K} \mathcal{T}^{(i)} + \sum_{i=1}^{L-K} d_i = \mathcal{D}_K + \sum_{i=1}^{L-K} d_i, \tag{2.43}$$

where the latter sum corresponds to the test statistics in the no-send region. The idea is that the test statistics of the secondary users not transmitting are replaced by a constant value denoted by d_i. Here, the value chosen for d_i is the conditional mean of the local test statistic $\mathcal{T}^{(i)}$ of the ith user in the no-send region under H_0. Note that, although d_i are constant, the value of the latter sum in (2.43) is a random variable since K is random. Moreover, the values of d_i need to be calculated and transmitted to the fusion center only once when the collaboration is initiated and whenever the communication rate constraints are changed.

In order to constrain the false alarm rate of the detection test, we need to establish the asymptotic distribution of (2.43) under H_0. Truncation of the test statistics due to censoring makes an analytic solution intractable. Hence, we have employed a numeric approximation. That is, we have derived a procedure for approximating the asymptotic distribution of (2.43) by numerically inverting the characteristic function using a Fourier series method. Detailed description of the proposed method may be found in Publications II and III.

The proposed censoring scheme may be directly applied to local tests that are under the null hypothesis chi-square distributed, such as the multicycle detectors of Section 2.4.4, the spatial sign detector of Section 2.4.8 (note that the test statistic in (2.35) has to multiplied by 2 to get $2N$

real degrees of freedom), and the energy detector, among others. Due to computational reasons for large number of degrees of freedom, a normal distribution approximation may be used. That is, if $X \sim \chi^2_k$, then as k goes to infinity, $\lim_{k\to\infty} X \overset{D}{=} N(k, 2k)$. The characteristic function as well as the mean and variance of a one-sidedly truncated normal distribution are given in Appendix A.

2.9 Sequential detection

In cognitive radio applications the detection time is an important performance criterion. Faster sensing allows for higher temporal utilization of the available spectral resources. However, it is important not to sacrifice detection performance when minimizing the detection time. Sequential detection aims at making the decision as soon as there is sufficient information available to make the decision at the specified error levels. A typical sequential detection test may be formulated as

$$\begin{aligned}
&\text{If } \mathcal{T}_n < \gamma_0 \Longrightarrow \text{Select } H_0,\\
&\text{If } \mathcal{T}_n > \gamma_1 \Longrightarrow \text{Select } H_1,\\
&\text{Otherwise} \Longrightarrow \text{take a new sample, i.e. } n = n + 1,
\end{aligned}$$

where $\mathcal{T}_n$ is the test statistic for n samples.

Another approach for sequential detection is quickest detection [161]. Quickest detection aims at detecting changes in the distribution of the observations as quickly as possible. The cumulative sum (CUSUM) test [162] is optimal for a non-Bayesian statistical quickest detection formulation [163]. Quickest detection methods for cognitive radios and sensor networks have been proposed in [164–166].

Sequential detection strategies may be employed both at the fusion center and at the local sensors. Reviews of sequential analysis and detection can be found in [118, 167, 168].

Many of the proposed sequential detectors are based on the sequential probability ratio test (SPRT) proposed in [169]. The SPRT has the smallest average sample number under both hypotheses among all tests with equal (or smaller) error probabilities. Sequential spectrum sensing schemes using the SPRT have been proposed in [111, 127, 170]. A single user sequential detection scheme based on truncated SPRT for ATSC pilot energy detection has been proposed in [170]. In [127], sequential collaborative energy detection at the fusion center has been proposed. [111] employs also a sequential detector at the fusion center. However, the proposed detector is based on the correlation detector of [110, 111] for detecting OFDM signals.

In Publication V, a single-user truncated sequential detection approach based on the spatial sign cyclic correlation estimator in (2.37) has been pro-

posed. The proposed test will be briefly described in the following. Detailed description may be found in Publication V.

2.9.1 Spatial sign cyclic correlation based sequential detection test

We define a truncated sequential detection test as follows

$$\begin{aligned} &\text{If } \lambda(n) \geq \gamma_s \text{ and } n \leq M_{\max}, && \text{Decide } H_1 \\ &\text{If } \lambda(n) < \gamma_s \text{ and } n = M_{\max}, && \text{Decide } H_0 \\ &\text{Otherwise}, && \text{Take a new sample, i.e., } n = n+1, \end{aligned} \tag{2.44}$$

where γ_s is the detection threshold, and $M_{\max}$ is the maximum number of samples that can be taken until a decision has to be made. The sequential detection test statistic is given by $\lambda(n) = \frac{1}{M_{\max}}||\hat{\boldsymbol{r}}_{S,n}(\alpha)||^2$ where the components of $\hat{\boldsymbol{r}}_{S,n}(\alpha)$ are calculated sequentially as follows

$$\hat{R}_{S,n}(\alpha,\tau) = \hat{R}_{S,n-1}(\alpha,\tau) + S(x(n))S(x^*(n+\tau))e^{-j2\pi\alpha n}, \quad n > 0, \tag{2.45}$$

and $\hat{R}_{S,0}(\alpha,\tau) = S(x(0))S(x^*(\tau))$. $S(\cdot)$ denotes the spatial sign function in (2.34).

In Publication V an upper bound for the false alarm rate of the sequential test has been established. This allows us to set the threshold according to $\beta = 2p(\lambda(M_{\max}) \geq \gamma_s|H_0)$ to constrain the false alarm rate below β. Under the null hypothesis $\lambda(M_{\max})$ is asymptotically chi-square distributed with N complex degrees of freedom where N is the number of lags.

Simulation experiments showing the considerable reductions in detection times compared to fixed sample size tests may be found in Publication V.

The proposed sequential detection test may be applied in collaborative detection as well. In sequential detection the secondary users will transmit their test statistic as soon as it exceeds the local test threshold. Hence, soft combining of the test statistics at the fusion center may result in a performance loss. Consequently, we propose a binary OR test for the sequential detection detector at the fusion center where each secondary user will send only their binary decision to the fusion center. The fusion center will accept H_1 if at least one of the secondary users has detected the primary user.

Assuming independence of the secondary user test statistics under the null hypothesis, the false alarm rate at the fusion center is given by $\beta_{FC} = 1 - \prod_{i=1}^{L}(1-\beta_i)$ where β_i are the false alarm rates of the secondary users.

2.10 Discussion

In this chapter, spectrum sensing methods for identifying underutilized radio spectrum have been reviewed. Spectrum sensing methods may be broadly

categorized to three classes: matched filter, energy based detection, and feature detection. Matched filter is a coherent detection technique that employs a correlator that is matched to the signal of interest or to specific parts of it, such as pilot and training sequences. Coherent processing provides very good performance in nominal conditions. However, matched filters are very sensitive to synchronization errors and multipath fading. In practice, the performance of matched filters may degrade significantly due to the aforementioned reasons. In addition, a separate matched filter is required for each different primary signal thus complicating the cognitive radio design.

Energy detection is suitable for random signal detection. It does not require any assumptions on the primary signal. Unfortunately, this also means that energy detection cannot distinguish among different signals or interference. Hence, ultimately, if efficient spectral opportunity utilization is desired, energy detection cannot be the only sensing approach. Moreover, energy detection is susceptible to noise uncertainty that renders detection below certain SNR impossible regardless of the number of samples (i.e., the SNR wall behavior). Hence, energy detection requires an accurate noise level estimate. The benefit of energy detection is that it is computationally very efficient.

Feature detection relies on detecting the primary signals based on deterministic or statistical properties of the signal. Since feature detection is based on extracted signal features, it allows distinction among signals with different features. In order to accomplish this, some knowledge about the primary signals and their properties is required. In general, feature detection has higher computational complexity than energy detection or matched filtering. One important subclass of feature detectors is the cyclostationarity-based detectors. Cyclostationarity-based detection is more robust against noise uncertainty than energy detection since noise is typically not cyclostationary. However, cyclostationarity-based detection can be very sensitive to synchronization errors resulting in carrier frequency and sampling clock frequency offsets.

In this chapter, the proposed cyclostationarity-based spectrum sensing algorithms have been briefly described. Detailed derivations may be found in Publications I-V. The proposed methods require only minimal prior knowledge about the primary signals. Only the knowledge of the cyclic frequencies of the primary systems and a few suitable time delays are required. The benefit of this is that sensitivity to non-idealities and synchronization errors such as carrier frequency offsets is reduced. In fact the proposed methods do not require the knowledge of the carrier frequency, unless the cyclic frequencies related to the carrier frequency are used as features. However, the caveat is that some performance loss may be sustained compared to detectors using full, explicit information in the form of the ideal spectral correlation function, if such information is in fact available. However, in practice, parameters such as pulse shapes and carrier frequencies are typically known

only approximately.

The proposed multicycle detectors improve performance compared to single-cycle detectors when the detected signal has multiple strong cyclic frequencies. Moreover, since the proposed detectors require only the asymptotic distribution of the cyclic correlation estimators to infer the asymptotic distribution of the test statistic, they may be applied in various different noise and interference environments. However, this does not mean that they are particularly robust to impulsive non-Gaussian noise and interference commonly observed in many wireless communication channels. The same applies to most cyclostationarity-based detectors. Hence, a robust nonparametric cyclostationarity-based detector that has very reliable performance in non-Gaussian heavy-tailed noise has been proposed. The downside of the proposed detector is that in Gaussian noise some performance loss may be sustained.

The proposed spatial sign cyclic correlation based detector is one of the few robust cyclostationarity-based detectors proposed in the literature. In [74], the locally-optimum multicycle detector for non-Gaussian noise has been derived. However, that detector as well as the corresponding suboptimal single-cycle detector requires the knowledge of the noise pdf. Our detector does not require the knowledge of the noise pdf. More generally speaking, although robust detection has very rich literature in the past [51,118,171,172], robust spectrum sensing has so far received relatively little attention in the cognitive radio research community. This is somewhat surprising considering the nature of the problem and the strict constraints on the interference the secondary users are allowed to inflict on the primary users. Hence, in spectrum sensing one should be especially concerned with the worst case performance in least-favorable conditions. Thus, one should focus on the robustness of spectrum sensing algorithms against deviations from model assumptions, such as the assumed noise model.

In conclusion, each of the three major classes has their advantages and disadvantages. Table 2.2 gives a summary evaluation of the characteristics of different detectors with an emphasis on cyclostationarity-based detectors. Selecting and designing the proper detection algorithm is very much application and primary system dependent. There may not be an algorithm that is best suited for every application. Hence, a very viable strategy is to use a library of different sensing algorithms, for example, both energy and feature detectors. In order to maximize the probability of spectral opportunity detection, the spectrum sensing approach should be primary-system-oriented. Hence, feature detection or matched filter should be used whenever a desired performance can be achieved with a computationally feasible algorithm. Otherwise energy detection may be used. However, as a first step of the spectrum sensing process, energy detection or spectral estimation could be used to provide a quick, coarse sensing in order to narrow the set of possibly available frequency bands that would then be checked using

Table 2.2: Comparison of different detectors. Note that the values give only a rough characterization of the properties relative to the other detectors. Sensitivity to synchronization errors refers to sensitivity to carrier frequency offset, sampling offset, phase offset, and deviations from the assumed prior knowledge. Robustness to noise uncertainty refers to uncertainty in the noise distribution and its parameters. † Robustness depends on the chosen nominal pdf.

Detector	**Computational complexity**	**Sensitivity to synchronization errors**	**Robustness to noise uncertainty**
Energy detector	Low	Low	Low
Matched filter	Moderate	Very High	Moderate
Cyclostationarity-based detectors:			
-Opt. MC det. in Gaussian noise $y_{mc}(t)$ [71]	High	Very High	Moderate
-Opt. MC det. in non-Gaussian noise Z^{MC} [74]	High	Very High	Moderate to Very High†
-SC detectors in Gaussian noise $\lvert y_{sc}^{\alpha}(t)\rvert$ [71]	High	High	Moderate
-SC detectors in non-Gaussian noise Z^{SC} [74]	High	High	Moderate to Very High†
-Suboptimum MC detector $y_{mcm}(t)$ [73]	High	Moderate	Moderate
-GLRT for cyclostationarity $\mathcal{T}_{xx}$ [5]	High	Moderate	Moderate
-GLRT MC detector [Publications I and III]	High	Moderate	Moderate
-Spatial sign detector [Publications IV and V]	Moderate	Moderate	Very High
-DVB-T detector $J_x(N_b)$ [85]	Moderate	Moderate	Moderate
-Spread-spectrum signal detector $J_e(V)$ [86]	Moderate	Moderate	Moderate
-Synchronized averaging-based test $\mathcal{L}$ [87]	High	Moderate	Moderate

computationally more complex feature detectors or matched filters. That is, the purpose of this initial step would be mainly to determine whether the power level at a given frequency band is below a level that could enable secondary user transmissions.

Regardless of which spectrum sensing algorithm is employed, each algorithm provides a trade-off between the probability of false alarm and the probability of missed detection. False alarms lead to overlooking spectrum opportunities whereas missed detections lead to collisions with the primary systems and thus reduced rate for both primary and secondary systems. Moreover, these probabilities depend also on the number of collaborating users and the employed fusion rule as well as on the number of samples. Selecting a proper detection threshold is a cross-layer optimization problem. Medium access control (MAC) layer protocols define the bounds for

the physical layer algorithms for obtaining a desired trade-off between false alarms and missed detections. Physical layer algorithms whose threshold can be set analytically to obtain a desired trade-off are preferred for their simplicity and predictability.

In addition to single-user tests, collaborative spectrum sensing tests and strategies have been reviewed. Moreover, the proposed cyclostationarity-based collaborative tests and strategies have been briefly described. Detailed derivations may be found in the Publications I-V. Collaboration among secondary users is at the core of an effective spectrum sensing system. Simulation results in Publications I-V show that the proposed collaborative tests significantly improve the reliability and performance in fading and shadowing environments. Moreover, the proposed censoring scheme provides highly improved energy efficiency by reducing the amount of control signaling and thus the number of secondary user transmissions. However, the proposed censoring scheme poses some limitations to the design of the cognitive radio system. The main assumption of the proposed censoring scheme affecting the cognitive radio system architecture and the selection of the spectrum sensing policies is the requirement of the knowledge of the number of secondary users sensing the same frequency band and primary system. Otherwise the fact that no secondary user test statistics have been received at the fusion center cannot be interpreted as the absence of the primary users and subsequently as a spectral opportunity.

Chapter 3

Radar waveform recognition

Modern radar systems typically employ pulse compression for increasing the energy of the transmitted signal without sacrificing range resolution and increasing the peak power of the radar [173]. Pulse compression is achieved by modulating the transmitted signal in such a way that the modulated signal compresses to a shorter signal with higher amplitude in the matched filter of the radar receiver. The aim of the radar waveform recognition is to recognize the employed pulse compression waveform of the radar signal. Applications of radar waveform recognition include spectrum management in civilian and military applications, signal reconnaissance, threat recognition and analysis, as well as design of effective jamming responses. In a crowded radio frequency spectrum the importance of automatic systems and intelligent receivers is emphasized. Friendly signals should be transmitted and received in a secure, efficient fashion. On the other hand, hostile signals transmitted by the adversaries should be identified and possibly jammed.

Since many of the modulation techniques employed in radars are employed also in communication signals, radar waveform recognition is closely related to automatic modulation recognition of communication signals. However, due to the different objectives of the underlying systems, the characteristics of the waveforms may be considerably different between communication and radar signals. Nevertheless, the methods and techniques employed for automatic modulation recognition of communication signals give considerable insight for radar waveform recognition as well. Moreover, some of the techniques may be directly employed or adapted, and similar signal features can be used for radar signals as well. Applications of automatic modulation recognition of communication signals include the same as the radar waveform recognition. In addition, automatic modulation recognition of communication signals may be used in blind receivers and in adaptive modulation systems as an intermediate step between signal detection and demodulation. Techniques such as automatic modulation recognition improve efficiency of wireless communication schemes by reducing the signaling overhead.

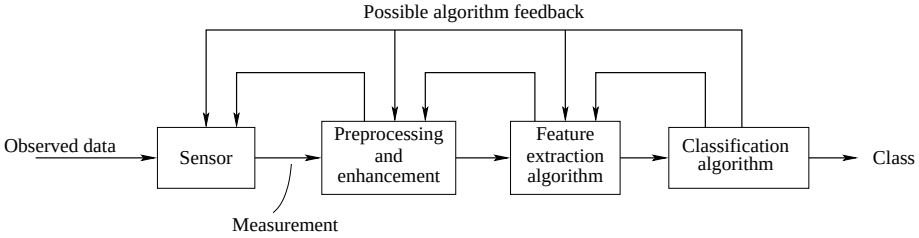

Figure 3.1: Typical pattern recognition system.

Automatic modulation recognition of communication signals has received considerable attention during the past two decades. A comprehensive survey of automatic modulation recognition and classification methods for communication signals may be found in [4]. The two main categories of automatic modulation recognition algorithms are the likelihood and feature based methods. The likelihood based approach calculates the likelihood of the received signal and compares it to a threshold to make a decision about the class. The feature based approach extracts features from the signal and bases the classification decision on the values of the extracted features.

In the following, radar waveform recognition methods are reviewed. Most of the proposed methods are based on features extracted from the measurements. Moreover, time-frequency distributions or features based on time-frequency distributions have often been employed. Fig. 3.1 illustrates the structure of a typical pattern recognition system. It consists of a sensor (i.e., in our case the sensor is the RF receiver including components such as the antenna and analog-to-digital converter), a preprocessing and enhancement mechanism for the measurements, a feature extraction algorithm and a classification algorithm. In addition, there may be data available that has already been classified. This data may be employed to train a supervised pattern recognition system.

In the following, we group the radar waveform recognition systems to time-frequency distribution based approaches and to other feature based approaches. In addition to the review of radar waveform recognition literature, the supervised radar waveform recognition system developed in this thesis work is briefly presented. The recognition system has been proposed and described in detail in Publications VI-VIII.

3.1 Advanced signal processing methods for radar waveform recognition

In [174], the applicability of time-frequency distributions (specifically the pseudo Wigner-Ville distribution, PWVD), quadrature mirror filter banks

(QMFB), and cyclostationary spectral analysis for the detection and classification of pulse compression radar signals is discussed. Large number of different waveforms, such as binary and polyphase codes, linear frequency modulation (LFM), frequency shift codes, as well as their combinations, are considered. The focus is to show what kind of information can be extracted from the intercepted signal using these methods and what are the distinctive characteristics or features of each waveform. It is observed that each of the three methods provides useful information for waveform recognition. However, no algorithms for automatic detection or classification of radar signals are presented. Nevertheless, a block diagram of an intercept receiver for detecting and classifying radar signals is drafted. The outlined intercept receiver uses neural network classifier to classify the 2-D images obtained from PWVD, QMFB, and cyclic spectrum analysis.

3.2 Time-frequency transform based radar waveform recognition

3.2.1 Morphologically processed Choi-Williams distribution based waveform recognition

In [175], a supervised radar waveform classification system based on time-frequency distribution images has been proposed. The estimated Choi-Williams distribution is considered as a 2D-image and processed using morphological image processing operations, dilation and erosion, to extract a binary feature image. The extracted binary feature image is fed to a supervised MLP classifier which performs the final classification. The continuous wave waveforms are classified to 5 classes: binary phase shift keying (BPSK), LFM, Frank codes, P4 codes, and polytime modulation T1. In the simulations, the proposed classification system achieved over 90 % overall correct classification rate at SNR of roughly 0 dB.

3.2.2 Pseudo Wigner-Ville distribution based estimation and classification of FM signals

In [176], a frequency modulation (FM) waveform classification algorithm based on the estimated instantaneous frequency has been proposed. The instantaneous frequency is estimated from the PWVD using the peak location for each time instant. Three different FM waveform models are defined and considered: LFM, sinusoidal FM, and "S"-shaped FM. The model parameters of each possible class are estimated using a statistical model for the estimated instantaneous frequency. Finally, a statistical hypothesis test based on the mean-square errors of the intercepted radar pulse and the estimated models is employed for classifying among the three different FM

waveform classes. The proposed method achieved over 90 % overall correct classification rate at SNR of -4 dB in the examples.

3.2.3 Short-time Fourier transform based waveform recognition

In [177], a channelized waveform recognition system based on the short time Fourier transform (STFT) has been proposed. The proposed algorithm obtains multiple time-frequency representations by averaging the estimated STFT using different integration lengths, hence providing better adaptation to signals with different lengths. The waveform classifier is a hierarchical classifier using threshold tests based on features extracted from the time-frequency distribution based instantaneous frequency estimate. Features extracted are the magnitude and error of a fitted linear model, as well as the maximum first-order difference of the instantaneous frequency. The proposed classifier is able to classify signals to four classes: LFM, phase shift keying (PSK), frequency shift keying (FSK), and non-modulated.

The classification performance of the proposed recognition system is analyzed using both simulated and real-world measured signals. Due to the channelized structure the classification performance varies heavily for different waveforms. In general, the performance for PSK and FSK signals occupying several channels is very poor because the filtering destroys the modulation information carried in the phase [177]. For the other waveforms considered as well as for the PSK and FSK signals when the signal bandwidth is small enough, 90 % correct classification rate is attained between SNRs of -5 dB and 8 dB depending on the waveform.

3.2.4 Atomic decomposition-based waveform recognition

In [178,179], atomic decomposition (AD)-based complex radar signal detection and classification has been proposed. AD represents the intercepted signal by the expansion of atoms, i.e., the basis functions forming a dictionary. In [178, 179], the employed dictionary of atoms is composed of chirplets. Fig. 3.2 presents the block diagram of the intercept receiver proposed in [178]. First, the analytic signal is obtained using the Hilbert transform. The analytic signal is then decomposed to atoms, after which the atoms are clustered. The purpose of the clustering stage is to group atoms coming from the same signal to the same cluster. Hence, the clustering stage enables classification of simultaneous signals. After the atoms have been assigned to different clusters, the signals corresponding to the clusters are reconstructed. The instantaneous frequencies are estimated from the reconstructed signals. The modulation recognition is based on features extracted from the estimate of each instantaneous frequency. Features extracted are the magnitude and error of a fitted linear model, as well as the

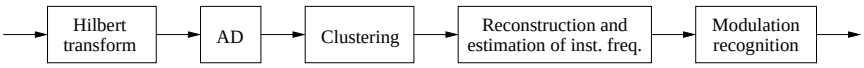

Figure 3.2: Block diagram of an atomic decomposition-based intercept receiver [178].

ratio of the error and squared magnitude, and the maximum deviation of the instantaneous frequency and the variance of a median-filtered instantaneous frequency. The modulation classifier is a hierarchical classifier based on threshold tests. Similarly as the STFT based classifier of [177], the proposed classifier is able to classify signals to four classes: LFM, PSK, FSK, and non-modulated.

The classification performance is tested using three test signals obtained from real radar and communication systems. The test signals are LFM, BPSK, and 2-FSK signals, respectively. Over 90 % correct classification rate is obtained for the BPSK signal (Barker-13 pulse) at SNR of -2 dB, and for the 2-FSK signal at SNR of 4 dB. For the LFM signal the correct classification rate is 100 % conditioned on detection for all tested SNRs.

In [179], the detection and estimation stage is improved by using the expectation maximization (EM) algorithm and an information theoretic criterion in addition to the AD. That is, the initial representation provided by the AD is improved using the EM algorithm that iteratively finds the ML estimate. Information theoretic criterion is then employed for the model order selection, i.e., for the detection of the number of signals. The authors employ their own information theoretic criterion that depends directly on the false alarm rate parameter. The improved method employing the EM algorithm and information theoretic criterion obtains a sparser representation, i.e. fewer atoms, than the original algorithm and hence has a more desirable performance in practical applications. However, its influence to waveform classification performance has not been studied in [179].

3.3 Other feature based approaches

3.3.1 Resemblance coefficient and wavelet based radar waveform recognition

Radar waveform recognition using, e.g., resemblance coefficient and wavelet packet decomposition features has been proposed in [180, 181]. In [180] supervised support vector machine (SVM) classifiers are employed while in [181] unsupervised classifiers, e.g. self-organizing maps (SOMs), are employed. The radar waveforms considered are carrier wave, BPSK, QPSK, multiple PSK, LFM, nonlinear FM (NLFM), frequency diversity (FD), and intrapulse frequency encoding (IPFE) radar signals. The performance of the proposed recognition systems has been analyzed using a dataset con-

sisting of radar signals with SNRs of 5 dB, 10 dB, 15 dB, and 20 dB. The best supervised classifier achieved an overall correct classification rate of 86 % while the best unsupervised classifier achieved an overall correct classification rate of 82 %. The classification rates are averages over the whole dataset containing signals with all the SNRs.

3.3.2 Symbolic time series analysis based features for radar waveform recognition

In [182], symbolic time series analysis based features for radar waveform recognition have been proposed. The intercepted radar signal is first quantized to form symbols. Symbols form a finite alphabet consisting of integers from 0 to $q-1$ where q is the alphabet size. For example, 0 and 1 are the symbols for an alphabet of size 2. Symbols are then grouped into words using a sliding window. Probability of each word is calculated. Finally, the entropy of the word distribution is calculated. The entropy values may be used as features. Discrimination capability of the proposed features is illustrated using seven different radar emitter signals. However, classification results have not been provided. The consider signals are carrier wave, BPSK, QPSK, LFM, NLFM, FSK, and chirp stepped-frequency encoding radar signals.

3.4 Supervised waveform recognition system based on time-frequency distribution features

In this section, the waveform recognition system proposed in Publications VI-VIII is briefly presented. Detailed description may be found in the publications.

3.4.1 Recognition system overview

The objective of the proposed radar waveform recognition system is to detect and classify intercepted radar pulses based on the pulse compression waveform. The intercepted waveforms are classified to eight classes: LFM, discrete frequency codes (Costas codes), binary phase, and Frank, P1, P2, P3, and P4 polyphase codes.

Fig. 3.3 depicts the block diagram of the waveform recognition system. First the signal is detected. After that the carrier frequency is estimated and removed. Here, the carrier frequency is defined as the center frequency of the signal's frequency band. We focus on the classification and assume that the radar pulse has already been successfully detected. The channel is assumed to be AWGN channel. That is, the intercepted discrete time signal is given by

$$y(n) = x(n) + w(n) = Ae^{j\phi(n)} + w(n), \tag{3.1}$$

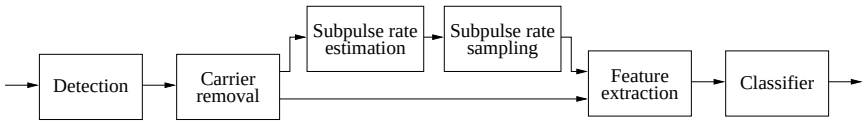

Figure 3.3: Block diagram of the waveform recognition system.

where $y(n)$ is the complex envelope of the intercepted radar signal, $x(n)$ is the complex envelope of the transmitted signal, and $w(n)$ is a complex circular white Gaussian noise process. A is a constant amplitude and $\phi(n)$ is the instantaneous phase of the complex envelope. Moreover, the signal is assumed to be a single pulse consisting of a single code period from a single radar emitter.

Many of the employed features are calculated directly from the complex envelope of (3.1). However, in order to extract detailed properties of the polyphase coded waveforms, the subpulse rate is estimated and the signal is sampled at the subpulse frequency. Cyclostationarity of the phase coded waveforms is utilized in the subpulse rate estimation by using a cyclic correlation based symbol rate estimator [183]. The subpulse rate estimation and sampling complete the preprocessing stage of the recognition system.

After the preprocessing has been completed, the features are calculated. Finally, the calculated feature vectors are inserted to the waveform classifier that performs the classification.

3.4.2 Waveform classifier

Fig. 3.4 shows the structure of the supervised waveform classifier. The waveform classifier comprises two independently operating parallel MLP networks. The MLP networks have different independently selected input feature vectors, although some of the features may be same. The main difference in the feature sets is that only the feature set for the network 2 includes features calculated from the subpulse rate sampled signal. This is because subpulse rate sampling is not feasible for LFM which does not have any subpulses. The same reason is behind the chosen classifier structure. That is, the classifier is divided to two parts in order to guarantee that the features calculated from the subpulse rate sampled signal do not affect the training or the classification of the frequency modulated waveforms.

The standard feed-forward MLP using conventional training, i.e. parameter optimization, is prone to overfit to the training data. Thus, two more complex MLP classifiers that provide better solutions against overfitting are employed. The classifiers are the ensemble averaging early-stop committee (ESC) [184] and the Bayesian MLP [185]. The idea is that both networks in Fig. 3.4 are either ESCs or Bayesian MLPs.

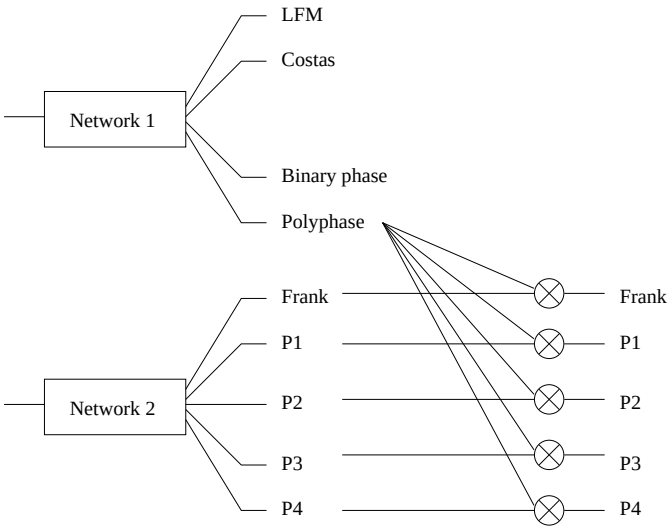

Figure 3.4: Waveform classifier comprising two parallel independent multilayer perceptron networks.

3.4.3 Feature extraction and selection

A large number of features suitable for recognizing the pulse compression waveforms have been explored. Moreover, a set of novel features specifically designed for radar signals has been proposed:

- Time-lag of the maximum cross-correlation between pulse and time-reversed pulse [Publications VI and VIII].
- Features calculated from the Choi-Williams distribution (CWD) [Publications VI and VIII]. These features include second-, third-, and fourth-order pseudo-Zernike moments as well as 3 other features targeting specific properties observed in the CWDs of the pulse compression waveforms. The three features are: the number of image components in the binary CWD, the time location of the peak power in the CWD, and the standard deviation of the width of the objects in the binary CWD.
- Features calculated from the instantaneous frequency estimated using the Wigner distribution with adaptive data-driven window length [Publication VIII]. The features are: the standard deviation of the instantaneous frequency, the ratio of the sidelobe and maximum of the autocorrelation of the instantaneous frequency, and a feature based on the statistical runs test on the instantaneous frequency. Before calculating each of the features, the instantaneous frequency is first preprocessed by removing the linear trend.

In addition, we have collected a set of features that have previously performed well in automatic modulation recognition of communication signals and that in our preliminary analysis appeared promising for radar waveform recognition as well. These include features based on instantaneous signal properties, second- and higher-order statistics, and power spectral densities. The features are:

- Standard deviation of the instantaneous phase [186] and frequency [187]. The instantaneous frequency was median-filtered as suggested in [178] to suppress the spikes caused by the phase changes in the phase coded signals.
- The bandwidth feature from [188] using symbol rate sampled signal. Thus, rendering the feature to a measure of the autocorrelation sidelobes.
- The difference of the beginning and ending phases of the pulse.
- Power spectral density (PSD) based features: symmetry [189], the maximum of the PSD [189], and the maximum of the PSD of the squared signal.
- Zero-lag moments of the complex envelope. Moments up to eighth-order without any complex conjugated components were used.
- Zero-lag cumulants of the complex envelope. Second- to sixth-order cumulants were used. See [190] for discussion of using cumulants of the complex envelope for classification of digital modulations.
- Diagonal slice of a third-order cumulant of the complex envelope. The lags used were –2, –1, 1, 2.

The final feature vectors employed in the classifiers have been selected using a mutual information based feature selection algorithm [191]. This removes redundant features and thus improves the computational complexity of the system. In our experiments, the number of selected features were 10 out of 11 and 9 out of 44 for the networks 1 and 2 in Fig. 3.4, respectively. The most informative features are the time-frequency distribution based features, the second moment of the complex envelope for the network 1, as well as the time-lag of the maximum cross-correlation between pulse and time-reversed pulse for the network 2.

3.5 Discussion

In this chapter, radar waveform recognition literature has been reviewed. The amount of published literature on radar waveform recognition is very

limited. Most of the published methods employ time-frequency distribution based approaches. Noise in time-frequency domain typically spreads to all frequencies at each time instant while the signal usually exists only at few specific frequencies at a time. Hence, time-frequency distributions provide powerful means for extracting the instantaneous properties of the received waveforms.

In addition to the literature review, an overview of the radar waveform recognition system proposed in Publications VI-VIII has been presented. The proposed recognition system employs a supervised classification approach for classifying intercepted radar pulses to common pulse compression waveform classes. The proposed approach is a feature based classification system. Special emphasis has been put on finding features based on time-frequency distributions.

Simulation results in Publication VIII show that the proposed waveform recognition system has very reliable performance in AWGN. The overall correct classification rate is over 90 % at SNR of 3 dB and over 98 % at SNR of 6 dB. Moreover, the proposed classification system generalizes well within the waveform classes. However, non-idealities such as carrier frequency offsets degrade the performance. Future work should focus on developing appropriate and reliable preprocessing algorithms and on decreasing the sensitivity to non-idealities.

The proposed approach relies on features based on time-frequency distributions, thus, showing resemblance to many of the other approaches reviewed in this chapter. However, the proposed features and the involved processing steps are novel. In pattern recognition the features are the key component for obtaining high performance. Moreover, typically the features are application specific.

Comparison of the classification performance of the different methods is in general very difficult because different authors have used different set of waveform classes as well as different data. Hence, one should not make any definitive conclusions based on the available information. However, we can make a couple of general observations. First, we have considered a more extensive set of waveform classes and signals than most previous works in the literature. Moreover, the performance of our classification system for individual classes appears to be roughly on the same level as the performance of the other systems that have considered fewer waveform classes. Thus, we can conclude that the proposed recognition system has very promising performance compared to the other systems proposed in the literature. However, unlike some of the other systems our approach considers only pulsed radar waveforms.

Finally, it is worth emphasizing the importance of data collection for training purposes. The performance and generalization capability of supervised classifiers depends heavily on the diversity and quality of the training data.

Chapter 4

Specific emitter identification

Specific emitter identification and RF fingerprinting are important tasks in both civilian and military applications. These tasks are typically performed by intercept receivers. The goal of specific emitter identification or RF fingerprinting is to identify the emitting device, not the message it is transmitting. Knowledge of the type and location of the adversary systems allows for building situational awareness needed for efficient operations. In case of a conflict it facilitates making correct decisions how to deploy troops and use resources as well as design and select proper countermeasures when necessary. The most important civilian applications of specific emitter identification and RF fingerprinting are spectrum management and wireless security applications. Security has become a primary concern in wireless networks in order to ensure secure communication between legitimate devices in a potentially hostile environment. Especially in ad-hoc networks innovative solutions are required. Emitter identification techniques may be used to improve the security of a wireless network by identifying and discriminating the rogue devices from the legitimate ones.

A typical identification system requires high fidelity acquisition of the signal of interest followed by preprocessing and enhancement stages, feature extraction from the signal, and finally the identification of the emitter. That is, the system structure follows the typical classification system structure illustrated in Fig. 3.1. The identification stage typically compares the extracted features to a known database of emitters. Moreover, the classifier or identifier may be supervised, i.e., trained using data that has already been classified. Alternatively at the initial stage of the system deployment or in case there is no existing database of emitters, the identification stage may perform clustering analysis in order to determine which signals come from the same emitter.

In this section, a literature review of specific emitter identification methods is given. Traditional electronic support receivers for radar signals employ features such as carrier frequencies, pulse repetition intervals, and pulse

widths [192]. However, although such information may provide additional or preliminary information for clustering the received signals, it does not allow distinguishing among emitters of the same type and model. Hence, we focus on methods based on detailed information that is unique to the specific device. This information includes intrapulse information for radar signals, such as rise and fall times as well as all other possible non-idealities of the emitted waveforms due to the properties of the physical components of the emitter [193–195]. For example, various transceiver imperfections and unintended modulations are useful features for emitter identification. For wireless communication transmitters the most commonly exploited distinguishing feature among different devices is the turn-on transient [196, 197]. That is, in general the identification is based on non-idealities that are unique to the emitter in question.

The chapter is structured as follows. First, the literature on RF fingerprinting of communication devices is reviewed. Then the specific emitter identification methods of radar signals are reviewed. These sections are relatively short since the amount of openly available literature, especially, on military applications is very limited. In addition, in this chapter, a robust likelihood ratio type test based on the estimated common modulation from a group of intercepted pulses is proposed for specific emitter identification. The proposed test is based on a robust M-estimation method for estimating a common modulation from a group of intercepted radar pulses. This method has been proposed in Publications IX and X. The developed M-estimation approach will be briefly presented in this chapter. Detailed description and derivation of the estimation algorithms as well as simulation results may be found in Publications IX and X.

4.1 Turn-on transient based RF fingerprinting

When a radio transmitter is turned on, the signal emitted generally shows a transient behavior with respect to the instantaneous frequency and amplitude. This turn-on transient may last from a few microseconds to few tens of milliseconds [196], depending on the type and model of the RF transmitter. The characteristics of the turn-on transient are typically distinctive even among transmitters of the same type and manufacturer [196, 197]. Identification of RF transmitters based on the turn-on transient signal has been considered in [196–204] for VHF FM radio transmitters, as well as Bluetooth and WLAN devices. Although the employed techniques may differ, common tasks to all approaches are the high fidelity acquisition of the signal of interest as well as the localization of the turn-on transient portion of the signal data. Typical approach then performs feature extraction followed by classification of the signal using known signal data stored in a database.

Features that have been proposed include statistical features of instan-

taneous signal properties [202], e.g. standard deviations of the normalized amplitude and phase, and discrete wavelet transform (DWT) based features [198, 202], e.g. standard deviation of the normalized amplitude of the DWT coefficients. Variance fractal dimension features have been proposed and employed in [196, 199]. The variance fractal dimension is related to the spread of the time variation of a time series (i.e., signal amplitude and/or phase in this case) at different time increments [196]. In [197], the raw instantaneous amplitude profiles of the transient are employed as features. In addition, principal component analysis (PCA) was applied for dimensionality reduction of the feature vector. Both approaches, i.e. with or without PCA, provided comparable performances.

Experimental results in [196] show that variation in ambient temperature and in power supply alters the characteristics of the turn-on transients. Robustness of the identification system to the variations in the environmental conditions and transmitter power supply levels may be improved by training the system with data measured under diverse circumstances, i.e. over a wide range of temperatures and transmitter power supply levels.

4.2 Matched filter based signal fingerprinting

In [205], a matched filter approach has been proposed and applied for identification of wired Ethernet devices. The matched filter is applied to a portion of the frame preamble common to all devices. At the beginning of each Ethernet frame there is a fixed 64-bit sequence used for synchronization. The employed matched filter includes the turn-on transient as well as the actual synchronization signal.

4.3 Electromagnetic signature identification of WLAN cards

In [206], the differences among different example WLAN card signals have been visually identified in time and frequency domain. Clear differences especially among cards by different manufacturers were observed. The observed differences in frequency domain were the symmetry of the passband, as well as the level and symmetry of the sidebands. Differences were observed in time domain at the depth of the zeros as well as in the smoothness of the waveforms. Moreover, the radiation patterns were observed to be different as well.

WLAN network interface card (NIC) identification using modulation features has been proposed in [207]. The proposed features include I/Q modulation features, such as phase and magnitude errors compared to the ideal constellation, I/Q origin offset, carrier frequency error between the ideal and observed, as well as correlation value to the SYNC sequence (a short signal

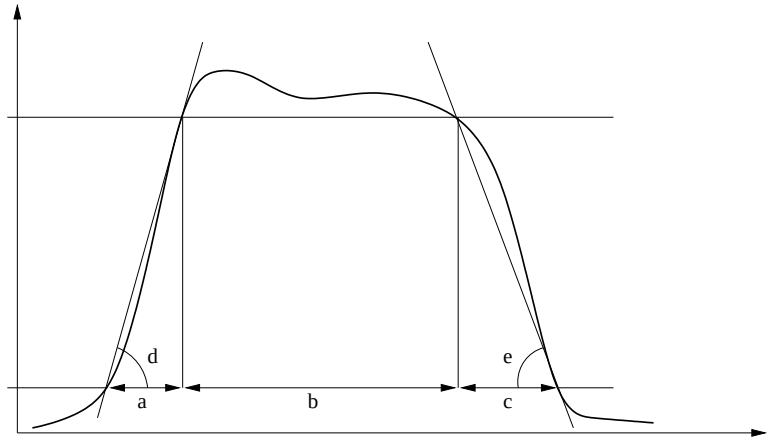

Figure 4.1: Pulse profile showing the following amplitude modulation features [208]: rise (a), slope (b), and fall (c) times, and rise (d) and fall (e) angles.

used for synchronization in IEEE 802.11 WLAN that precedes the encoded data). Over 99 % correct identification accuracy was achieved using an SVM classifier for identifying 138 identical NICs from the same manufacturer.

4.4 Specific emitter identification using intrapulse features

Specific emitter identification using features extracted from intrapulse data has been studied in [208, 209]. The authors use both amplitude and frequency modulation features. The amplitude modulation features are: the rise, slope, and fall times of the pulse, the rise, fall, and pulse angles, as well as the pulse point. The pulse point is the intersection point of the lines defined by the rise and fall angles, and pulse angle is the corresponding angle between the intersecting lines. Fig. 4.1 illustrates many of the amplitude modulation features. The frequency modulation features are: the frequency waveform vector, the frequency modulation angle, and the regression line of the frequency modulation.

To eliminate redundant and uninformative features, the authors employ and compare two methods for feature selection: linear discriminant analysis (LDA) and PCA. The employed classifier is a minimum distance classifier where different distance measures have been used, e.g., Euclidean and Mahalanobis distance. Both LDA and PCA gave similar classification results.

The proposed classification system using the new intrapulse features was observed to give superior performance on real radar data compared to a system based on traditional features used in electronic support (ES) receivers,

such as carrier frequency, pulse repetition frequency, and pulse width. Using the intrapulse features the proposed classification system was able to classify correctly all the test signals because the intrapulse features were sufficiently distinct among different emitters.

4.5 Information theoretic criterion and intrapulse information based approach for radar pulse deinterleaving

In [210–212], clustering algorithms using minimum description length (MDL) criterion and intrapulse information for emitter number detection and pulse classification have been proposed. The proposed methods are more of deinterleaving methods based on intrapulse information than identification methods. In addition, the proposed methods are able to effectively determine the number of emitters.

First, the intercepted pulses are preprocessed to remove nuisance parameters. The nuisance parameters are estimated and their value is normalized to a desired reference value. These nuisance parameters are: the initial amplitude and phase of the received pulse, the time delay of the received pulse with respect to the reference, and the carrier frequency of the intercepted pulse. In addition, the pulses are compressed using wavelet decomposition.

The preprocessed pulses are then clustered using an MDL based algorithm. The proposed algorithms may be divided to offline [210, 211] and online [212] algorithms. The offline algorithm [210,211] requires all the data before the clustering can be performed whereas the online algorithm [212] classifies the pulses and updates the cluster structure as more data is intercepted. The proposed offline clustering algorithm operates iteratively starting from one cluster, and then increasing the number of clusters one by one until a preselected upper bound for the number of clusters is reached. At each step, a new clustering for the increased number of clusters is obtained by generating new candidate partitions and selecting the one with the minimum description length. The online clustering starts from one cluster and employs the same MDL criterion for splitting and merging existing clusters as more pulses are intercepted. In [212], an online competitive learning algorithm is proposed as well. However, it has clearly inferior performance especially for distinguishing among closely related clusters. In the experiments, both the offline and online MDL algorithms achieved over 90 % correct classification rate in several different experiments.

4.6 Radar emitter identification using time-frequency distributions with optimized kernels

In [213, 214], a classification method using time-frequency distributions for radar emitter identification has been proposed. The method is based on finding a class dependent kernel function optimized to discriminate among multiple classes of signals.

The optimized kernel is found by maximizing the mean-square distance between representations obtained by multiplying the time-frequency distributions of the different classes with the kernel. In practice, the binary kernel mask is formed by selecting a set of best kernel points on training data according to the Fisher's linear discriminant ratio.

The intercepted radar pulses are classified using a multivariate Gaussian classifier. The class mean and covariance statistics employed by the classifier model are estimated from the training data. Before the classification, the radar pulse is first preprocessed. The mean and standard deviation of the radar pulse are estimated and normalized. Then the center frequency of the pulse is estimated and removed. After the preprocessing, the time-frequency distribution is estimated and multiplied with the binary kernel mask. Finally, the multivariate Gaussian classifier is employed.

The authors have tested three different time-frequency distributions: the Rihaczek, the Wigner-Ville (WV), and the STFT time-frequency distributions [215]. The Rihaczek and WV achieved identical classification performance that was far superior to the performance of the STFT. Under timing jitter of $\pm$ one sample and SNR of 14 dB in AWGN channel the Rihaczek and WV distribution based classifiers achieved an overall correct classification rate of 92.4 % for a case of four different emitters.

4.7 Maximum likelihood estimation and identification of radar pulse modulation

Statistical methods for the estimation of the common modulation from a group of intercepted radar pulses have been developed in [216]. A maximum likelihood (ML) estimator for the amplitude and phase modulation of the radar pulses is derived. The noise is assumed to be additive white Gaussian.

In order to calculate the ML estimate, the intercepted pulses are first preprocessed. The preprocessing consists of estimating the time and frequency alignment parameters of the intercepted pulses and then aligning the pulses in time and frequency using the acquired estimates. After the preprocessing, the ML estimate can be calculated. For this purpose, computationally efficient methods are proposed. The power method is employed to calculate the ML estimate of the pulse modulation. This reduces the number of operations comparable to those of conventional averaging methods.

The performance of the ML estimator is compared to separate averaging of the phase and amplitude profiles. The ML estimator accuracy is reported to be clearly better, especially, when the intercepted pulses have a large range of different SNRs. In addition, the ML estimator can be used for phase coded radar as well, unlike averaging which cannot be used for the phase coded signals due to the difficulties with unwrapping the phase for such signals.

In the second part of the work, a GLRT for testing the similarity of modulation of two different groups of pulses is derived. That is, for deciding whether both groups of pulses (a group can also consist of only one pulse) are from the same radar emitter.

The method relies on successful time and frequency alignment of the pulses. Consequently, the main cause of errors is misalignment either in time or frequency. In Publications IX and X, a robust M-estimation method has been proposed for the estimation of the common modulation from a group of intercepted radar pulses. The M-estimation approach provides robustness against preprocessing errors as well as against deviations from the model assumptions, such as the nominal Gaussian noise model. The proposed approach will be briefly presented next. In addition, a robust likelihood ratio type test based on the estimated modulation profiles is proposed for specific emitter identification.

4.8 M-estimation based radar pulse modulation estimation and identification

As already mentioned, one of the main causes of error in ML estimation of the common modulation from a group pulses are the errors made in the alignment of the pulses in time and frequency. Misalignment of the pulses results in large errors that are not well represented by the assumed Gaussian noise model. In Publications IX and X, a robust M-estimation method for estimating the common modulation from a group of intercepted radar pulses has been proposed. The intuitive idea in using an M-estimator instead of an ML estimator is that the M-estimator assigns a smaller weight for the pulses/samples that cause large errors, for example, due to misalignment in either time or frequency. Moreover, the performance of the M-estimators does not degrade as much as performance of the ML estimator when the model assumptions do not hold. In particular, when the noise distribution differs from the one assumed by the ML estimator, it may lose its performance rapidly. The main ideas of the proposed M-estimation algorithms are presented in the following. Detailed description and derivation of the estimation algorithms as well as simulation results may be found in Publications IX and X.

The proposed identification method for radar emitters in [216] is a GLRT

based on the estimated modulation profiles. However, the GRLT may be very sensitive to even small deviations from the model assumptions. In the following, a robust likelihood ratio-type test is proposed for radar emitter identification. The proposed robust likelihood ratio-type test is a robust generalization of the GLRT.

4.8.1 Signal model

The employed signal model is presented in the following. The sampling rate is assumed to be sufficiently high to record the modulations of the pulses faithfully. In addition, it is assumed that each intercepted pulse consists of N_S complex samples from a single mode of a radar with a buffer of samples recorded before and after the pulse.

The preprocessed complex pulse vectors $\boldsymbol{z}_k,\ k = 1, \ldots, N_P$, from a single mode of the same radar emitter are assumed to be given by

$$\boldsymbol{z}_k = A_k \boldsymbol{\Omega}(\nu_k)\boldsymbol{\mu} + \boldsymbol{\epsilon}_k, \quad k = 1, \ldots, N_P, \tag{4.1}$$

where A_k are the complex amplitudes of the pulses and $\boldsymbol{\mu}$ is a fixed unit vector representing the basic pulse modulation. The $\boldsymbol{\epsilon}_k$ are i.i.d. circular complex noise vectors satisfying $E(\boldsymbol{\epsilon}) = \mathbf{0}$, $E(\boldsymbol{\epsilon}\boldsymbol{\epsilon}^H) = \sigma^2 \boldsymbol{I}$, and $E(\boldsymbol{\epsilon}\boldsymbol{\epsilon}^T) = \mathbf{0}$. Here, $E(\cdot)$ denotes the expectation operator, $(\cdot)^T$ denotes the transpose, $(\cdot)^H$ denotes the conjugate transpose, σ^2 is the noise variance assumed to be known, and $\boldsymbol{I}$ is an $N_S \times N_S$ identity matrix.

The parameter ν_k is the remaining frequency offset of the kth pulse after the preprocessing, and the frequency shift operator $\boldsymbol{\Omega}(\omega)$ is a matrix given by [216]

$$\Omega(\nu)_{kn} = \exp(-jn\nu)\delta_{kn}, \tag{4.2}$$

where δ_{kn} is the Kronecker delta (i.e. $\delta_{kn} = 1$, if $k = n$, otherwise 0) and j is the imaginary unit.

4.8.2 Estimation process

Fig. 4.2 shows the block diagram of the estimation process. The first stage is a preprocessing stage. The objective of the preprocessing is to estimate the time and frequency shift parameters τ and ω necessary to align the pulses with the modulation profile $\boldsymbol{\mu}$. The time alignment of the pulses is assumed to be exact after the preprocessing. Hence, only frequency offsets ν may possibly remain. The preprocessing stages are explained in detail in Publication IX. After the preprocessing, the common modulation profile is estimated from the aligned pulses. The estimation stage is a combination of an iterative reweighted least-squares (IRLS) procedure and the scaled conjugate gradient (SCG) algorithm.

The task is to find M-estimates for $\boldsymbol{\mu}$, A_k's, and ν_k's. The idea is to use SCG to update the estimates of ν_k's, and in each iteration of the SCG to

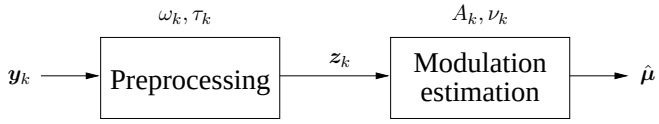

Figure 4.2: Block diagram of the estimation process. The parameters τ_k and ω_k are the circular time and frequency shifts required to align the kth pulse with the modulation profile $\boldsymbol{\mu}$. A_k are the complex amplitudes of the pulses and ν_k are the remaining frequency offsets after the preprocessing.

employ the IRLS procedure to calculate the estimates for $\boldsymbol{\mu}$ and A_k's while keeping the estimates of ν_k's fixed. Two M-estimates have been derived in Publications IX and X: one that employs only one weight parameter for each pulse and one that employs different weight parameter for each sample of the pulses. A complete description of the estimation process as well as simulation results is given in Publications IX and X.

The IRLS procedure converges in few steps. Moreover, each step of the IRLS procedure consists of an iterative procedure that also converges in only few steps. The SCG algorithm may take a few more iterations before convergence, typically converging in 10–100 iterations. However, there is no guarantee of global convergence. That is, the algorithm may converge also to a local optimum. In order to alleviate the problem, multiple starting points for the iteration may be applied. Moreover, a more accurate preprocessing algorithm for estimating the carrier frequencies would provide better first estimates for the carrier frequency offsets.

4.8.3 Hypothesis testing

The primary goal in estimating a common modulation from a group of pulses is to use the estimated modulation profile for identifying the radar emitter. In this section a robust likelihood ratio-type test is proposed for radar emitter identification.

We employ the hypothesis testing approach proposed in [216] for the identification of radar emitters. Assuming two groups of pulses $\{\boldsymbol{z}_k^{(1)}, k = 1, \ldots, N_P^{(1)}\}$ and $\{\boldsymbol{z}_k^{(2)}, k = 1, \ldots, N_P^{(2)}\}$, the problem is to determine whether these groups have a common modulation according to the model (4.1) or not. That is, the hypothesis H_0 is tested against H_1 where

$$H_0 : \boldsymbol{\mu}^{(1)} = \boldsymbol{\mu}^{(2)}$$
$$H_1 : \boldsymbol{\mu}^{(1)} \neq \boldsymbol{\mu}^{(2)},$$

where $\boldsymbol{\mu}^{(1)}$ and $\boldsymbol{\mu}^{(2)}$ denote the underlying modulation profiles of the first and second group of pulses, respectively.

According to the null hypothesis H_0, the two groups of pulses have a common modulation denoted here by $\boldsymbol{\mu}^{(c)}$, i.e. $\boldsymbol{\mu}^{(c)} = \boldsymbol{\mu}^{(1)} = \boldsymbol{\mu}^{(2)}$. Thus, the pulses constitute a single group of pulses, i.e. $\{\boldsymbol{z}^{(c)}\} = \{\boldsymbol{z}^{(1)}\} \cup \{\boldsymbol{z}^{(2)}\}$.

In [216] the hypothesis problem is solved using the GLRT. In GLRT the unknown modulation profiles and parameters are estimated using conventional ML estimators. However, the GRLT is very sensitive even to small deviations from the model assumptions, such as time and frequency alignment errors. Hence, we employ a robust likelihood ratio-type test [217] that is not as sensitive to deviations from model assumptions as the GLRT. The robust likelihood ratio-type test is the corresponding likelihood ratio-type test for M-estimators. The robust likelihood ratio-type test is given by the test statistic [217]

$$\begin{aligned} S_{N_P} &= 2 \sum_{\boldsymbol{z} \in \{\boldsymbol{z}^{(c)}\}} \sum_{n=1}^{N_S} [\rho(r^0_{\boldsymbol{z},n}/\sigma) - \rho(r^1_{\boldsymbol{z},n}/\sigma)] \\ &= 2 \sum_{k=1}^{N_P^{(1)}} \sum_{n=1}^{N_S} \left[\rho\left(\frac{z_k^{(1)}(n) - \hat{A}_{k,c}\Omega(\hat{\nu}_{k,c})_{nn}\hat{\mu}_c(n)}{\sigma} \right) \right. \\ &\qquad \left. - \rho\left(\frac{z_k^{(1)}(n) - \hat{A}_{k,1}\Omega(\hat{\nu}_{k,1})_{nn}\hat{\mu}_1(n)}{\sigma} \right) \right] \\ &\quad + 2 \sum_{k=1}^{N_P^{(2)}} \sum_{n=1}^{N_S} \left[\rho\left(\frac{z_k^{(2)}(n) - \hat{A}_{k,c}\Omega(\hat{\nu}_{k,c})_{nn}\hat{\mu}_c(n)}{\sigma} \right) \right. \\ &\qquad \left. - \rho\left(\frac{z_k^{(2)}(n) - \hat{A}_{k,2}\Omega(\hat{\nu}_{k,2})_{nn}\hat{\mu}_2(n)}{\sigma} \right) \right] \end{aligned} \tag{4.3}$$

where $r^0_{\boldsymbol{z},n}$ and $r^1_{\boldsymbol{z},n}$ are the residual errors of the models under the null and alternative hypothesis, respectively. The residual errors $r^0_{\boldsymbol{z},n}$ and $r^1_{\boldsymbol{z},n}$ are calculated using the M-estimates under the null and alternative hypothesis, respectively. That is, under H_0 the profile $\hat{\boldsymbol{\mu}}_c$ is estimated from $\{\boldsymbol{z}^{(c)}\}$ and under H_1 the two profiles $\hat{\boldsymbol{\mu}}_1$ and $\hat{\boldsymbol{\mu}}_2$ are estimated independently from the two groups of pulses $\{\boldsymbol{z}^{(1)}\}$ and $\{\boldsymbol{z}^{(2)}\}$, respectively.

The ρ function is a symmetric real-valued function that reduces the influence of outliers, i.e., highly deviating observations. We chose for the simulations the Huber ρ function given by [218]

$$\rho(r) = \begin{cases} |r|^2/2, & \text{for } |r| < c, \\ c|r| - c^2/2, & \text{for } |r| \geq c, \end{cases} \tag{4.4}$$

where c is a tuning constant. The value c employed in the simulations was experimentally selected as 1.345. Note that the residual errors r are

normalized by the scale σ in (4.3) where σ is the standard deviation of the noise. We assume σ to be known.

Under the null hypothesis, $\boldsymbol{\mu}^{(c)} = \boldsymbol{\mu}^{(1)} = \boldsymbol{\mu}^{(2)}$. Hence, the robust likelihood ratio-type test statistic S_{N_P} is under the null hypothesis asymptotically distributed as (see Appendix B for proof)

$$S_{N_P} \sim M_{2N_S+4N_S}(\cdot;\lambda) = M_{6N_S}(\cdot;\lambda), \tag{4.5}$$

where $M_{6N_S}(\cdot;\lambda)$ denotes the cumulative distribution function (cdf) of a random variable $\sum_{i=1}^{6N_S} \lambda_i x_i^2$ where x_i are independent standard normal random variables. λ_i are the eigenvalues of the matrix

$$\boldsymbol{W} = \begin{bmatrix} -\boldsymbol{B}_\theta(\boldsymbol{\theta}_0)\boldsymbol{A}_\theta^{-T}(\boldsymbol{\theta}_0) & -\boldsymbol{B}_{\theta\gamma}(\boldsymbol{\theta}_0,\boldsymbol{\gamma}_0)\boldsymbol{A}_\gamma^{-T}(\boldsymbol{\gamma}_0) \\ \boldsymbol{B}_{\gamma\theta}(\boldsymbol{\gamma}_0,\boldsymbol{\theta}_0)\boldsymbol{A}_\theta^{-T}(\boldsymbol{\theta}_0) & \boldsymbol{B}_\gamma(\boldsymbol{\gamma}_0)\boldsymbol{A}_\gamma^{-T}(\boldsymbol{\gamma}_0) \end{bmatrix}, \tag{4.6}$$

where $\boldsymbol{\theta}_0$ is a $2N_S \times 1$ vector of the real and imaginary parts of $\boldsymbol{\mu}^{(c)}$ stacked to the same vector and $\boldsymbol{\gamma}_0 = \left[\boldsymbol{\theta}_0, \boldsymbol{\theta}_0\right]^T$ is a $4N_S \times 1$ vector. The matrices $\boldsymbol{A}$ and $\boldsymbol{B}$ are defined by

$$\boldsymbol{A}(\boldsymbol{\theta}_0) = -E\left[\frac{\partial \boldsymbol{\psi}}{\partial \boldsymbol{\theta}}(\boldsymbol{z},\boldsymbol{\theta}_0)\right], \tag{4.7}$$

$$\boldsymbol{B}(\boldsymbol{\theta}_0,\boldsymbol{\gamma}_0) = E\left[\boldsymbol{\psi}(\boldsymbol{z},\boldsymbol{\theta}_0)\boldsymbol{\psi}(\boldsymbol{z},\boldsymbol{\gamma}_0)^T\right], \tag{4.8}$$

where $\boldsymbol{\psi} = \frac{\partial \rho}{\partial \boldsymbol{\theta}}$. Moreover, $\boldsymbol{B}(\boldsymbol{\theta})$ is a shorthand for $\boldsymbol{B}(\boldsymbol{\theta},\boldsymbol{\theta})$. In order to save computation, we can approximate the asymptotic distribution as follows.

The sum of the eigenvalues equals the trace of the matrix. Consequently,

$$\operatorname{tr}(\boldsymbol{W}) = \operatorname{tr}((\boldsymbol{B}_\gamma(\boldsymbol{\gamma}_0)\boldsymbol{A}_\gamma^{-T}(\boldsymbol{\gamma}_0))_{(22)}) = \sum_{i=1}^{6N_S} \lambda_i, \tag{4.9}$$

where $(\boldsymbol{B}_\gamma(\boldsymbol{\gamma}_0)\boldsymbol{A}_\gamma^{-T}(\boldsymbol{\gamma}_0))_{(22)}$ denotes the lower right $2N_S \times 2N_S$ dimensional diagonal block of the matrix $\boldsymbol{B}_\gamma(\boldsymbol{\gamma}_0)\boldsymbol{A}_\gamma^{-T}(\boldsymbol{\gamma}_0)$. The first equality follows from the fact that under the null hypothesis the matrix $\boldsymbol{B}_\theta(\boldsymbol{\theta}_0)\boldsymbol{A}_\theta^{-T}(\boldsymbol{\theta}_0)$ equals the upper left $2N_S \times 2N_S$ dimensional diagonal block of the matrix $\boldsymbol{B}_\gamma(\boldsymbol{\gamma}_0)\boldsymbol{A}_\gamma^{-T}(\boldsymbol{\gamma}_0)$. Hence, it follows

$$\operatorname{tr}(\boldsymbol{W}) = \sum_{n=2N_S+1}^{4N_S} \frac{E\left[\psi(\boldsymbol{z},\boldsymbol{\gamma})_n^2\right]}{E\left[\frac{\partial \psi(\boldsymbol{z},\boldsymbol{\gamma})_n}{\partial \gamma_n}\right]} = T, \tag{4.10}$$

where the subscript n denotes the nth component.

The asymptotic distribution of the normalized test statistic under the null hypothesis can now be approximated by

$$t^{-1} S_{N_P} \sim \chi^2_{2N_S}, \tag{4.11}$$

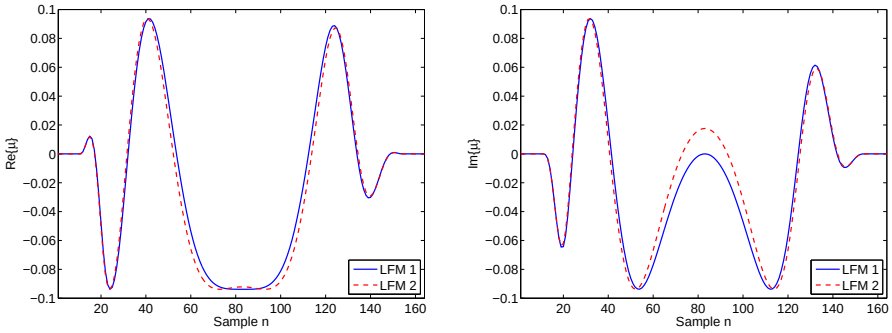

Figure 4.3: Real and imaginary parts of the two LFM pulse profiles ($N_S = 144$ plus a buffer of zeros at both ends of the pulse). The correlation difference between the two pulses is $1 - |\boldsymbol{\mu}_1^H \boldsymbol{\mu}_2|^2 \approx 0.00164$.

where $t = \frac{1}{2N_S} T$.

In order to make a decision between the hypotheses, the test statistic in (4.11) is compared to a threshold, i.e. $t^{-1} S_{N_P} \underset{H_0}{\overset{H_1}{\gtrless}} \eta$. The threshold η is defined by the equation $\alpha = p(t^{-1} S_{N_P} > \eta | H_0)$ where α is the false alarm rate. In this case the false alarm rate denotes the probability of identifying the two emitters as different when in reality they are the same.

4.8.4 Simulation experiments

The performance of the proposed M-estimation based identification technique is considered here using simulations in circularly symmetric complex Gaussian distributed noise. In order to demonstrate the high resolution of the proposed method, we employ two LFM test pulses that deviate only slightly from each other. The two pulses have identical amplitude profiles, hence, the differences between the pulses are in the phase profile. The difference is that the second pulse, i.e. LFM 2, has 2 % larger frequency sweep than the first pulse. Fig. 4.3 illustrates the differences between the two modulation profiles. The correlation difference between the two pulses is $1 - |\boldsymbol{\mu}_1^H \boldsymbol{\mu}_2|^2 \approx 0.00164$.

Figs. 4.4 and 4.5 depict the probability of identification as a function of the number of pulses for two cases when the reference and intercepted emitters are the same and when they are not the same, respectively. The pulse SNRs were selected randomly between 18 and 20 dB. The curves in the figures are averages over 5000 experiments.

In our experiments we noticed that the established asymptotic distribution holds only approximately. The mode of the distribution is well matched to the empirical distribution. However, the variance of the empirical distribution can be considerably larger than the variance of the established

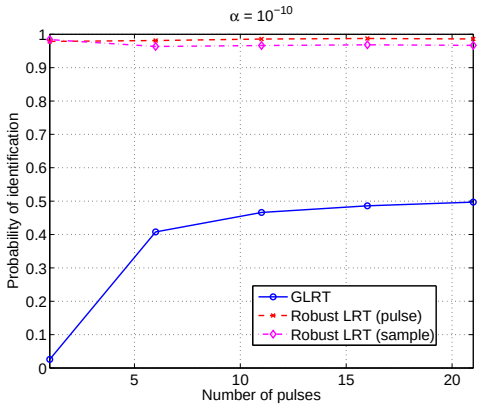

Figure 4.4: Number of pulses vs. probability of identification for LFM pulses with pulse SNRs between 18 and 20 dB ($N_S = 144$). The modulation profiles of the intercepted and reference emitters are identical (both are LFM 1). The modulation profile of the reference emitter has been calculated from 30 LFM pulses with the same SNR regime. The false alarm rate parameter α is 10^{-10}.

asymptotic distribution. The reason for this appears to be the remaining misalignment of the pulses in time and frequency. That is, the estimation algorithm does not necessarily reach the global optimum. The misalignment of the pulses is also the reason for the bad performance of the GLRT since the errors due to misalignment are not well represented by the Gaussian noise model. The consequence of this is that for the robust tests the false alarm rate parameter should be selected very small, e.g. $10^{-8} - 10^{-12}$, in order to enable high identification probability of emitters. Consequently, in Figs. 4.4 and 4.5 the false alarm rate parameter was chosen as $\alpha = 10^{-10}$.

Fig. 4.5 shows that as the number of intercepted pulses increases the probability of false identification decreases. For one intercepted pulse the probability of false identification is close to one for the robust tests. This is characteristic for the proposed methods. It is due to the fact that that particular pulse's influence is reduced due to large errors when the modulation profile is estimated under the null hypothesis. Only when the number of intercepted pulses increases closer to the number of pulses from the reference emitter, the cumulative influence of the pulses starts to have a significant effect on the estimate under the null hypothesis.

4.9 Discussion

In this chapter, specific emitter identification/RF fingerprinting methods have been reviewed. Identification of both radar and communication devices, in particular distinguishing among devices of the same type and model, is

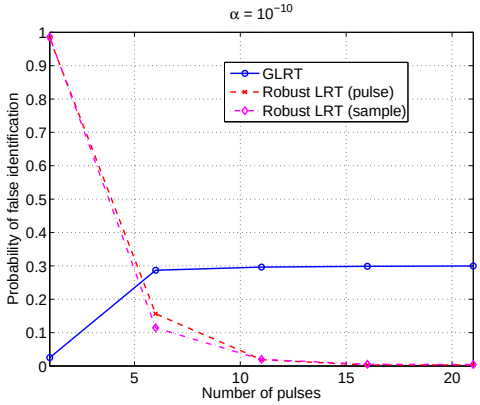

Figure 4.5: Number of pulses vs. probability of false identification for LFM pulses with pulse SNRs between 18 and 20 dB ($N_S = 144$). The correlation difference between the modulation profiles of the intercepted and reference emitters is $1 - |\boldsymbol{\mu}_1^H \boldsymbol{\mu}_2|^2 \approx 0.00164$. The modulation profile of the reference emitter has been calculated from 30 LFM pulses with the same SNR regime. The false alarm rate parameter α is 10^{-10}.

based ultimately on the characteristics of each emitter's signal specific to that particular emitter. These unintentional features or characteristics originate from different properties of the physical components and are typically of transient nature. Their origin has been attributed to different sources, such as the acquisition characteristics of phase-locked-loop frequency synthesis systems, modulator subsystems, RF amplifiers, antenna, switch and relay characteristics [196].

In addition to unintentional modulations, intentional modulations can be used to distinguish among different emitters as well. This requires that the intentional modulation is the same in each pulse or signal emitted by the same emitter. Hence, it is more suited for identifying radars than communication devices since traditional radars employ the same signal when operating in the same mode. However, the trend is to employ low-probability-of-intercept (LPI) radars that change their operation mode and transmit signals in an agile, intelligent manner, such as random radars [219] and cognitive radars [220]. These concepts are aimed more at future radar systems. More of a short-term ongoing trend in modern radar design is to use long duration pulses or even continuous wave signals to lower the peak power and thus to make them less vulnerable to interception [221]. This presents an additional challenge to the modern intercept receivers. They must be able to operate when both pulsed and continuous wave signals are present. This additional challenge is apparent for the intercept receivers using a feature based approach, such as the one presented in Section 4.4. Use of the proposed amplitude modulation features, such as rise and fall times and angles,

is limited to pulsed radars. This may call for a hierarchical system that first classifies the signal either to pulsed or continuous wave signals, and then proceeds on identifying the emitter using features suited to the type of the signal.

Another challenge to intercept receivers is added by varying conditions, such as temperature changes, different transmit powers, physical age of the components, etc., that may change the characteristics of the physical components and thus the unintentional modulations as well. Moreover, propagation channel effects, such as multipath and interference, further complicate the identification process.

In general, the amount of open literature, in particular on identification of radar emitters, is very limited. Hence, it is difficult to assess reliably what is the state-of-the-art in the field. However, the ML estimation based approach of [216], chosen as the starting point for the algorithm proposed in this thesis, has the potential to distinguish among a very large set of different emitters. The time-frequency distribution based approach of [213, 214] may not scale as nicely for a very large set of potential emitters due to the difficulty and complexity of calculating the class-dependent kernel from the training data. However, it has good performance in low SNR regimes due to the use of time-frequency distributions. The intrapulse feature-based approach of [208, 209] could potentially scale to a large number of different emitters. However, the performance using the suggested features may not allow precise identification among emitters of the same type. Moreover, the intrapulse clustering methods of [210–212] are intended more for deinterleaving the intercepted pulses than identifying the emitters.

In this chapter, a robust M-estimation based radar emitter identification method has been proposed. The proposed identification method consists of robust M-estimation of the common modulation from a group of intercepted pulses and the subsequent hypothesis test. The simulation results have shown that the proposed identification method has very good resolution for distinguishing among emitters with very similar modulation profiles. In addition, the use of M-estimation techniques improves the robustness against preprocessing errors and departures from the assumed noise model, thus enabling more reliable performance than the ML estimation based approach of [216].

A drawback of the proposed method is that the memory requirements of the robust tests are high. All the pulses have to be saved in order to be able to calculate the M-estimates under the null hypothesis. It would be of great importance to develop ways of reducing the memory and computational requirements of the proposed methods, preferably allowing identification to be made based only on the estimated modulation profiles similarly as in [216], thus, not requiring the storage of the intercepted pulses.

Finally, the proposed robust test is not suitable for identifying single pulses unlike most of the methods found in the literature. Hence, some

other strategy has to be employed for the initial clustering of the intercepted pulses. This could, for example, be a simple test based on the correlation difference that is compared to a fixed threshold. Another interesting strategy could be to fix the weight of the single intercepted pulse to one when calculating the M-estimate under the null hypothesis. Hence, not enabling the M-estimation algorithm to decrease the weight and thus reduce the influence of the intercepted pulse.

Chapter 5

Conclusion

The use of radio frequencies has increased dramatically during the past few decades. As a result, the radio frequency spectrum is becoming more and more crowded. Efficient and reliable operation in this crowded environment calls for flexible and intelligent automatic systems capable of adapting to the existing radio environment. In order to facilitate learning and adaptation, these systems must observe the radio environment. That is, they must sense the spectrum and become aware its state. Cognitive radios and cognitive radars are future communication and radar devices that are capable of learning from the environment. Spectrum sensing operations such as detection, spectrum estimation, waveform or modulation recognition, and specific emitter identification are examples of tasks that future communication and radar systems, such as cognitive radios and radars, need to perform for optimum performance.

In this thesis, spectrum sensing methods and algorithms for cognitive radios and radar intercept receivers have been proposed. The main application considered for cognitive radios in this thesis has been dynamic spectrum access. In order to find spectral opportunities while maintaining the interference caused to the primary systems below an allowed level the cognitive radios or secondary users must sense the radio frequency spectrum. In this thesis, cyclostationarity-based spectrum sensing algorithms have been proposed. The proposed algorithms require minimal assumptions about the primary user systems. The use of cyclostationarity allows distinction among primary systems, secondary systems, and interference exhibiting cyclostationarity at different cyclic frequencies. Spectrum sensing algorithms that employ multiple cyclic frequencies to improve the performance have been proposed. Robust nonparametric fixed sample size and sequential cyclostationarity-based detectors have been proposed. Robust detectors have practical importance in wireless communications systems where noise and interference is commonly non-Gaussian. Sequential detection reduces the average detection time required for a desired performance. In addition,

collaborative sensing schemes have been considered and proposed. Collaborative spectrum sensing among spatially dispersed secondary users allows mitigating shadowing and multipath fading effects through spatial diversity. In addition, for a given performance level, simpler local detectors can be used and the coverage of the sensing system improved. Moreover, energy efficiency of collaborative spectrum sensing has been considered. Transmission of local spectrum sensing statistics to the fusion center causes overhead traffic that congests the control channel and drains the batteries of the mobile terminals. In this thesis, a censoring scheme in which only informative local test statistics are transmitted to the fusion center has been proposed for collaborative spectrum sensing. The proposed scheme has been seen to have extremely reliable performance even under very strict communication rate constraints. The drop in performance compared to the uncensored collaborative scheme has been seen to be minimal.

In the future, the big challenge will be on developing collaborative strategies and especially sensing policies for collaborative sensing that incorporate the use of the physical layer algorithms. Moreover, the access policy and the sensing policy should be connected to each other. The outcome of the past access decisions and resulting channel throughputs could be used to improve the sensing policy. There exists several studies discussing and proposing sensing and access policies for cognitive radios [9–12, 222–225]. However, so far most of them do not consider collaboration among secondary users. In particular, most of the proposed sensing policies consider spectrum sensing to be performed individually by each of the secondary users without taking into account or allowing user collaboration. However, the study of physical layer algorithms suggests that collaboration among secondary users is necessary for reliable performance in difficult fading environments. In addition, there is still room for improvement in the performance and reliability of the physical layer algorithms. Issues such as reporting channel errors and correlated shadowing have so far received relatively little attention.

In addition to detection, waveform recognition and specific emitter identification using intercept receivers have been considered as well. The focus has been on radar signals and systems. A radar waveform classification system has been proposed. The proposed system classifies an intercepted radar pulse to one of eight different classes based on the pulse compression waveform: LFM, Costas codes, binary phase codes, and Frank, P1, P2, P3, and P4 polyphase codes. Novel time-frequency distribution based features have been proposed. Cyclostationarity of the phase coded waveforms has been utilized as well. The proposed classification system employs a hierarchical supervised classifier structure based on neural networks. Simulation results have shown that the proposed waveform recognition system has very reliable performance in AWGN. The overall correct classification rate has been seen to be over 98 % at SNR of 6 dB.

The proposed waveform classification system considers only pulsed radar

systems. Future development should focus on extending the classification system to continuous wave radar signals since the trend in modern radar systems is to use longer pulses or continuous wave signals due to their LPI properties. Some of the features, such as the moments and cumulants of the complex envelope, may be directly applied to continuous wave signals as well. However, for example, the time-frequency distribution based features have to be adapted to continuous wave signals. If the continuous wave signal consists of a repeating modulation sequence, the extension could be achieved by estimating the modulation period and dividing the intercepted signal to segments each containing one modulation period. Feature calculation could then be performed for each segment separately or for the average of the segments. In addition to continuous wave signals, other waveform classes could be considered as well.

In addition, a robust M-estimation based likelihood ratio-type test has been proposed for radar emitter identification. The proposed test uses M-estimation to estimate a common modulation from a group of intercepted pulses. The robust likelihood ratio-type test is based on the estimated modulation profiles. The proposed test has been seen to have very reliable performance with extremely good resolution for distinguishing among emitters with similar modulation profiles.

The proposed radar emitter identification method has very high memory requirements. Moreover, it is not suitable for identifying single pulses. Future work should aim at reducing the memory requirements of the proposed method as well as providing a solution for single pulse identification. Possible solutions to these problems have been discussed at the end of Chapter 4. Moreover, similarly as the waveform classification system, the proposed specific emitter identification method should also be extended to continuous wave signals.

Bibliography

[1] J. Mitola III and G. Q. Maguire, Jr., "Cognitive radio: making software radios more personal," *IEEE Personal Communications*, vol. 6, no. 4, pp. 13–18, Aug. 1999.

[2] J. Mitola III, "Cognitive radio: an integrated agent architecture for software defined radio," Ph.D. dissertation, Royal Institute of Technology (KTH), Stockholm, Sweden, 2000.

[3] M. J. Riezenman, "Cellular security: better, but foes still lurk," *IEEE Spectrum*, vol. 37, no. 6, pp. 39–42, Jun. 2000.

[4] O. A. Dobre, A. Abdi, Y. Bar-Ness, and W. Su, "Survey of automatic modulation classification techniques: classical approaches and new trends," *IET Communications*, vol. 1, no. 2, pp. 137–156, Apr. 2007.

[5] A. V. Dandawaté and G. B. Giannakis, "Statistical tests for presence of cyclostationarity," *IEEE Transactions on Signal Processing*, vol. 42, no. 9, pp. 2355–2369, Sep. 1994.

[6] Q. Zhao and B. M. Sadler, "A survey of dynamic spectrum access," *IEEE Signal Processing Magazine*, vol. 24, no. 3, pp. 79–89, May 2007.

[7] M. M. Buddhikot, "Understanding dynamic spectrum access: Models, taxonomy and challenges," in *Proc. of the IEEE International Symposium on New Frontiers in Dynamic Spectrum Access Networks (DySPAN)*, Apr. 17–21, 2007.

[8] W. Lehr and J. Crowcroft, "Managing shared access to a spectrum commons," in *Proc. of the 1st IEEE International Symposium on New Frontiers in Dynamic Spectrum Access Networks (DySPAN)*, Nov. 8–11, 2005, pp. 420–444.

[9] Q. Zhao, L. Tong, A. Swami, and Y. Chen, "Decentralized cognitive MAC for opportunistic spectrum access in ad hoc networks: A POMDP framework," *IEEE Journal of Selected Areas in Communications*, vol. 25, no. 3, pp. 589–600, Apr. 2007.

[10] H.-S. Chen, W. Gao, and D. G. Daut, "Spectrum sensing for wireless microphone signals," in *Proc. of the 5th IEEE Annual Communications Society Conference on Sensor, Mesh and Ad Hoc Communications and Networks. SECON Workshops '08*, Jun. 16–20, 2008, pp. 1–5.

[11] Y. Chen, Q. Zhao, and A. Swami, "Distributed spectrum sensing and access in cognitive radio networks with energy constraint," *IEEE Transactions on Signal Processing*, vol. 57, no. 2, pp. 783–797, Feb. 2009.

[12] Q. Zhao, B. Krishnamachari, and K. Liu, "On myopic sensing for multi-channel opportunistic access: Structure, optimality, and performance," *IEEE Transactions on Wireless Communications*, vol. 7, no. 12, pp. 5431–5440, Dec. 2008.

[13] S. H. A. Ahmad, M. Liu, T. Javidi, Q. Zhao, and B. Krishnamachari, "Optimality of myopic sensing in multichannel opportunistic access," *IEEE Transactions on Information Theory*, 2009, to appear.

[14] R. S. Sutton and A. G. Barto, *Reinforcement Learning: An Introduction*. MIT Press, Cambridge, MA, 1998, a Bradford Book, 322 pages.

[15] S. Haykin, *Neural networks: a comprehensive foundation*, 2nd ed. Prentice-Hall, Inc., 1999, 842 pages.

[16] M. Maskery, V. Krishnamurthy, and Q. Zhao, "Game theoretic learning and pricing for dynamic spectrum access in cognitive radio," in *Cognitive Wireless Communication Networks*, E. Hossain and V. K. Bhargava, Eds. Springer, 2007, ch. 11.

[17] A. Motamedi and A. Bahai, "Optimal channel selection for spectrum-agile low-power wireless packet switched networks in unlicensed bands," *EURASIP Journal on Wireless Communications and Networking*, vol. 2008, Article ID 896420, 10 pages, 2008.

[18] D. Cabric, S. M. Mishra, and R. W. Brodersen, "Implementation issues in spectrum sensing for cognitive radios," in *Proc. of the 38th Asilomar Conference on Signals, Systems and Computers*, vol. 1, Nov. 7–10, 2004, pp. 772–776.

[19] I. F. Akyildiz, W.-Y. Lee, M. C. Vuran, and S. Mohanty, "Next generation/dynamic spectrum access/cognitive radio wireless networks: A survey," *Computer Networks*, vol. 50, no. 13, pp. 2127–2159, Sep. 2006.

[20] A. Ghasemi and E. S. Sousa, "Spectrum sensing in cognitive radio networks: requirements, challenges and design trade-offs," *IEEE Communications Magazine*, vol. 46, no. 4, pp. 32–39, Apr. 2008.

[21] S. Haykin, "Cognitive radio: brain-empowered wireless communications," *IEEE Journal of Selected Areas in Communications*, vol. 23, no. 2, pp. 201–220, Feb. 2005.

[22] ——, "Fundamental issues in cognitive radio," in *Cognitive Wireless Communication Networks*, E. Hossain and V. K. Bhargava, Eds. Springer, 2007, ch. 1.

[23] T. C. Clancy, "Formalizing the interference temperature model," *Wireless Communications and Mobile Computing*, vol. 7, no. 9, pp. 1077–1086, Nov. 2007.

[24] FCC, "FCC order no. 07-78, terminate the proceeding ET Docket no. 03-237," May 2007.

[25] Q. Zhao, "Spectrum opportunity and interference constraint in opportunistic spectrum access," in *Proc. of the IEEE International Conference on Acoustics, Speech and Signal Processing (ICASSP)*, vol. 3, Apr. 15–20, 2007, pp. 605–608.

[26] Q. Zhao, W. Ren, and A. Swami, "Spectrum opportunity detection: How good is listen-before-talk?" in *Proc. of the 41st Asilomar Conference on Signals, Systems and Computers*, Nov. 4–7, 2007, pp. 767–771.

[27] T. X. Brown, "An analysis of unlicensed device operation in licensed broadcast service bands," in *Proc. of the 1st IEEE International Symposium on New Frontiers in Dynamic Spectrum Access Networks (DySPAN)*, Nov. 8–11, 2005, pp. 11–29.

[28] D. Cabric, A. Tkachenko, and R. Brodersen, "Spectrum sensing measurements of pilot, energy, and collaborative detection," in *Proc. of the Military Communications Conference (MILCOM)*, Oct. 23–25 2006, pp. 1–7.

[29] D. Cabric, "Addressing the feasibility of cognitive radios," *IEEE Signal Processing Magazine*, vol. 25, no. 6, pp. 85–93, Nov. 2008.

[30] S. V. Nagaraj, "Entropy-based spectrum sensing in cognitive radio," *Signal Processing*, vol. 89, no. 2, pp. 174–180, Feb. 2009.

[31] M. Muterspaugh, H. Liu, and W. Gao, "Thomson proposal outline for WRAN," Nov. 2005, IEEE 802.22-05/0096r1.

[32] D. Birru, V. Gaddam, C. Cordeiro, K. Challapali, M. Bellek, P. Pirat, L. Escobar, and D. Callonnec, "A cognitive PHY/MAC proposal for IEEE 802.22 WRAN systems," Nov. 2005, IEEE 802.22-05/0103r0.

[33] H.-S. Chen, W. Gao, and D. G. Daut, "Signature based spectrum sensing algorithms for IEEE 802.22 WRAN," in *Proc. of the IEEE International Conference on Communications (ICC)*, Jun. 24–28, 2007, pp. 6487–6492.

[34] H. Urkowitz, "Energy detection of unknown deterministic signals," *Proceedings of the IEEE*, vol. 55, no. 4, pp. 523–531, Apr. 1967.

[35] S. M. Kay, *Fundamentals of Statistical Signal Processing: Volume 2, Detection Theory.* Upper Saddle River, NJ: Prentice-Hall, 1998, 672 pages.

[36] J. Moragues, L. Vergara, J. Gosálbez, and I. Bosch, "An extended energy detector for non-Gaussian and non-independent noise," *Signal Processing*, vol. 89, no. 4, pp. 656–661, Apr. 2009.

[37] A. Sonnenschein and P. M. Fishman, "Radiometric detection of spread-spectrum signals in noise of uncertain power," *IEEE Transactions on Aerospace and Electronic Systems*, vol. 28, no. 3, pp. 654–660, Jul. 1992.

[38] R. Tandra and A. Sahai, "SNR walls for signal detection," *IEEE Journal of Selected Topics in Signal Processing*, vol. 2, no. 1, pp. 4–17, Feb. 2008.

[39] D. J. Torrieri, *Principles of Military Communication Systems.* Dedham, MA: Artech, 1981, 298 pages.

[40] J. Lehtomäki, "Analysis of energy based signal detection," Ph.D. dissertation, Faculty of Technology, University of Oulu, 2005, [Online]. Available: http://herkules.oulu.fi/isbn9514279255/.

[41] A. Ghasemi and E. S. Sousa, "Opportunistic spectrum access in fading channels through collaborative sensing," *Journal of Communications*, vol. 2, no. 2, pp. 71–82, Mar. 2007.

[42] J. Ma and Y. Li, "Soft combination and detection for cooperative spectrum sensing in cognitive radio networks," in *Proc. of the IEEE Global Communications Conference (GLOBECOM)*, Nov. 26–30, 2007, pp. 3139–3143.

[43] H. Kim and K. G. Shin, "In-band spectrum sensing in cognitive radio networks: energy detection or feature detection?" in *Proc. of the 14th ACM International Conference on Mobile Computing and Networking (MobiCom)*, Sep. 14–19, 2008, pp. 14–25.

[44] J. J. Lehtomäki, M. Juntti, and H. Saarnisaari, "CFAR strategies for channelized radiometer," *IEEE Signal Processing Letters*, vol. 12, no. 1, pp. 13–16, Jan. 2005.

[45] V. I. Kostylev, "Energy detection of a signal with random amplitude," in *Proc. of the IEEE International Conference on Communications (ICC)*, vol. 3, Apr. 28–May 2, 2002, pp. 1606–1610.

[46] F. F. Digham, M.-S. Alouini, and M. K. Simon, "On the energy detection of unknown signals over fading channels," in *IEEE International Conference on Communications (ICC)*, vol. 5, May 11–15, 2003, pp. 3575–3579.

[47] A. Ghasemi and E. S. Sousa, "Collaborative spectrum sensing for opportunistic access in fading environments," in *Proc. of the 1st IEEE International Symposium on New Frontiers in Dynamic Spectrum Access Networks (DySPAN)*, Nov. 8–11, 2005, pp. 131–136.

[48] ——, "Impact of user collaboration on the performance of sensing-based opportunistic spectrum access," *Proc. of the 64th IEEE Vehicular Technology Conference (VTC-2006 Fall)*, pp. 1–6, Sep. 25–28, 2006.

[49] S. M. Mishra, R. W. Brodersen, S. T. Brink, and R. Mahadevappa, "Detect and avoid: an ultra-wideband/WiMAX coexistence mechanism [Topics in radio communications]," *IEEE Communications Magazine*, vol. 45, no. 6, pp. 68–75, Jun. 2007.

[50] H. Urkowitz, "Energy detection of a random process in colored Gaussian noise," *IEEE Transactions on Aerospace and Electronic Systems*, vol. AES-5, no. 2, pp. 156–162, Mar. 1969.

[51] S. A. Kassam, *Signal Detection in Non-Gaussian Noise*. New York: Springer-Verlag, 1988, 234 pages.

[52] C. Cordeiro, M. Ghosh, D. Cavalcanti, and K. Challapali, "Spectrum sensing for dynamic spectrum access of TV bands," in *Proc. of the 2nd International Conference on Cognitive Radio Oriented Wireless Networks and Communications (CrownCom)*, Jul. 31–Aug. 3, 2007, pp. 225–233.

[53] N. M. Neihart, S. Roy, and D. J. Allstot, "A parallel, multi-resolution sensing technique for multiple antenna cognitive radios," in *Proc. of the IEEE International Symposium on Circuits and Systems (ISCAS)*, May 27–30, 2007, pp. 2530–2533.

[54] A. Pandharipande and J.-P. M. G. Linnartz, "Performance analysis of primary user detection in a multiple antenna cognitive radio," in *Proc. of the IEEE International Conference on Communications (ICC)*, Jun. 24–28, 2007, pp. 6482–6486.

[55] S. M. Kay and S. L. Marple, Jr., "Spectrum analysis—a modern perspective," *Proceedings of the IEEE*, vol. 69, no. 11, pp. 1380–1420, Nov. 1981.

[56] P. Stoica and R. L. Moses, *Introduction to Spectral Analysis*. Upper Saddle River, NJ: Prentice Hall, 1997, 319 pages.

[57] ——, *Spectral Analysis of Signals*. Upper Saddle River, NJ: Prentice Hall, 2005, 452 pages.

[58] H. Sarvanko, M. Mustonen, A. Hekkala, A. Mämmelä, M. Matinmikko, and M. Katz, "Cooperative and noncooperative spectrum sensing techniques using Welch's periodogram in cognitive radios," in *Proc. of the 1st International Workshop on Cognitive Radio and Advanced Spectrum Management (COGART)*, Feb. 14, 2008, pp. 1–5.

[59] B. Farhang-Boroujeny, "Filter bank spectrum sensing for cognitive radios," *IEEE Transactions on Signal Processing*, vol. 56, no. 5, pp. 1801–1811, May.

[60] C. M. Spooner, "Multi-resolution white-space detection for cognitive radio," in *Proc. of the Military Communications Conference (MILCOM)*, Oct. 29–31, 2007, pp. 1–9.

[61] Z. Tian and G. B. Giannakis, "A wavelet approach to wideband spectrum sensing for cognitive radios," in *Proc. of the 1st International Conference on Cognitive Radio Oriented Wireless Networks and Communications (CrownCom)*, Jun. 8–10, 2006, pp. 1–5.

[62] ——, "Compressed sensing for wideband cognitive radios," in *IEEE International Conference on Acoustics, Speech and Signal Processing (ICASSP)*, vol. 4, Apr. 15–20, 2007, pp. 1357–1360.

[63] Y. L. Polo, Y. Wang, A. Pandharipande, and G. Leus, "Compressive wide-band spectrum sensing," in *Proc. of the IEEE International Conference on Acoustics, Speech and Signal Processing (ICASSP)*, Apr. 19–24, 2009, pp. 2337–2340.

[64] Y. Wang, A. Pandharipande, Y. L. Polo, and G. Leus, "Distributed compressive wide-band spectrum sensing," in *Proc. of the Information Theory and Applications Workshop (ITA)*, Feb. 8–13, 2009, pp. 178–183.

[65] Y. Hur, J. Park, W. Woo, K. Lim, C.-H. Lee, H. Kim, and J. Laskar, "A wideband analog multi-resolution spectrum sensing (MRSS) technique for cognitive radio (CR) systems," in *Proc. of the IEEE International Symposium on Circuits and Systems (ISCAS)*, May 21–24, 2006, pp. 4090–4093.

[66] J. Park, Y. Hur, T. J. Song, K. Kim, J. Lee, K. Lim, C.-H. Lee, H. S. Kim, and J. Laskar, "Implementation issues of a wideband multi-resolution spectrum sensing (MRSS) technique for cognitive radio (CR) systems," in *Proc. of the 1st International Conference on Cognitive Radio Oriented Wireless Networks and Communications (CrownCom)*, Jun. 8–10, 2006, pp. 1–5.

[67] Y. Youn, H. Jeon, H. Jung, and H. Lee, "Discrete wavelet packet transform based energy detector for cognitive radios," in *Proc. of the 65th IEEE Vehicular Technology Conference (VTC-2007 Spring)*, Apr. 22–25, 2007, pp. 2641–2645.

[68] J. J. Lehtomäki, J. Vartiainen, M. Juntti, and H. Saarnisaari, "Spectrum sensing with forward methods," in *Proc. of the Military Communications Conference (MILCOM)*, Oct. 23–25, 2006, pp. 1–7.

[69] ——, "CFAR outlier detection with forward methods," *IEEE Transactions on Signal Processing*, vol. 55, no. 9, pp. 4702–4706, Sep. 2007.

[70] J. Vartiainen, H. Sarvanko, J. Lehtomäki, M. Juntti, and M. Latva-aho, "Spectrum sensing with LAD-based methods," in *Proc. of the 18th IEEE International Symposium on Personal, Indoor and Mobile Radio Communications (PIMRC)*, Sep. 3–7, 2007, pp. 1–5.

[71] W. A. Gardner, "Signal interception: A unifying theoretical framework for feature detection," *IEEE Transactions on Communications*, vol. 36, no. 8, pp. 897–906, Aug. 1988.

[72] W. A. Gardner and C. M. Spooner, "Signal interception: Performance advantages of cyclic-feature detectors," *IEEE Transactions on Communications*, vol. 40, no. 1, pp. 149–159, Jan. 1992.

[73] ——, "Detection and source location of weak cyclostationary signals: Simplifications of the maximum-likelihood receiver," *IEEE Transactions on Communications*, vol. 41, no. 6, pp. 905–916, Jun. 1993.

[74] L. Izzo, L. Paura, and M. Tanda, "Signal interception in non-Gaussian noise," *IEEE Transactions on Communications*, vol. 40, no. 6, pp. 1030–1037, Jun. 1992.

[75] P. Rostaing, E. Thierry, and T. Pitarque, "Asymptotic performance analysis of the single-cycle detector," in *Proc. of the European Signal Processing Conference (EUSIPCO)*, Sep. 10–13, 1996.

[76] ——, "Asymptotic performance analysis of cyclic detectors," *IEEE Transactions on Communications*, vol. 47, no. 1, pp. 10–13, Jan. 1999.

[77] W. A. Gardner, A. Napolitano, and L. Paura, "Cyclostationarity: Half a century of research," *Signal Processing*, vol. 86, no. 4, pp. 639–697, Apr. 2006.

[78] W. A. Gardner, "Spectral correlation of modulated signals: Part I—analog modulation," *IEEE Transactions on Communications*, vol. COM-35, no. 6, pp. 584–594, Jun. 1987.

[79] W. A. Gardner, W. A. Brown, III, and C.-K. Chen, "Spectral correlation of modulated signals: Part II—digital modulation," *IEEE Transactions on Communications*, vol. COM-35, no. 6, pp. 595–601, Jun. 1987.

[80] A. Napolitano and C. M. Spooner, "Cyclic spectral analysis of continuous-phase modulated signals," *IEEE Transactions on Signal Processing*, vol. 49, no. 1, pp. 30–44, Jan. 2001.

[81] H. Bölcskei, "Blind estimation of symbol timing and carrier frequency offset in wireless ofdm systems," *IEEE Transactions on Communications*, vol. 49, no. 6, pp. 988–999, Jun. 2001.

[82] M. Öner and F. Jondral, "On the extraction of the channel allocation information in spectrum pooling systems," *IEEE Journal on Selected Areas in Communications*, vol. 25, no. 3, pp. 558–565, Apr. 2007.

[83] A. Tkachenko, D. Cabric, and R. W. Brodersen, "Cyclostationary feature detector experiments using reconfigurable BEE2," in *Proc. of the 2nd IEEE International Symposium on New Frontiers in Dynamic Spectrum Access Networks (DySPAN)*, Apr. 17–20, 2007, pp. 216–219.

[84] E. Serpedin, F. Panduru, I. Sari, and G. B. Giannakis, "Bibliography on cyclostationarity," *Signal Processing*, vol. 85, no. 12, pp. 2233–2303, Dec. 2005.

[85] P. Jallon, "An algorithm for detection of DVB-T signals based on their second-order statistics," *EURASIP Journal on Wireless Communications and Networking*, vol. 2008, Article ID 538236, 9 pages, 2008.

[86] ——, "A spread signals detection algorithm based on the second order statistics in semi-blind contexts," in *Proc. of the 3rd International Conference on Cognitive Radio Oriented Wireless Networks and Communications (CrownCom)*, May 15–17, 2008.

[87] M. Ghozzi, M. Dohler, F. Marx, and J. Palicot, "Cognitive radio: methods for the detection of free bands," *C. R. Physique*, vol. 7, no. 7, pp. 794–804, Sep. 2006.

[88] P. Marques, J. Bastos, and A. Gameiro, "Sensing UMTS bands using cyclostationarity features and cooperation between opportunistic terminals," in *Proc. of the 3rd International Conference on Cognitive Radio Oriented Wireless Networks and Communications (CrownCom)*, May 15–17, 2008.

[89] L. P. Goh, Z. Lei, and F. Chin, "Feature detector for DVB-T signal in multipath fading channel," in *Proc. of the 2nd International Conference on Cognitive Radio Oriented Wireless Networks and Communications (CrownCom)*, Jul. 31–Aug. 3, 2007, pp. 234–240.

[90] M. Öner and F. Jondral, "Air interface identification for software radio systems," *International Journal of Electronics and Communications*, vol. 61, no. 2, pp. 104–117, Feb. 2007.

[91] W. A. Gardner, *Statistical Spectral Analysis: A Nonprobabilistic Theory.* Englewood Cliffs, NJ: Prentice-Hall, 1988, 566 pages.

[92] J. Möttönen and H. Oja, "Multivariate spatial sign and rank methods," *Journal of Nonparametric Statistics*, vol. 5, no. 2, pp. 201–213, 1995.

[93] S. Visuri, V. Koivunen, and H. Oja, "Sign and rank covariance matrices," *Journal of Statistical Planning and Inference*, vol. 91, no. 2, pp. 557–575, Dec. 2000.

[94] O. A. Yeste-Ojeda and J. Grajal, "Detection of unknown signals based on spectral correlation measurements," in *Proc. of the 14th European Signal Processing Conference (EUSIPCO)*, Sep. 4–8, 2006.

[95] R. S. Roberts, W. A. Brown, and H. H. Loomis, Jr., "Computationally efficient algorithms for cyclic spectral analysis," *IEEE Signal Processing Magazine*, vol. 8, no. 2, pp. 38–49, Apr. 1991.

[96] H.-S. Chen, W. Gao, and D. G. Daut, "Spectrum sensing using cyclostationary properties and application to IEEE 802.22 WRAN," in *Proc. of the IEEE Global Communications Conference (GLOBECOM)*, Nov. 26–30, 2007, pp. 3133–3138.

[97] A. Fehske, J. Gaeddart, and J. H. Reed, "A new approach to signal classification using spectral correlation and neural networks," in *Proc. of the 1st IEEE International Symposium on New Frontiers in Dynamic Spectrum Access Networks (DySPAN)*, Nov. 8–11, 2005.

[98] K. Kim, I. A. Akbar, K. K. Bae, J.-S. Urn, C. M. Spooner, and J. H. Reed, "Cyclostationary approaches to signal detection and classification in cognitive radio," in *Proc. of the 2nd IEEE International Symposium on New Frontiers in Dynamic Spectrum Access Networks (DySPAN)*, Apr. 17–20, 2007, pp. 212–215.

[99] C. R. C. da Silva, B. Choi, and K. Kim, "Distributed spectrum sensing for cognitive radio systems," in *Proc. of the Information Theory and Applications Workshop (ITA)*, Jan. 29–Feb. 2, 2007, pp. 120–123.

[100] W. C. Headley, J. D. Reed, and C. R. C. da Silva, "Distributed cyclic spectrum feature-based modulation classification," in *Proc. of the IEEE Wireless Communications and Networking Conference (WCNC)*, Mar. 31–Apr. 3, 2008, pp. 1200–1204.

[101] C. M. Spooner, "Classification of co-channel communication signals using cyclic cumulants," in *Proc. of the 29th Asilomar Conference on Signals, Systems and Computers*, vol. 1, Oct. 30–Nov. 1, 1995, pp. 531–536.

[102] C. M. Spooner, W. A. Brown, and G. K. Yeung, "Automatic radio-frequency environment analysis," in *Proc. of the 34th Asilomar Conference on Signals, Systems and Computers*, vol. 1, Oct. 29–31, 2000, pp. 1181–1186.

[103] C. M. Spooner, "On the utility of sixth-order cyclic cumulants for rf signal classification," in *Proc. of the 35th Asilomar Conference on Signals, Systems and Computers*, vol. 1, Nov. 4–7, 2001, pp. 890–897.

[104] O. A. Dobre, A. Abdi, Y. Bar-Ness, and W. Su, "Cyclostationarity-based blind classification of analog and digital modulations," in *Proc. of the Military Communications Conference (MILCOM)*, Oct. 23–25, 2006, pp. 1–7.

[105] M. K. Tsatsanis and G. B. Giannakis, "Transmitter induced cyclostationarity for blind channel equalization," *IEEE Transactions on Signal Processing*, vol. 45, no. 7, pp. 1785–1794, Jul. 1997.

[106] P. D. Sutton, K. E. Nolan, and L. E. Doyle, "Cyclostationary signatures in practical cognitive radio applications," *IEEE Journal of Selected Areas in Communications*, vol. 26, no. 1, pp. 13–24, Jan. 2008.

[107] K. Maeda, A. Benjebbour, T. Asai, T. Furuno, and T. Ohya, "Recognition among OFDM-based systems utilizing cyclostationarity-inducing transmission," in *Proc. of the 2nd IEEE International Symposium on New Frontiers in Dynamic Spectrum Access Networks (DySPAN)*, Apr. 17–20, 2007.

[108] ——, "Cyclostationary-inducing transmission methods for recognition among OFDM-based systems," *EURASIP Journal on Wireless Communications and Networking*, vol. 2008, Article ID 586172, 14 pages, 2008.

[109] T. Yücek and H. Arslan, "Spectrum characterization for opportunistic cognitive radio systems," in *Proc. of the Military Communications Conference (MILCOM)*, Oct. 23–25, 2006, pp. 1–6.

[110] S. Chaudhari, J. Lundén, and V. Koivunen, "Collaborative autocorrelation-based spectrum sensing of OFDM signals in cognitive radios," in *Proc. of the 42nd Annual Conference on Information Sciences and Systems (CISS)*, Mar. 19–21, 2008, pp. 191–196.

[111] S. Chaudhari, V. Koivunen, and H. V. Poor, "Autocorrelation-based decentralized sequential detection of OFDM signals in cognitive radios," *IEEE Transactions on Signal Processing*, vol. 57, no. 7, pp. 2690–2700, Jul. 2009.

[112] ——, "Distributed autocorrelation-based sequential detection of OFDM signals in cognitive radios," in *Proc. of the 3rd International Conference on Cognitive Radio Oriented Wireless Networks and Communications (CrownCom)*, May 15–17, 2008, pp. 1–6.

[113] S.-Y. Tu, K.-C. Chen, and R. Prasad, "Spectrum sensing of OFDMA systems for cognitive radios," in *Proc. of the 18th IEEE International Symposium on Personal, Indoor and Mobile Radio Communications (PIMRC)*, Sep. 3–7, 2007, pp. 1–5.

[114] Y. Zeng and Y.-C. Liang, "Spectrum-sensing algorithms for cognitive radio based on statistical covariances," *IEEE Transactions on Vehicular Technology*, vol. 58, no. 4, pp. 1804–1815, May 2009.

[115] ——, "Eigenvalue based spectrum sensing algorithms for cognitive radio," Apr. 2008, [Online.] Available: http://arxiv.org/abs/0804.2960v1 [Accessed: Nov. 3, 2008].

[116] B. Wild and K. Ramchandran, "Detecting primary receivers for cognitive radio applications," in *Proc. of the 1st IEEE International Symposium on New Frontiers in Dynamic Spectrum Access Networks (DySPAN)*, Nov. 8–11, 2005, pp. 124–130.

[117] R. Viswanathan and P. K. Varshney, "Distributed detection with multiple sensors: Part I — fundamentals," *Proceedings of the IEEE*, vol. 85, no. 1, pp. 54–63, Jan. 1997.

[118] R. S. Blum, S. A. Kassam, and V. H. Poor, "Distributed detection with multiple sensors: Part II — advanced topics," *Proceedings of the IEEE*, vol. 85, no. 1, pp. 64–79, Jan. 1997.

[119] P. K. Varshney, *Distributed detection and data fusion.* New York: Springer-Verlag, 1996, 292 pages.

[120] A. Paulraj, R. Nabar, and D. Gore, *Introduction to Space-Time Wireless Communications.* Cambridge University Press, 2003, 277 pages.

[121] M. Gudmundson, "Correlation model for shadow fading in mobile radio systems," *Electronics Letters*, vol. 27, no. 23, pp. 2145–2146, 1991.

[122] C. Cordeiro and D. Challapali, K. Birru, "IEEE 802.22: An introduction to the first wireless standard based on cognitive radios," *Journal of Communications*, vol. 1, no. 1, pp. 38–47, Apr. 2006.

[123] S. J. Shellhammer, "Spectrum sensing in IEEE 802.22," in *Proc. of the IAPR Workshop on Cognitive Information Processing (CIP)*, Jun. 9–10, 2008.

[124] E. Visotsky, S. Kuffner, and R. Peterson, "On collaborative detection of TV transmissions in support of dynamic spectrum sharing," in *Proc. of the 1st IEEE International Symposium on New Frontiers in Dynamic Spectrum Access Networks (DySPAN)*, Nov. 8–11, 2005, pp. 338–345.

[125] A. Ghasemi and E. S. Sousa, "Asymptotic performance of collaborative spectrum sensing under correlated log-normal shadowing," *IEEE Communications Letters*, vol. 11, no. 1, pp. 34–36, Jan. 2007.

[126] S. M. Mishra, A. Sahai, and R. W. Brodersen, "Cooperative sensing among cognitive radios," in *Proc. of the IEEE International Conference on Communications (ICC)*, vol. 4, Jun. 11–15, 2006, pp. 1658–1663.

[127] A. Taherpour, Y. Norouzi, M. Nasiri-Kenari, A. Jamshidi, and Z. Zeinalpour-Yazdi, "Asymptotically optimum detection of primary user in cognitive radio networks," *IET Communications*, vol. 1, no. 6, pp. 1138–1145, Dec. 2007.

[128] F. E. Visser, G. J. M. Janssen, and P. Pawelczak, "Multinode spectrum sensing based on energy detection for dynamic spectrum access," in *Proc. of the IEEE Vehicular Technology Conference (VTC-2008 Spring)*, May 11–14, 2008, pp. 1394–1398.

[129] S. Kyperountas, N. Correal, Q. Shi, and Z. Ye, "Performance analysis of cooperative spectrum sensing in Suzuki fading channels," in

Proc. of the 2nd International Conference on Cognitive Radio Oriented Wireless Networks and Communications (CrownCom), Jul. 31–Aug. 3, 2007, pp. 428–432.

[130] E. Peh and Y.-C. Liang, "Optimization for cooperative sensing in cognitive radio networks," in *Proc. of the IEEE Wireless Communications and Networking Conference (WCNC)*, Mar. 11–15, 2007, pp. 27–32.

[131] W. Zhang, R. K. Mallik, and K. B. Letaief, "Signal detection for OFDM/OQAM system using cyclostationary signatures," in *Proc. of the IEEE International Conference on Communications (ICC)*, May 19–23, 2008, pp. 3411–3415.

[132] Z. Quan, S. Cui, A. H. Sayed, and H. V. Poor, "Spatial-spectral joint detection for wideband spectrum sensing in cognitive radio networks," in *Proc. of the IEEE International Conference on Acoustics, Speech and Signal Processing (ICASSP)*, Mar. 31–Apr. 4, 2008, pp. 2793–2796.

[133] ——, "Wideband spectrum sensing in cognitive radio networks," in *Proc. of the IEEE International Conference on Communications (ICC)*, May 19–23, 2008, pp. 901–906.

[134] Z. Quan, S. Cui, H. V. Poor, and A. H. Sayed, "Collaborative wideband sensing for cognitive radios," *IEEE Signal Processing Magazine*, vol. 25, no. 6, pp. 60–73, Nov. 2008.

[135] Z. Quan, S. Cui, A. H. Sayed, and H. V. Poor, "Optimal multiband joint detection for spectrum sensing in cognitive radio networks," *IEEE Transactions on Signal Processing*, vol. 57, no. 3, pp. 1128–1140, Mar. 2009.

[136] N. Ansari, J.-G. Chen, and Y.-Z. Zhang, "Adaptive decision fusion for unequiprobable sources," *IEE Proceedings — Radar, Sonar and Navigation*, vol. 144, no. 3, pp. 105–111, Jun 1997.

[137] N. Mansouri and M. Fathi, "Simple counting rule for optimal data fusion," in *Proc. of the IEEE Conference on Control Applications (CCA)*, vol. 2, Jun. 23–25, 2003, pp. 1186–1191.

[138] L. Chen, J. Wang, and S. Li, "An adaptive cooperative spectrum sensing scheme based on the optimal data fusion rule," in *Proc. of the 4th International Symposium on Wireless Communication Systems (ISWCS)*, Oct. 17–19, 2007, pp. 582–586.

[139] G. Ganesan and L. Ye, "Cooperative spectrum sensing in cognitive radio, part II: Two user networks," *IEEE Transactions on Wireless Communications*, vol. 6, no. 6, pp. 2204–2213, Jun. 2007.

[140] ——, "Cooperative spectrum sensing in cognitive radio, part II: Multiuser networks," *IEEE Transactions on Wireless Communications*, vol. 6, no. 6, pp. 2214–2222, Jun. 2007.

[141] G. Ganesan, L. Ye, B. Bing, and S. Li, "Spatiotemporal sensing in cognitive radio networks," *IEEE Journal of Selected Areas in Communications*, vol. 26, no. 1, pp. 5–12, Jan. 2008.

[142] J. Unnikrishnan and V. V. Veeravalli, "Cooperative sensing for primary detection in cognitive radio," *IEEE Journal of Selected Topics in Signal Processing*, vol. 2, no. 1, pp. 18–27, Feb. 2008.

[143] S. C. A. Thomopoulos and L. Zhang, "Distributed decision fusion in the presence of networking delays and channel errors," *Information Sciences*, vol. 66, no. 1–2, pp. 91–118, Dec. 1992.

[144] B. Chen, R. Jiang, T. Kasetkasem, and P. K. Varshney, "Channel aware decision fusion in wireless sensor networks," *IEEE Transactions on Signal Processing*, vol. 52, no. 12, pp. 3454–3458, Dec. 2004.

[145] R. Niu, B. Chen, and P. Varshney, "Fusion of decisions transmitted over rayleigh fading channels in wireless sensor networks," *IEEE Transactions on Signal Processing*, vol. 54, no. 3, pp. 1018–1027, Mar. 2006.

[146] B. Chen and P. K. Willett, "On the optimality of the likelihood-ratio test for local sensor decision rules in the presence of nonideal channels," *IEEE Transactions on Information Theory*, vol. 51, no. 2, pp. 693–699, Feb. 2005.

[147] Z. Quan, S. Cui, and A. H. Sayed, "Optimal linear cooperation for spectrum sensing in cognitive radio networks," *IEEE Journal of Selected Topics in Signal Processing*, vol. 2, no. 1, pp. 28–40, Feb. 2008.

[148] C. Sun, W. Zhang, and K. B. Letaief, "Cluster-based cooperative spectrum sensing in cognitive radio systems," in *Proc. of the IEEE International Conference on Communications (ICC)*, Jun. 24–28, 2007, pp. 2511–2515.

[149] C. Rago, P. Willett, and Y. Bar-Shalom, "Censoring sensors: A low-communication-rate scheme for distributed detection," *IEEE Transactions on Aerospace and Electronic Systems*, vol. 32, no. 2, pp. 554–568, Apr. 1996.

[150] S. Appadwedula, V. V. Veeravalli, and D. L. Jones, "Robust and locally-optimum decentralized detection with censoring sensors," in *Proc. of the 5th International Conference on Information Fusion (FUSION)*, Jul. 8–11, 2002, pp. 56–63.

[151] S. Appadwedula, "Energy-efficient sensor networks for detection applications," Ph.D. dissertation, University of Illinois at Urbana-Champaign, 2003.

[152] S. Appadwedula, V. V. Veeravalli, and D. L. Jones, "Energy-efficient detection in sensor networks," *IEEE Journal on Selected Areas in Communications*, vol. 23, no. 4, pp. 693–702, Apr. 2005.

[153] ——, "Decentralized detection with censoring censors," *IEEE Transactions on Signal Processing*, vol. 56, no. 4, pp. 1362–1373, Apr. 2008.

[154] R. Jiang and B. Chen, "Fusion of censored decisions in wireless sensor networks," *IEEE Transactions on Wireless Communications*, vol. 4, no. 6, pp. 2668–2673, Nov. 2005.

[155] R. S. Blum and B. M. Sadler, "Energy efficient signal detection in sensor networks using ordered transmissions," *IEEE Transactions on Communications*, vol. 56, no. 7, pp. 3229–3235, Jul. 2008.

[156] C.-T. Yu and P. K. Varshney, "Bit allocation for discrete signal detection," *IEEE Transactions on Communications*, vol. 46, no. 2, pp. 173–175, Feb. 1998.

[157] ——, "Paradigm for distributed detection under communication rate constraints," *Optical Engineering*, vol. 37, no. 2, pp. 417–426, Feb. 1998.

[158] C.-H. Lee and W. Wolf, "Energy efficient techniques for cooperative spectrum sensing in cognitive radios," in *Proc. of the 5th IEEE Consumer Communications and Networking Conference (CCNC)*, Jan. 10–12, 2008, pp. 968–972.

[159] C. Sun, W. Zhang, and K. B. Letaief, "Cooperative spectrum sensing for cognitive radios under bandwidth constraints," in *Proc. of the IEEE Wireless Communications and Networking Conference (WCNC)*, Mar. 11–15, 2007, pp. 1–5.

[160] K. B. Letaief and W. Zhang, "Cooperative spectrum sensing," in *Cognitive Wireless Communication Networks*, E. Hossain and V. K. Bhargava, Eds. Springer, 2007, ch. 4.

[161] H. V. Poor and O. Hadjiliadis, *Quickest Detection*. Cambridge University Press, 2009, 244 pages.

[162] E. S. Page, "Continuous inspection schemes," *Biometrika*, vol. 41, no. 1–2, pp. 100–115, 1954.

[163] G. V. Moustakides, "Optimal stopping times for detecting changes in distributions," *The Annals of Statistics*, vol. 14, no. 4, pp. 1379–1387, 1986.

[164] L. Lai, Y. Fan, and H. V. Poor, "Quickest detection in cognitive radio: A sequential change detection framework," in *Proc. of the IEEE Global Communications Conference (GLOBECOM)*, Nov. 30–Dec. 4, 2008, pp. 1–5.

[165] H. Li, C. Li, and H. Dai, "Quickest spectrum sensing in cognitive radio," in *Proc. of the 42nd Annual Conference on Information Sciences and Systems (CISS)*, Mar. 19–21, 2008, pp. 203–208.

[166] V. V. Veeravalli, "Decentralized quickest change detection," *IEEE Transactions on Information Theory*, vol. 47, no. 4, pp. 1657–1665, May 2001.

[167] S. Tantaratana, "Some recent results on sequential detection," in *Advances in Statistical Signal Processing-Vol. 2: Signal Detection*, H. V. Poor and J. B. Thomas, Eds. Greenwich, CT: JAI, 1993.

[168] T. L. Lai, "Sequential analysis: Some classical problems and new challenges," *Statistica Sinica*, vol. 11, no. 2, pp. 303–408, Apr. 2001.

[169] A. Wald, "Sequential tests of statistical hypothesis," *The Annals of Mathematical Statististics*, vol. 16, no. 2, pp. 117–186, Apr. 1945.

[170] N. Kundargi and A. Tewfik, "Sequential pilot sensing of ATSC signals in IEEE 802.22 cognitive radio networks," in *Proc. of the IEEE International Conference on Acoustics, Speech and Signal Processing (ICASSP)*, Mar. 31–Apr. 4, 2008, pp. 2789–2792.

[171] S. A. Kassam and H. V. Poor, "Robust techniques for signal processing: A survey," *Proceedings of the IEEE*, vol. 73, no. 3, pp. 433–482, Mar. 1985.

[172] S. A. Kassam, "Nonparametric signal detection," in *Advances in Statistical Signal Processing*, H. V. Poor and J. B. Thomas, Eds. JAI Press Inc., 1993, pp. 66–91.

[173] B. L. Lewis, F. F. Kretschmer, Jr., and W. W. Shelton, *Aspects of radar signal processing.* Artech House, Inc., 1986, 568 pages.

[174] P. E. Pace, *Detecting and classifying low probability of intercept radar.* Artech House, 2004, 484 pages.

[175] E. R. Zilberman and P. E. Pace, "Autonomous time-frequency morphological feature extraction algorithm for LPI radar modulation classification," in *Proc. of the IEEE International Conference on Image Processing (ICIP)*, Oct. 8–11, 2006, pp. 2321–2324.

[176] C. De Luigi and C. Jauffret, "Estimation and classification of FM signals using time frequency transforms," *IEEE Transactions on Aerospace and Electronic Systems*, vol. 41, no. 2, pp. 421–437, Apr. 2005.

[177] G. López-Risueño, J. Grajal, and A. Sanz-Osorio, "Digital channelized receiver based on time-frequency analysis for signal interception," *IEEE Transactions on Aerospace and Electronic Systems*, vol. 41, no. 3, pp. 879–898, Jul. 2005.

[178] G. López-Risueño, J. Grajal, and O. Yeste-Ojeda, "Atomic decomposition-based radar complex signal interception," *IEE Proceedings – Radar, Sonar and Navigation*, vol. 150, no. 4, pp. 323–331, Aug. 2003.

[179] G. López-Risueño and J. Grajal, "Multiple signal detection and estimation using atomic decomposition and EM," *IEEE Transactions on Aerospace and Electronic Systems*, vol. 42, no. 1, pp. 84–102, Jan. 2006.

[180] G. Zhang, "Intra-pulse modulation recognition of advanced radar emitter signals using intelligent recognition method," in *Rough Sets and Knowledge Technology, Lecture Notes in Computer Science*, G. W. et al., Ed. Springer Verlag Berlin Heidelberg, 2006, pp. 707–712.

[181] G. Zhang, H. Rong, and W. Jin, "Intra-pulse modulation recognition of unknown radar emitter signals using support vector clustering," in *Fuzzy Systems and Knowledge Discovery, Lecture Notes in Computer Science*, L. W. et al., Ed. Springer Verlag Berlin Heidelberg, 2006, pp. 420–429.

[182] T.-W. Chen and W.-D. Jin, "Feature extraction of radar emitter signals based on symbolic time series analysis," in *Proc. of the 2007 International Conference on Wavelet Analysis and Pattern Recognition (ICWAPR)*, Nov. 2–4, 2007, pp. 1277–1282.

[183] P. Ciblat, P. Loubaton, E. Serpedin, and G. B. Giannakis, "Asymptotic analysis of blind cyclic correlation-based symbol-rate estimators," *IEEE Transactions on Information Theory*, vol. 48, no. 7, pp. 1922–1934, Jul. 2002.

[184] C. M. Bishop, *Neural networks for pattern recognition.* Oxford University Press, 1995.

[185] R. M. Neal, *Bayesian learning for neural networks*, ser. Lecture Notes in Statistics. New York: Springer-Verlag, 1996, vol. 118, 204 pages.

[186] A. K. Nandi and E. E. Azzouz, "Automatic analogue modulation recognition," *Signal Processing*, vol. 46, no. 2, pp. 211–222, Oct. 1995.

[187] M. L. D. Wong and A. K. Nandi, "Automatic digital modulation recognition using artificial neural network and genetic algorithm," *Signal Processing*, vol. 84, no. 2, pp. 351–365, Feb. 2004.

[188] S. J. Roome, "Classification of radar signals in modulation domain," *Electronics Letters*, vol. 28, no. 8, pp. 704–705, Apr. 1992.

[189] A. K. Nandi and E. E. Azzouz, "Algorithms for automatic modulation recognition of communication signals," *IEEE Transactions on Communications*, vol. 46, no. 4, pp. 431–436, Apr. 1998.

[190] A. Swami and B. M. Sadler, "Hierarchical digital modulation classification using cumulants," *IEEE Transactions on Communications*, vol. 48, no. 3, pp. 416–429, Mar. 2000.

[191] N. Kwak and C.-H. Choi, "Input feature selection by mutual information based on Parzen window," *IEEE Transactions on Pattern Analysis and Machine Intelligence*, vol. 24, no. 12, pp. 1667–1671, Dec. 2002.

[192] R. G. Wiley, *ELINT: The interception and analysis of radar signals*. Boston: Artech House, 2006, 478 pages.

[193] L. E. Langley, "Specific emitter identification (SEI) and classical parameter fusion technology," in *Proc. of the WESCON/'93*, Sep. 28–30, 1993, pp. 377–381.

[194] I. Kimber, "Generic techniques for the identification of wanted and unwanted modulations on pulses," in *IEE Colloquium on Signal Processing in Electronic Warfare*, Jan. 31, 1994, pp. 5/1–5/4.

[195] K. I. Talbot, P. R. Duley, and M. H. Hyatt, "Specific emitter identification and verification," *Technology Review Journal*, pp. 113–133, Spring/Summer 2003.

[196] Ö. H. Tekbaş, N. Serinken, and O. Üreten, "An experimental performance evaluation of a novel radio-transmitter identification system under diverse environmental conditions," *Canadian Journal of Electrical and Computer Engineering*, vol. 29, no. 3, pp. 203–209, Jul. 2004.

[197] O. Üreten and N. Serinken, "Wireless security through RF fingerprinting," *Canadian Journal of Electrical and Computer Engineering*, vol. 32, no. 1, pp. 27–33, Winter 2007.

[198] R. D. Hippenstiel and Y. Payal, "Wavelet based transmitter identification," in *Proc. of the 4th International Symposium on Signal Processing and Its Applications (ISSPA)*, vol. 2, Aug. 25–30, 1996, pp. 740–742.

[199] D. Shaw and W. Kinsner, "Multifractal modelling of radio transmitter transients for classification," in *Proc. of the IEEE Conference on Communications, Power and Computing (WESCANEX)*, May 22–23, 1997, pp. 306–312.

[200] O. Üreten and N. Serinken, "Bayesian detection of WiFi transmitter RF fingerprints," *Electronics Letters*, vol. 41, no. 6, pp. 373–374, Mar. 2005.

[201] J. Hall, M. Barbeau, and E. Kranakis, "Detection of transient in radio frequency fingerprinting using signal phase," in *Proc. of the 3rd IASTED International Conference on Wireless and Optical Communications (WOC)*, Jul. 14–16, 2003, pp. 13–18.

[202] ——, "Enhancing intrusion detection in wireless networks using radio frequency fingerprinting," in *Proc. Communications, Internet, and Information Technology (CIIT)*, Nov. 22–24, 2004.

[203] ——, "Detection of rogue devices in Bluetooth networks using radio frequency fingerprinting," in *Proc. of the IASTED International Conference on Communications and Computer Networks (CCN)*, Oct. 4–6, 2006.

[204] J. Hall, "Detection of rogue devices in wireless networks," Ph.D. dissertation, School of Computer Science, Carleton University, Ottawa, 2006.

[205] R. M. Gerdes, T. E. Daniels, M. Mina, and S. F. Russell, "Device identification via analog signal fingerprinting: a matched filter approach," in *Proc. of the 13th Annual Symposium on Network and Distributed System Security (NDSS)*, Feb. 2–3, 2006.

[206] K. A. Remley, C. A. Grosvenor, R. T. Johnk, D. R. Novotny, P. D. Hale, M. D. McKinley, A. Karygiannis, and E. Antonakakis, "Electromagnetic signatures of WLAN cards and network security," in *Proc. of the 5th IEEE International Symposium on Signal Processing and Information Technology (ISSPIT)*, Dec. 18–21, 2005, pp. 484–488.

[207] V. Brik, S. Banerjee, M. Gruteser, and S. Oh, "Wireless device identification with radiometric signatures," in *Proc. of the 14th ACM International Conference on Mobile Computing and Networking (MobiCom)*, Sep. 14–19, 2008, pp. 116–127.

[208] A. Kawalec and R. Owczarek, "Radar emitter recognition using intrapulse data," in *Proc. of the 15th International Conference on Microwaves, Radar and Wireless Communications (MIKON)*, vol. 2, May 17–19, 2004, pp. 435–438.

[209] ——, "Specific emitter identification using intrapulse data," in *Proc. of the European Radar Conference (EuRAD)*, Oct. 14–15, 2004, pp. 249–252.

[210] J. Liu, S. Gao, Z.-Q. Luo, T. N. Davidson, and J. P. Y. Lee, "The minimum description length criterion applied to emitter number detection and pulse classification," in *Proc. 9th IEEE Signal Processing Workshop on Statistical Signal and Array Processing (SSAP)*, Sep. 14–16, 1998, pp. 172–175.

[211] K. M. Wong, Z.-Q. Luo, J. Liu, J. P. Y. Lee, and S. W. Gao, "Radar emitter classification using intrapulse data," *International Journal of Electronics and Communications*, pp. 324–332, Dec. 1999.

[212] J. Liu, J. P. Y. Lee, L. Li, Z.-Q. Luo, and K. M. Wong, "Online clustering algorithms for radar emitter identification," *IEEE Transactions on Pattern Analysis and Machine Intelligence*, vol. 27, no. 8, pp. 1185–1196, Aug. 2005.

[213] B. W. Gillespie and L. E. Atlas, "Optimization of time and frequency resolution for radar transmitter identification," in *Proc. IEEE International Conference on Acoustics, Speech, and Signal Processing (ICASSP)*, vol. 3, Mar. 15–19, 1999, pp. 1341–1344.

[214] ——, "Optimizing time-frequency kernels for classification," *IEEE Transactions on Signal Processing*, vol. 49, no. 3, pp. 485–496, Mar. 2001.

[215] L. Cohen, "Time-frequency distributions-a review," *Proceedings of the IEEE*, vol. 77, no. 7, pp. 941–981, Jul. 1989.

[216] S. D. Howard, "Estimation and correlation of radar pulse modulations for electronic support," in *Proc. of the IEEE Aerospace Conference*, vol. 5, Mar. 8–15, 2003, pp. 2065–2072.

[217] S. Heritier and E. Ronchetti, "Robust bounded-influence tests in general parametric models," *Journal of the American Statistical Association*, vol. 89, no. 427, pp. 897–904, Sep. 1994.

[218] P. J. Huber, *Robust Statistics*. New York: John Wiley & Sons, 1981, 308 pages.

[219] G.-S. Liu, H. Gu, W.-M. Su, H.-B. Sun, and J.-H. Zhang, "Random signal radar — a winner in both the military and civilian operating environments," *IEEE Transactions on Aerospace and Electronic Systems*, vol. 39, no. 2, pp. 489–498, Apr. 2003.

[220] S. Haykin, "Cognitive radar: A way of the future," *IEEE Signal Processing Magazine*, vol. 23, no. 1, pp. 30–40, Jan. 2006.

[221] A. G. Stove, A. L. Hume, and C. J. Baker, "Low probability of intercept radar strategies," *IEE Proceedings – Radar, Sonar and Navigation*, vol. 151, no. 5, pp. 249–260, Oct. 2004.

[222] P. Chaporkar and A. Proutiere, "Optimal joint probing and transmission strategy for maximizing throughput in wireless systems," *IEEE Journal of Selected Areas in Communications*, vol. 26, no. 8, pp. 1546–1555, Oct. 2008.

[223] G. Scutari, D. P. Palomar, and S. Barbarossa, "Cognitive MIMO radio: Competitive optimality design based on subspace projections," *IEEE Signal Processing Magazine*, vol. 25, no. 6, pp. 46–59, Nov. 2008.

[224] H. Jiang, L. Lai, R. Fan, and H. V. Poor, "Optimal selection of channel sensing order in cognitive radio," *IEEE Transactions on Wireless Communications*, vol. 8, no. 1, pp. 297–307, Jan. 2009.

[225] A. T. Hoang, Y.-C. Liang, D. T. C. Wong, Y. Zeng, and R. Zhang, "Opportunistic spectrum access for energy-constrained cognitive radios," *IEEE Transactions on Wireless Communications*, vol. 8, no. 3, pp. 1206–1211, Mar. 2009.

[226] Q. H. Vuong, "Likelihood ratio tests for model selection and nonnested hypotheses," *Econometrica*, vol. 57, no. 2, pp. 307–333, Mar. 1993.

[227] L. A. Stefanski and D. D. Boos, "The calculus of M-estimation," *The American Statistician*, vol. 56, no. 1, pp. 29–38, Feb. 2002.

[228] M. Bilodeau and D. Brenner, *Theory of Multivariate Statistics*, ser. Springer Texts in Statistics. New York: Springer-Verlag, 1999, 288 pages.

Appendix A

Characteristic function of a truncated normal distributed random variable

A one-sidedly truncated normal distribution is given by

$$f(x) = \begin{cases} \frac{1}{1-F\left(\frac{t-\mu}{\sigma}\right)} \frac{1}{\sqrt{2\pi}\sigma} \exp\left(-\frac{(x-\mu)^2}{2\sigma^2}\right) & , x \geq t, \\ 0 & , x < t, \end{cases} \tag{A.1}$$

where μ and σ^2 are the mean and variance of the underlying normal distribution $N(\mu, \sigma^2)$, respectively, and $F(x)$ is the cdf of the standard normal distribution $N(0, 1)$.

The characteristic function of a random variable X distributed according to (A.1) is given by

$$\Phi(\omega) = \frac{1}{1 - F\left(\frac{t-\mu}{\sigma}\right)} \exp\left(j\mu\omega - \frac{\sigma^2\omega^2}{2}\right) \left(1 - F\left(\frac{t - (\mu + j\sigma^2\omega)}{\sigma}\right)\right), \tag{A.2}$$

where j is the imaginary unit.

The mean of a one-sidedly truncated normal distributed random variable X is given by

$$E[X] = \mu + \frac{\sigma}{1 - F\left(\frac{t-\mu}{\sigma}\right)} f\left(\frac{t-\mu}{\sigma}\right), \tag{A.3}$$

and the variance is given by

$$\mathrm{Var}(X) = \mu^2 + \sigma^2 + \frac{1}{1 - F\left(\frac{t-\mu}{\sigma}\right)} \left(2\mu\sigma f\left(\frac{t-\mu}{\sigma}\right) + \frac{1}{\sqrt{2\pi}}\sigma\left(t-\mu\right) \exp\left(-\frac{(t-\mu)^2}{2\sigma}\right)\right). \tag{A.4}$$

Appendix B

Asymptotic distribution of the robust likelihood-ratio type test

The asymptotic distribution of the robust likelihood ratio-type test in general parametric models for real valued data has been derived in [217]. In the following, we derive the asymptotic distribution of the robust likelihood ratio-type test in general parametric models for complex valued data. The derivation follows the derivation of the asymptotic distribution of the classical GLRT in [226]. Note that the following is not a rigorous proof, it is merely an outline.

We start by deriving an intermediate result, the asymptotic distribution of the M-estimator for complex valued data, required in the final derivation. The derivation of the asymptotic distribution of the M-estimator for complex valued data follows the derivation for real valued data in [227].

B.1 Asymptotic distribution of the M-estimator

Let $\boldsymbol{\theta}_0$ and $\hat{\boldsymbol{\theta}}_n$ denote the true parameter value and its M-estimate obtained from n samples, respectively. Let us stack the real and imaginary parts of the difference vector $\hat{\boldsymbol{\theta}}_n - \boldsymbol{\theta}_0$ separately to the same vector and denote it by $\boldsymbol{d}_n$, i.e.

$$\boldsymbol{d}_n = \begin{bmatrix} \mathrm{Re}\{(\hat{\theta}_n - \theta_0)_1\} \\ \mathrm{Im}\{(\hat{\theta}_n - \theta_0)_1\} \\ \mathrm{Re}\{(\hat{\theta}_n - \theta_0)_2\} \\ \mathrm{Im}\{(\hat{\theta}_n - \theta_0)_2\} \\ \vdots \\ \mathrm{Re}\{(\hat{\theta}_n - \theta_0)_p\} \\ \mathrm{Im}\{(\hat{\theta}_n - \theta_0)_p\} \end{bmatrix} = \begin{bmatrix} (\hat{\theta}_n - \theta_0)_{1,r} \\ (\hat{\theta}_n - \theta_0)_{1,i} \\ (\hat{\theta}_n - \theta_0)_{2,r} \\ (\hat{\theta}_n - \theta_0)_{2,i} \\ \vdots \\ (\hat{\theta}_n - \theta_0)_{p,r} \\ (\hat{\theta}_n - \theta_0)_{p,i} \end{bmatrix} \tag{B.1}$$

where the first subindex denotes the respective component and the second the real or imaginary part.

The M-estimator $\hat{\boldsymbol{\theta}}_n$ of $\boldsymbol{\theta_0}$ is defined by

$$\sum_{i=1}^{n} \boldsymbol{\psi}(\boldsymbol{z}_i, \hat{\boldsymbol{\theta}}_n) = \mathbf{0}, \tag{B.2}$$

where $\boldsymbol{z}_1, \ldots, \boldsymbol{z}_n$ are independent random vectors. The $\boldsymbol{\psi}$ function is the derivative of the ρ function defined as

$$\boldsymbol{\psi} = \frac{\partial \rho}{\partial \boldsymbol{\theta}} = \begin{bmatrix} \frac{\partial \rho}{\partial \theta_{1,r}} \\ \frac{\partial \rho}{\partial \theta_{1,i}} \\ \vdots \\ \frac{\partial \rho}{\partial \theta_{p,r}} \\ \frac{\partial \rho}{\partial \theta_{p,i}} \end{bmatrix} = \begin{bmatrix} \psi_{1,r} \\ \psi_{1,i} \\ \vdots \\ \psi_{p,r} \\ \psi_{p,i} \end{bmatrix}. \tag{B.3}$$

Assuming that the $\boldsymbol{\psi}$ function is suitably smooth, the Taylor expansion of $\boldsymbol{g}_n(\boldsymbol{\theta}) = n^{-1} \sum_{i=1}^{n} \boldsymbol{\psi}(\boldsymbol{z}_i, \boldsymbol{\theta})$ gives

$$\mathbf{0} = \boldsymbol{g}_n(\hat{\boldsymbol{\theta}}) = \boldsymbol{g}_n(\boldsymbol{\theta}_0) + \frac{\partial \boldsymbol{g}_n}{\partial \boldsymbol{\theta}}(\boldsymbol{\theta}_0)\boldsymbol{d}_n + \boldsymbol{o}_p(1),$$

where notation $\boldsymbol{o}_p(1)$ indicates a quantity that converges in probability to zero.

For large enough n, $\frac{\partial \boldsymbol{g}_n}{\partial \boldsymbol{\theta}}(\boldsymbol{\theta}_0)$ is expected to be nonsingular. Rearrangement gives

$$\sqrt{n}\boldsymbol{d}_n = \left(-\frac{\partial \boldsymbol{g}_n}{\partial \boldsymbol{\theta}}(\boldsymbol{\theta}_0) \right)^{-1} \sqrt{n}\boldsymbol{g}_n(\boldsymbol{\theta}_0) + \sqrt{n}\boldsymbol{o}_p'(1). \tag{B.4}$$

Under suitable regularity conditions as $n \to \infty$, the weak law of large numbers gives

$$-\frac{\partial \boldsymbol{g}_n}{\partial \boldsymbol{\theta}}(\boldsymbol{\theta}_0) = -n^{-1} \sum_{i=1}^{n} \frac{\partial \boldsymbol{\psi}}{\partial \boldsymbol{\theta}}(\boldsymbol{z}_i, \boldsymbol{\theta}_0) \xrightarrow{P} -E\left[\frac{\partial \boldsymbol{\psi}}{\partial \boldsymbol{\theta}}(\boldsymbol{z}, \boldsymbol{\theta}_0) \right] = \boldsymbol{A}(\boldsymbol{\theta}_0), \tag{B.5}$$

where $\frac{\partial \boldsymbol{\psi}}{\partial \boldsymbol{\theta}}$ is given by

$$\frac{\partial \boldsymbol{\psi}}{\partial \boldsymbol{\theta}} = \begin{bmatrix} \frac{\partial \psi_{1,r}}{\partial \theta_{1,r}} & \frac{\partial \psi_{1r}}{\partial \theta_{1,i}} & \cdots & \frac{\partial \psi_{1,r}}{\partial \theta_{p,r}} & \frac{\partial \psi_{1,r}}{\partial \theta_{p,i}} \\ \frac{\partial \psi_{1,i}}{\partial \theta_{1,r}} & \frac{\partial \psi_{1,i}}{\partial \theta_{1,i}} & \cdots & \frac{\partial \psi_{1,i}}{\partial \theta_{p,r}} & \frac{\partial \psi_{1,i}}{\partial \theta_{p,i}} \\ \vdots & \vdots & \ddots & \vdots & \vdots \\ \frac{\partial \psi_{p,r}}{\partial \theta_{1,r}} & \frac{\partial \psi_{p,r}}{\partial \theta_{1,i}} & \cdots & \frac{\partial \psi_{p,r}}{\partial \theta_{p,r}} & \frac{\partial \psi_{p,r}}{\partial \theta_{p,i}} \\ \frac{\partial \psi_{p,i}}{\partial \theta_{1,r}} & \frac{\partial \psi_{p,i}}{\partial \theta_{1,i}} & \cdots & \frac{\partial \psi_{p,i}}{\partial \theta_{p,r}} & \frac{\partial \psi_{p,i}}{\partial \theta_{p,i}} \end{bmatrix}. \tag{B.6}$$

The central limit theorem gives (as $n \to \infty$)

$$\sqrt{n}\boldsymbol{g}_n(\boldsymbol{\theta}_0) \xrightarrow{D} N(\mathbf{0}, \boldsymbol{B}(\boldsymbol{\theta}_0)), \text{ where } \boldsymbol{B}(\boldsymbol{\theta}_0) = E\left[\boldsymbol{\psi}(\boldsymbol{z}, \boldsymbol{\theta}_0)\boldsymbol{\psi}(\boldsymbol{z}, \boldsymbol{\theta}_0)^T\right]. \quad \text{(B.7)}$$

The last term in (B.4) convergences in probability to zero vector in most situations provided that $\boldsymbol{\psi}$ is sufficiently smooth and $\boldsymbol{\theta}$ has a fixed dimension [218].

From the above results and from the multivariate Slutsky's theorem [228, p. 78], it follows that as $n \to \infty$

$$\sqrt{n}\boldsymbol{d}_n \xrightarrow{D} N(\mathbf{0}, \boldsymbol{V}(\boldsymbol{\theta}_0)), \text{ where } \boldsymbol{V}(\boldsymbol{\theta}_0) = \boldsymbol{A}(\boldsymbol{\theta}_0)^{-1}\boldsymbol{B}(\boldsymbol{\theta}_0)\boldsymbol{A}(\boldsymbol{\theta}_0)^{-T}. \quad \text{(B.8)}$$

B.2 Asymptotic distribution of the robust likelihood ratio-type test

Denote $u_n(\boldsymbol{\theta}) = \sum_{i=1}^n \rho(\boldsymbol{z}_i, \boldsymbol{\theta})$ and $v_n(\boldsymbol{\gamma}) = \sum_{i=1}^n \rho(\boldsymbol{z}_i, \boldsymbol{\gamma})$ where $\boldsymbol{\theta} \in \mathbb{R}^{2p}$ and $\boldsymbol{\gamma} \in \mathbb{R}^{2q}$ are the parameter vectors of the models of the null and alternative hypothesis, respectively. The true parameter values are denoted by $\boldsymbol{\theta}_0$ and $\boldsymbol{\gamma}_0$, respectively. Note that the real and imaginary parts are stacked separately to the vectors, i.e. for example $\boldsymbol{\theta} = \left[\theta_{1,r}, \theta_{1,i}, \ldots, \theta_{p,r}, \theta_{p,i}\right]^T$.

The robust likelihood ratio-type test is now given by

$$S_n = 2[u_n(\hat{\boldsymbol{\theta}}_n) - v_n(\hat{\boldsymbol{\gamma}}_n)]. \quad \text{(B.9)}$$

From the Taylor expansion of $u_n(\boldsymbol{\theta}_0)$ around $\hat{\boldsymbol{\theta}}_n$, it is obtained

$$u_n(\boldsymbol{\theta}_0) = u_n(\hat{\boldsymbol{\theta}}_n) + \frac{n}{2}\boldsymbol{d}_n^T \boldsymbol{A}_\theta(\hat{\boldsymbol{\theta}}_n)\boldsymbol{d}_n + o_p(1). \quad \text{(B.10)}$$

Similarly,

$$v_n(\boldsymbol{\gamma}_0) = v_n(\hat{\boldsymbol{\gamma}}_n) + \frac{n}{2}\boldsymbol{f}_n^T \boldsymbol{A}_\gamma(\hat{\boldsymbol{\gamma}}_n)\boldsymbol{f}_n + o_p(1), \quad \text{(B.11)}$$

where $\boldsymbol{f}_n$ is similarly to $\boldsymbol{d}_n$ given by

$$\boldsymbol{f}_n = \begin{bmatrix} (\hat{\gamma}_n - \gamma_0)_{1,r} \\ (\hat{\gamma}_n - \gamma_0)_{1,i} \\ (\hat{\gamma}_n - \gamma_0)_{2,r} \\ (\hat{\gamma}_n - \gamma_0)_{2,i} \\ \vdots \\ (\hat{\gamma}_n - \gamma_0)_{q,r} \\ (\hat{\gamma}_n - \gamma_0)_{q,i} \end{bmatrix}. \quad \text{(B.12)}$$

Subtracting (B.10) from (B.11) and multiplying the result with 2 gives

$$\begin{aligned} 2[u_n(\hat{\boldsymbol{\theta}}_n) - v_n(\hat{\boldsymbol{\gamma}}_n)] = 2[u_n(\boldsymbol{\theta}_0) - v_n(\boldsymbol{\gamma}_0)] - n\boldsymbol{d}_n^T \boldsymbol{A}_\theta(\hat{\boldsymbol{\theta}}_n)\boldsymbol{d}_n \\ + n\boldsymbol{f}_n^T \boldsymbol{A}_\gamma(\hat{\boldsymbol{\gamma}}_n)\boldsymbol{f}_n + o_p(1). \end{aligned} \quad \text{(B.13)}$$

This can be written as

$$2[u_n(\hat{\boldsymbol{\theta}}_n) - v_n(\hat{\boldsymbol{\gamma}}_n)] = 2[u_n(\boldsymbol{\theta}_0) - v_n(\boldsymbol{\gamma}_0)] + n \begin{bmatrix} \boldsymbol{d}_n \\ \boldsymbol{f}_n \end{bmatrix}^T \boldsymbol{Q}_n \begin{bmatrix} \boldsymbol{d}_n \\ \boldsymbol{f}_n \end{bmatrix} + o_p(1), \quad \text{(B.14)}$$

where $\boldsymbol{Q}_n$ is a block-diagonal matrix given by

$$\boldsymbol{Q}_n = \begin{bmatrix} -\boldsymbol{A}_\theta(\hat{\boldsymbol{\theta}}_n) & \mathbf{0} \\ \mathbf{0} & \boldsymbol{A}_\gamma(\hat{\boldsymbol{\gamma}}_n) \end{bmatrix}. \quad \text{(B.15)}$$

Assuming that the functional form is the same under both the null and alternative hypothesis, then $u_n(\boldsymbol{\theta}_0) - v_n(\boldsymbol{\gamma}_0) = 0$. Furthermore, from the multivariate central limit theorem and Appendix B.1, it follows (as $n \to \infty$)

$$\sqrt{n} \begin{bmatrix} \boldsymbol{d}_n \\ \boldsymbol{f}_n \end{bmatrix} \xrightarrow{D} N(\mathbf{0}, \boldsymbol{\Sigma}), \quad \text{(B.16)}$$

and

$$\boldsymbol{Q}_n \xrightarrow{P} \boldsymbol{Q} = \begin{bmatrix} -\boldsymbol{A}_\theta(\boldsymbol{\theta}_0) & \mathbf{0} \\ \mathbf{0} & \boldsymbol{A}_\gamma(\boldsymbol{\gamma}_0) \end{bmatrix}, \quad \text{(B.17)}$$

where

$$\boldsymbol{\Sigma} = \begin{bmatrix} \boldsymbol{A}_\theta^{-1}(\boldsymbol{\theta}_0)\boldsymbol{B}_\theta(\boldsymbol{\theta}_0)\boldsymbol{A}_\theta^{-T}(\boldsymbol{\theta}_0) & \boldsymbol{A}_\theta^{-1}(\boldsymbol{\theta}_0)\boldsymbol{B}_{\theta\gamma}(\boldsymbol{\theta}_0, \boldsymbol{\gamma}_0)\boldsymbol{A}_\gamma^{-T}(\boldsymbol{\gamma}_0) \\ \boldsymbol{A}_\gamma^{-1}(\boldsymbol{\gamma}_0)\boldsymbol{B}_{\gamma\theta}(\boldsymbol{\gamma}_0, \boldsymbol{\theta}_0)\boldsymbol{A}_\theta^{-T}(\boldsymbol{\theta}_0) & \boldsymbol{A}_\gamma^{-1}(\boldsymbol{\gamma}_0)\boldsymbol{B}_\gamma(\boldsymbol{\gamma}_0)\boldsymbol{A}_\gamma^{-T}(\boldsymbol{\gamma}_0) \end{bmatrix}. \quad \text{(B.18)}$$

Consequently, the test statistic is asymptotically distributed as [226, Lemma 3.2]

$$2[u_n(\hat{\boldsymbol{\theta}}_n) - v_n(\hat{\boldsymbol{\gamma}}_n)] \sim M_{2(p+q)}(\cdot; \lambda), \quad \text{(B.19)}$$

where $M_{2(p+q)}(\cdot; \lambda)$ denotes the cdf of a random variable $\sum_{i=1}^{2(p+q)} \lambda_i x_i^2$ where x_i are independent standard normal random variables. λ_i are the eigenvalues of $\boldsymbol{Q}\boldsymbol{\Sigma}$ and are real (possibly negative) valued. The matrix $\boldsymbol{Q}\boldsymbol{\Sigma}$ is given by

$$\boldsymbol{Q}\boldsymbol{\Sigma} = \begin{bmatrix} -\boldsymbol{B}_\theta(\boldsymbol{\theta}_0)\boldsymbol{A}_\theta^{-T}(\boldsymbol{\theta}_0) & -\boldsymbol{B}_{\theta\gamma}(\boldsymbol{\theta}_0, \boldsymbol{\gamma}_0)\boldsymbol{A}_\gamma^{-T}(\boldsymbol{\gamma}_0) \\ \boldsymbol{B}_{\gamma\theta}(\boldsymbol{\gamma}_0, \boldsymbol{\theta}_0)\boldsymbol{A}_\theta^{-T}(\boldsymbol{\theta}_0) & \boldsymbol{B}_\gamma(\boldsymbol{\gamma}_0)\boldsymbol{A}_\gamma^{-T}(\boldsymbol{\gamma}_0) \end{bmatrix}. \quad \text{(B.20)}$$